United Nations ECE/TRANS/WP.29/2025/85

Economic and Social Council

Distr.: General
9 April 2025

Original: English

Economic Commission for Europe

Inland Transport Committee

World Forum for Harmonization of Vehicle Regulations

196th session
Geneva, 24–27 June 2025
Item 14.2.2. of the provisional agenda
Consideration and vote by AC.3 of draft UN GTRs and/or draft amendments to established UN GTRs, if any

Proposal for a Final status report on the development of Amendment 2 to UN GTR No. 24

Submitted by the Working Party on Pollution and Energy*

The text reproduced below was adopted by the Working Party on Pollution and Energy (GRPE) at its ninety-second session (ECE/TRANS/WP.29/GRPE/92, para. XX). It is based on informal document GRPE-92-30-Rev.1. It is submitted to the World Forum for Harmonization of Vehicle Regulations (WP.29) and to the Administrative Committee (AC.3) for consideration at their June 2025 sessions.

* In accordance with the programme of work of the Inland Transport Committee for 2025 as outlined in proposed programme budget for 2025 (A/79/6 (Sect. 20), table 20.6), the World Forum will develop, harmonize and update UN Regulations in order to enhance the performance of vehicles. The present document is submitted in conformity with that mandate.

I. Introduction

1. Over recent years there has been a sharp increase in international interest to characterise non-exhaust emissions of particles from road transport. Until recently, exhaust sources dominated road transport emissions, and all regulatory efforts have been aiming at their reduction. As exhaust emissions were reduced due to increasingly stringent regulations, the relative contribution of non-exhaust emissions to overall ambient concentrations of particulate matter increased.

2. Most manufacturers produce vehicles for a global market, or at least for several regions. Since manufacturers tend to cater to the preferences, needs, and lifestyles of specific geographic regions, vehicle designs will vary worldwide. As compliance with different emission standards in each region can create burdens from an administrative and vehicle design point of view, vehicle manufacturers tend to have a strong interest in harmonising brake emission test procedures and performance requirements on a global scale. Global harmonisation is also of interest to regulators as it offers more efficient development and adaptation to technical progress, potential collaborations with market surveillance, and facilitates the exchange of information between regulatory authorities.

3. In this context, stakeholders launched the work for this United Nations Global Technical Regulation (UN GTR) on Worldwide harmonised Light vehicle Test Procedures (WLTP) for particle emissions from brake wear. This UN GTR aims to harmonise test procedures for emissions from Light-Duty Vehicles (LDV) to the extent possible. Laboratory test procedures need to represent real driving conditions as much as possible and to enable a direct comparison between the performance of vehicles during certification procedures and in real life. However, this aspect puts some limitations on the level of harmonisation to be achieved. Furthermore, different countries will show varying levels of development, population densities, and costs associated with braking system technology. Consequently, the regulatory stringency of legislation is expected to vary from region to region for the foreseeable future. Therefore, the definition of emission limit values is not part of this UN GTR. Nevertheless, the long-term goal is still to define globally harmonized performance requirements and emission limits in forthcoming amendments to this UN GTR.

4. UN GTRs are intended to be implemented into regional legislation by as many Contracting Parties as possible. The selection of vehicle categories to be covered by the scope of regional legislation represents a challenge as it depends on regional conditions that cannot be anticipated. However, according to the provisions of the 1998 UNECE agreement, a UN GTR being implemented by a Contracting Party must apply to all vehicles, conditions, and equipment falling under its formal scope. Therefore, care must be taken in developing the scope of the UN GTR, as an unduly large formal scope may prevent or hamper its implementation into regional legislation. For this reason, the formal scope of this UN GTR is limited to LDVs up to 3500 kg. This limitation does not, however, indicate that the scope of this UN GTR should not be applied to a larger group of vehicle categories when implemented into regional legislation. Indeed, Contracting Parties are encouraged to do so if this is feasible and appropriate from a technical, economical, and administrative point of view.

5. A harmonised approach for measuring brake particle emissions would allow manufacturers to better understand the behaviour of different brake systems, reduce inconsistencies in results and; therefore, compare them more efficiently, and develop strategies to decrease brake emissions.

6. This version of the UN GTR does not contain test requirements specific to other types of vehicles e.g. non-road machinery, special purpose, and heavy-duty vehicles. Thus, these vehicles are not included in the scope of this UN GTR. However, Contracting Parties may apply the provisions within this UN GTR to such vehicles to the extent possible from a technical point of view, and complement them with additional provisions in regional legislation e.g. brake emission testing with different types of friction materials or mating parts.

II. Principles

7. Discussions among the members of the PMP IWG a number of requirements for a brake emissions measurement system:

(a) The procedure should be consistent and repeatable with little variation, to minimize the need for repeated tests and prevent opportunities for selective reporting (or “cherry picking”);

(b) The procedure should be sufficiently robust to evaluate all brake assemblies, including those that currently exist in the market, and those that may reasonably be anticipated to emerge in the future;

(c) Third-party verification of brake emissions measured by the method, and of any manufacturer-provided inputs, should be possible;

(d) The test burden imposed by the procedure should be reasonable, so that the cost and the amount of work necessary to certify the brake emissions should not be prohibitive.

8. Additional discussion as to how the PMP IWG considered these requirements in development of the UN GTR, and discussion of all of the technical approaches considered, can be found in the Technical Background section of this UN GTR.

III. Technical part and contributions of the different task forces to the UN GTR

A. Hardware requirements

1. Overall system layout

9. Figure 1 provides an indicative layout that includes the minimum required subsystems to carry out a brake emissions test using a brake dynamometer. The illustrated layout features a climatic conditioning unit with variable flow fan(s) that supplies the setup with conditioned air. The conditioned air enters a brake enclosure designed to fit the entire assembly of the brake under testing. The brake dynamometer enables and controls the testing of the brake. The enclosure is directly connected to the sampling tunnel near the end of which the sampling probes are mounted. The sampling probes are used to extract the aerosol from the tunnel towards the PM and PN measurement setup. A flow measurement device is installed in the tunnel downstream of the sampling plane. The positioning and dimensions of the different elements are indicative. More details regarding the different elements of the setup are given below in this paragraph and the corresponding paragraphs of the UN GTR.

Figure 1

Indicative layout for performing brake emissions test in the laboratory. 1 represents the climatic conditioning unit with variable flow blower(s), air temperature, and air humidity control; 2 represents the cooling air filtering medium; 3 represents the cooling air temperature and humidity sensors; 4 represents the brake enclosure; 5 represents the brake assembly; 6 represents the brake dynamometer (not shown); 7 represents the sampling tunnel; 8 represents the sampling plane; 9 represents the PM and PN instrumentation; 10 represents the air flow rate measurement element.

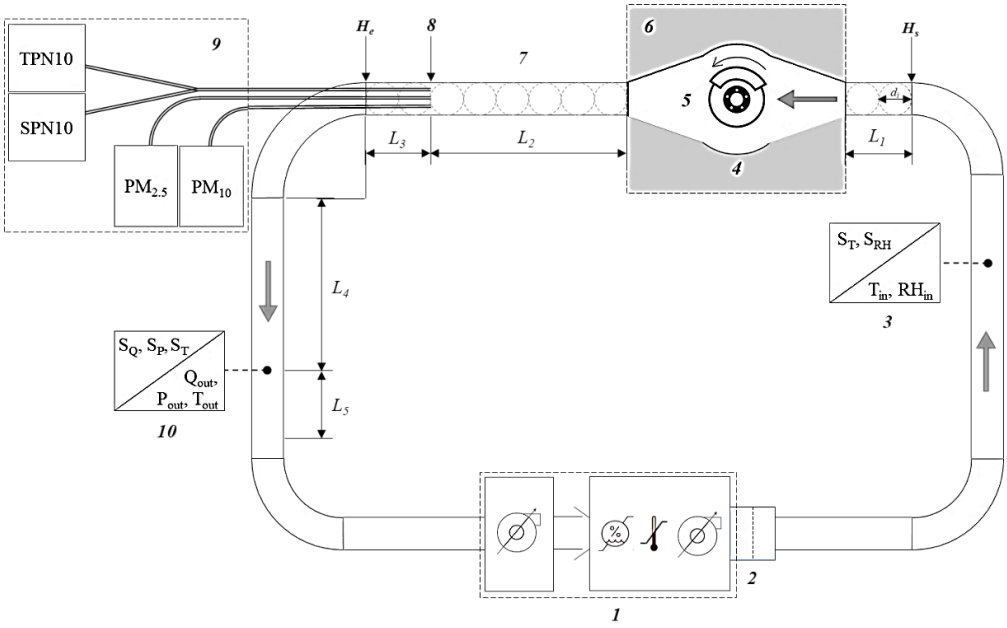

2. Brake dynamometer and automation

10. The brake dynamometer is a technical system that provides controlled kinetic energy to the brake under test. Figure 2 provides a layout of the test system with the brake dynamometer and shows the interactions with the minimum subsystems required to execute a brake emissions test. More details are given in the actual text of the UN GTR. It has been agreed that the brake dynamometer shall consist of at least the following elements: (a) A variable-speed electric motor to accelerate or keep the rotational speed constant; (b) A servo controller to actuate the brake under testing; (c) A mechanical assembly to mount the brake under testing, allow free rotation of the disc or drum, and absorb the reaction forces from braking; (d) A rigid structure to mount all the mandatory subsystems. The structure shall be capable of absorbing the forces and torque generated by the brake under testing; (e) Sensors and devices to collect data and monitor the operation of the test system. The specifications described above have been developed taking into account input from brake dynamometer manufacturers and considering the state-of-the-art of these devices in the market.

11. Integral to the test system is the automation, controls, and data acquisition system (S2). It continuously controls the rotational speed of the motor as well as the operation and the interactions between the different systems (S3, S4, S5). The automation, control, and data acquisition system perform all the functions that enable the brake emissions test. It accelerates the brake during acceleration events, maintains constant speed during cruise events, and modulates the frictional torque during deceleration events to reduce the kinetic energy of the rotating masses. Additionally, it provides an interface to the operator, stores the data from the test, and handles the interfaces with other systems in the testing facility. The software that operates the test system shall be capable of performing at least the following functions: (a) Execute the driving cycle automatically by operating all the closed-loop processes (mainly for brake controls, cooling air handling, and emissions measurements instruments); (b) Continuously sample and record data from all relevant sensors to generate the outputs defined in this UN GTR; (c) Monitor signals, messages, alarms, or emergency stops from the operator and the different systems connected to the test system. During the ILS, it was demonstrated that some of the current systems were not able to execute the

WLTP-Brake cycle correctly. Therefore, it was decided to mandate a series of checks to confirm the feasibility of the automation, controls, and data acquisition system to perform tests the correctly. These are presented in the relevant clause discussing the WLTP-Brake cycle. Additionally, many of current systems in the market cannot handle non-friction functions like regenerative braking in real time. This is one of the reasons for selecting full-friction testing with the application of the coefficients for testing non-friction braking as explained later in the report.

Figure 2

Brake dynamometer and automation systems in the overall test layout. S1: Brake dynamometer, S2: Automation, control, and data acquisition system, S3: Climatic conditioning unit, S4: Brake enclosure and sampling plane, S5: Emissions measurement system. C1 and C2: Testing facility energy controls and monitoring system. The grey arrow represents the aerosol sample from the brake under testing.

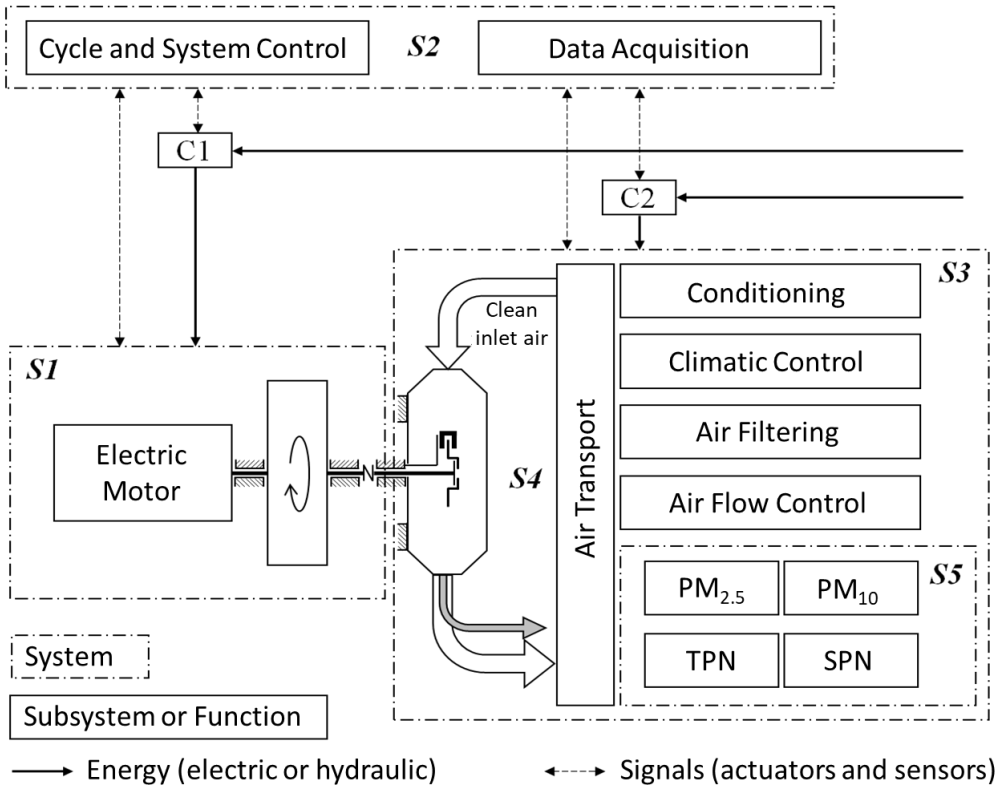

3. Brake enclosure design

12. High-level design requirements for the enclosure were defined for the ILS to achieve maximum transport efficiency, maximum particle distribution and uniformity, and minimum residence time. It was requested to avoid sharp bends and abrupt changes in cross-section with the aim of reducing flow recirculation zones. Gradual changes in the cross-section were permitted; however, it was recommended to apply smooth transition angles to overcome these cross-section changes and avoid the application of higher than 90° bends. It was strongly recommended to avoid oversized enclosures due to higher residence times and increased particle losses. It was also recommended to use electropolished surfaces or other electrically conductive material for the design of the inner walls of the enclosure to avoid particle losses by electrostatic deposition. Table 1 provides an overview of the main enclosure characteristics from testing facilities that performed successful emission measurement tests [1] and agreed to disclose the dimensions. The code of the testing facilities is not provided due to confidentiality issues.

Table 1
Overview of the main enclosure characteristics from testing facilities that performed successful emission measurement tests. SST stands for stainless steel. N/A stands for not available.

Lab	*Orientation*	*Inclination*	*Length (mm)*	*Height (mm)*	*Depth (mm)*	*h_B/h_D (%)*	*Material*	*Volume (m^3)*
1	Horizontal	None	1200	550	400	60%	SST with electropolish	0.10
2	Horizontal	None	1489	696	290	100%	#400 Buffing	N/A
3	vertical	N/A	760	760	460	N/A	Aluminium	0.21
4	Horizontal	None	1200	550	400	60%	SST with electropolish	0.14
5	Horizontal	None	1200	550	400	60%	SST with electropolish	0.14
6	Horizontal	None	1342	720	410	72%	SST with a polished finish	<0.30

13. A "universal" rhombus shape as shown in Figure 3 has been proposed for harmonizing the enclosure design. More specifically, the brake enclosure shall have two conical or trapezoidal sections intersecting with a cylinder at the centre concentric to the axis of the brake rotation. Four out of six labs that provided information on the enclosure's shape applied this design. Several other testing facilities have already opted for a similar design. The enclosure is defined by one horizontal and four vertical planes. Plane A1 represents the horizontal level aligned with the axis of the brake rotation and the axis of the inlet and outlet ducts. Plane A represents the vertical plane aligned with the enclosure's inlet. Plane B represents the vertical plane at the end of the transition from the inlet duct to the central section of the enclosure. Plane C is defined by the largest brake assembly applied on the vehicles that fall under the scope of this GTR (i.e., brake disc of 450 mm diameter). Plane D represents the vertical plane aligned with the axis of the brake rotation.

Figure 3
Indicative schematic representation of the brake enclosure and main proposed dimensions.

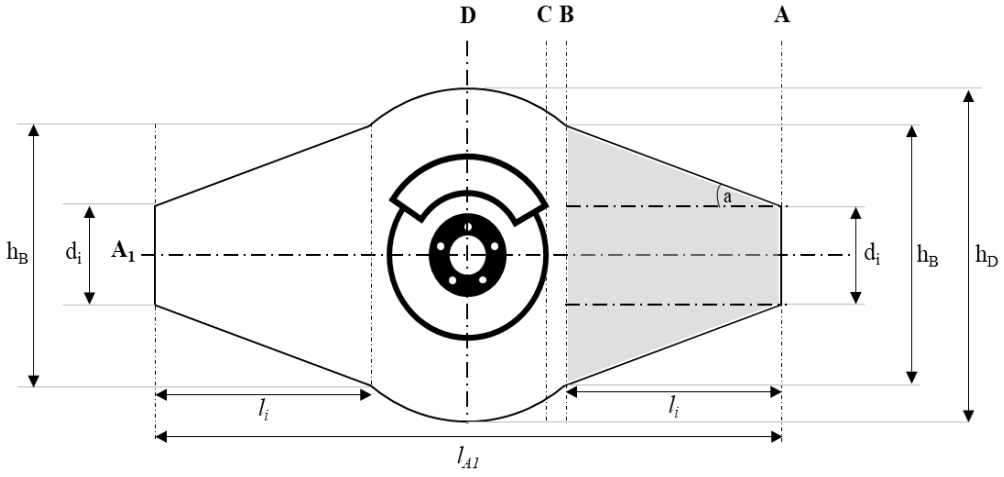

14. The enclosure shall be designed symmetrically to Planes A1 and D for harmonization purposes. Other types of design were discussed; however, the PMP did not receive any experimental data demonstrating the feasibility of non-symmetrical designs for performing brake emissions measurements. Despite there is no evidence that a vertical layout favours or

penalizes emission levels compared to a horizontal layout, it was agreed to mandate only a horizontal layout for harmonization purposes.

15. Some of the testing facilities that used an enclosure with a height of 550 mm reported difficulties in handling the brake when larger diameter brakes are tested. Thus, it was proposed to define a minimum allowed height of 600 mm to ensure that the enclosure fits the largest brake assembly applied to vehicles within the scope of the UN GTR (i.e., brake disc of 450 mm diameter). A maximum allowed height of 750 mm to avoid an oversized enclosure was also defined based on the dimensions provided by the testing facilities. Similarly, it has been defined that Plane A1's length shall be between 1200 mm and 1400 mm, while the enclosure's axial depth is proposed to be between 400-500 mm. Finally, the height at Plane B (h_B) shall be designed such that the h_B/h_D ratio is always greater than 60% (h_B/h_D > 60%) following the example of all testing facilities at the ILS. Detailed specifications regarding the dimensions are provided in the text of the UN GTR.

16. Regarding the residence time, LINK Engineering presented an analysis for a symmetrical design following the specifications defined in the UN GTR. Table 2 illustrates the different scenarios that were simulated in the study through Computational Fluid Dynamics (CFD) simulations. It is demonstrated that residence time is quite low regardless of the differences in the tested parameters when such a design is adopted. The authors concluded that the residence time is mainly determined by the air flow level [2]. Overall, it is concluded that the proposed design fulfils the requirement for minimum residence time in the enclosure.

Table 2
Overview of the main enclosure characteristics from testing facilities that performed successful emission measurement tests. CW stands for clockwise and CCW for counter-clockwise.

Run	*Airflow (m^3/h)*	*Brake size*	*Rotor design*	*Brake rotation*	*Brake speed (rpm)*	*Fixture*	*Residence Time (s)*
1	400	Small	Solid	CCW	900	Post	0.40
2	400	Large	Solid	CCW	400	Knuckle	0.35
3	1000	Large	Vented	CCW	900	Knuckle	0.22
4	400	Large	Vented	CW	900	Post	0.35
5	1000	Small	Solid	CW	900	Knuckle	0.17
6	1000	Large	Solid	CW	400	Post	0.20
7	400	Small	Vented	CW	400	Knuckle	0.37
8	1000	Small	Vented	CCW	400	Post	0.23

17. Another fundamental requirement for the enclosure design relates to the need for maximum particle distribution and uniformity. It has been agreed to allow for the use of flow straighteners or diffusion plates at the inlet's side upstream of Plane B to ensure the highest possible level of uniform flow at Plane C. To ensure air speed uniformity, it has been mandated to measure the air speed values at nine positions in Plane C as defined in Figure 4. Details regarding the design of Plane C and the execution of the measurement are provided in the main text of the UN GTR. The measurement shall be carried out at the minimum and maximum operational flows of the system. The cross-section area at the enclosure inlet shall be designed so that the air speed at Plane C remains below ±35% of the arithmetic mean of all measurements for a given flow. The main concept for confirming air speed uniformity follows the approach defined in ISO-9096.

Figure 4
Reference positions for air speed verification.

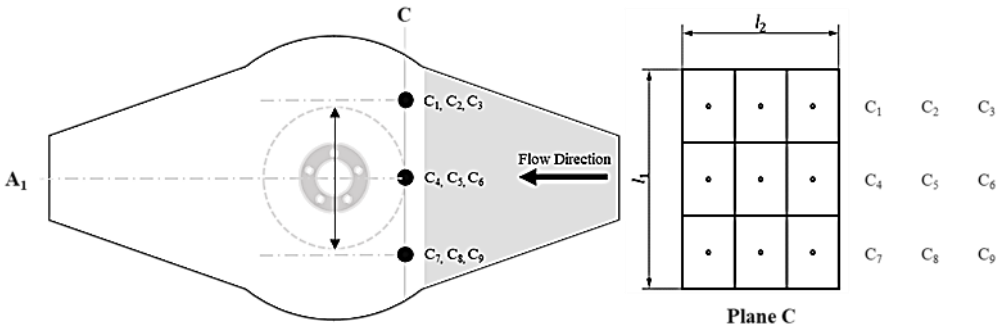

18. Two testing facilities already confirmed through measurement campaigns that the proposed design fulfils the criteria for speed uniformity set out in the UN GTR. Moreover, it has been indicated that the air speed at Plane C may remain below ±20% of the arithmetic mean of all measurements; however, it was decided to allow for the relaxed target of ±35%.

4. Brake fixture and calliper

19. During the ILS it was requested by the testing facilities to position the calliper in a way to minimize potential interference with the incoming cooling air. It was recommended to install the calliper at the upper part of the disc in a position between 1-2 o´clock or 10-11 o´clock considering the direction of evacuation. The brake disc shall have rotated in the direction of the evacuation independently of the orientation of the duct (Counter Clock Wise - CCW if the incoming cooling air flows in a direction from right to the left or Clock Wise - CW when the incoming cooling air flows in a direction from left to the right). No specification was set for the fixture style. Table 3 provides an overview of the fixture style, disc rotation direction, and calliper position during the ILS.

Table 3
Overview of the fixture type, disc rotation direction, and calliper position during the ILS. L0-U stands for the universal fixture without a wheel hub – L0-P stands for the post-style fixture with a wheel hub – L1 stands for the knuckle fixture with a wheel hub.

Lab	*Lab B*	*Lab C*	*Lab D*	*Lab F*	*Lab G*	*Lab H*	*Lab J*	*Lab K*	*Lab L*	*Lab M*	*Lab N*	*Lab P*	*Lab Q*	*Lab R*	*Lab S*	*Lab T*
Fixture Style	L0-U	L0-U	L0-U	L0-U	Other	Other	L0-U	L1	L0-U	L0-U	L0-P	L1	L0-P	L0-U	N/A	L0-P
Disc Rotation Direction	CCW	CCW	CCW	N/A	CCW	CCW	CCW	CCW	CW	CCW	CCW	CW	CCW	CCW	CW	CW
Caliper Position (o'clock)	11	9	3	8	10	10	11	12	9	9	10	12	11	10	1-2	2

20. It was agreed that the installation position of the brake assembly shall always be at the centre of the brake enclosure. This was applied by most labs during the ILS. This requirement is much easier to fulfil due to the symmetrical design of the enclosure. The support fixture of the brake assembly shall allow the brake to freely rotate by 360° with low or no friction and without exhibiting vibration or oscillations during testing. It was agreed that the brake system shall be mounted on the dynamometer using either a Universal-style (L0-U) or Post-style (L0-P) brake fixture. Different variations of L0-U and L0-P fixtures are allowed. 11 of 15 labs used these types of fixtures during the ILS. Knuckle fixtures are not permitted since it has been reported that they might collect particles during the emissions test. More details regarding the fixture specifications are provided in the main text of the UN GTR. The brake disc or drum shall always rotate in the direction of the evacuation. 15 of 16 labs followed this requirement during the ILS; therefore, it is not possible to extract a solid conclusion about

whether the opposite direction negatively influences emissions. Even though in vehicle applications the rotation is in the opposite direction, the objective of the method is to direct all particles towards the sampling tunnel with the minimum possible losses. For this reason, it has been mandated to harmonize the method for all testing facilities applying the direction of the evacuation.

21. A wide variety of calliper orientations were tested during the ILS. Labs G, J, L, S, and T provided PM10 measurements closer to PM10 average value for the reference brake (Figure 5). These labs applied various orientations mostly at the upper part of the disc. However, it is not possible to extract solid conclusions on how the calliper orientation influences PM emissions. JARI performed internal measurements applying all calliper orientations and found that the measured PM10 is within ±20%. This variation falls within the measurement variability for PM10 emissions. For harmonization purposes, it was proposed to install the calliper in a fixed position (12 o'clock) differently than recommended during the ILS. It is not allowed to apply for a different calliper position even if the actual vehicle featuring the tested brake applies a different orientation. The vehicle orientation is irrelevant since the enclosure is a closed system (unlike the vehicle's wheel) where the aim is to collect the particles efficiently, direct them towards the sampling plane, and keep the temperature regimes at certain levels. Finally, Computational Fluid Dynamic (CFD) studies show a minor effect of the calliper orientation in particle mixing and evacuation time [2].

Figure 5

PM emissions for the reference brake in mg/km per brake corner for selected labs. The upper line represents the PM10 average. The lower line represents the PM2.5 average.

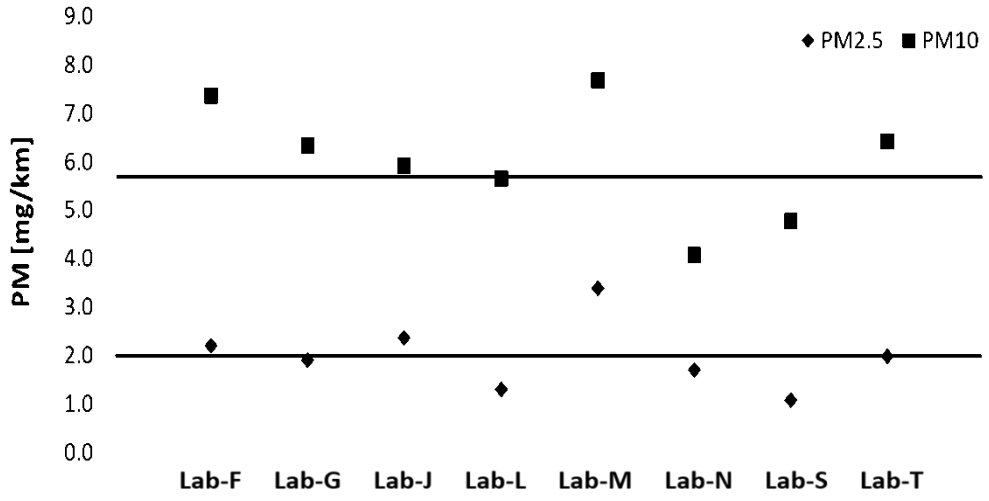

5. Measurement of the brake temperature

22. During the ILS, it was mandatory to use embedded thermocouples for the measurement of the brake disc and drum temperature. The testing facilities were requested to locate the disc thermocouple in the outboard plate rubbing surface – radially positioned 10 mm outwards of the centre of the friction path – and recessed (0.5±0.1) mm deep into the face of the disc. Similarly, the labs were instructed to locate the drum thermocouple at the centre of the friction path (0.5±0.1) mm deep in the inside surface of the brake drum. The ISO 26867 performance test makes reference to the 0.5 mm depth. TF1 adopted this requirement as it has been a common practice in the industry. The ±0.1mm is to allow for some flexibility. It was also recommended to measure the brake pad or shoe temperature parallel to the disc temperature. It was recommended to embed one thermocouple at a depth of 1.0 mm near the centre of the friction surface on each pad. For brake shoes, it was recommended to embed one thermocouple at a depth of 1.0 mm near the centre of the friction surface of the most heavily loaded shoe. The testing facilities shall have paid special attention to the tear, wear, and routing (to allow free calliper movement) of the thermocouple wire for inner pads.

23. Figure 6 shows the average and maximum temperature recorded in all ILS tests with all brakes. A careful look into the data shows that different testing facilities measured generally similar average brake temperatures for the same brakes. Differences of a maximum of 20°C were observed for the reference brake which was tested by all testing facilities. Brake #2 (Br2) and Br3 average temperatures were at the same level and always within 15°C. The highest differences in the average temperature were observed with Br5b. The maximum temperatures showed higher deviations which is normal since it is a single-point temperature. Taking into account the differences in the execution of the test among the various facilities (e.g., problems in the correct execution of the cycle, tests carried out with lower kinetic energy), it was concluded that the performance of the embedded thermocouples, as well as the instructions for their installation, are adequate. More details regarding the specifications are provided in the main text of the UN GTR.

Figure 6
Average and maximum brake temperature recorded during the ILS by all testing facilities with all brakes.

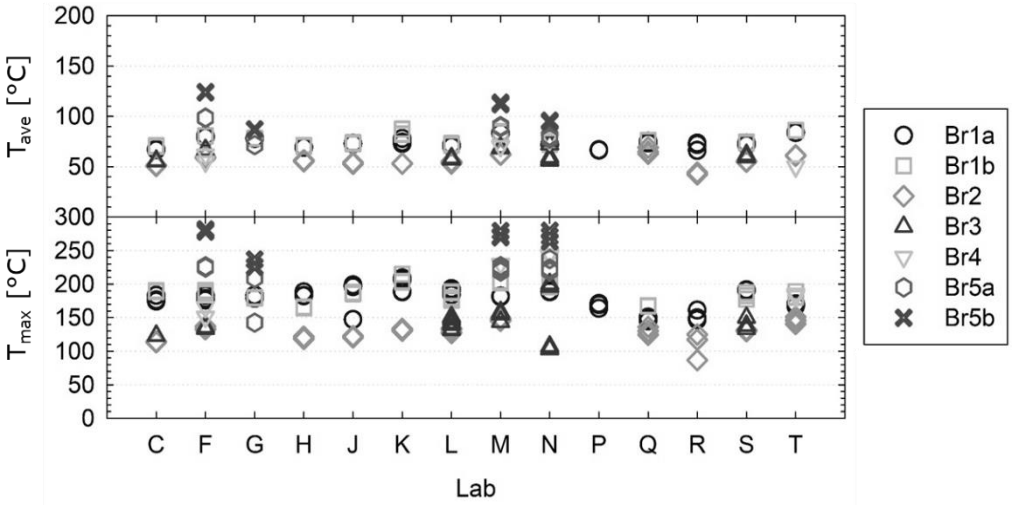

24. Figure 7 shows the proper installation of embedded thermocouples for brake discs and drums. Regarding the temperature measurement of the friction material, during the ILS Lab N noticed that the pad thermocouple was causing a tight fit causing excessive drag while conducting the cooling air adjustment for Br3. Several other testing facilities reported similar issues in the past and commented that the installation of the thermocouple is not easy as described in the protocol – a thermocouple placed 1 mm below the surface may result in the brake pad material being crumbled in this area. Additionally, the installation of the thermocouple wire on the back plate may result in additional brake torque which would affect particle measurement due to the narrow space between the brake pad and the brake calliper. Therefore, it was decided to amend the specification for the measurement of pad/shoe temperature from the UN GTR. Indeed, this information has been useful for research purposes; however, when it comes to regulatory testing the protocol shall ensure that no interferences or artificial temperature increases are caused. Therefore, the installation of embedded or other types of thermocouples for measuring brake pad or shoe temperature in the context of this UN GTR is strongly discouraged.

Figure 7
Schematic installation of embedded thermocouples for brake discs (upper part) and drums (lower part).

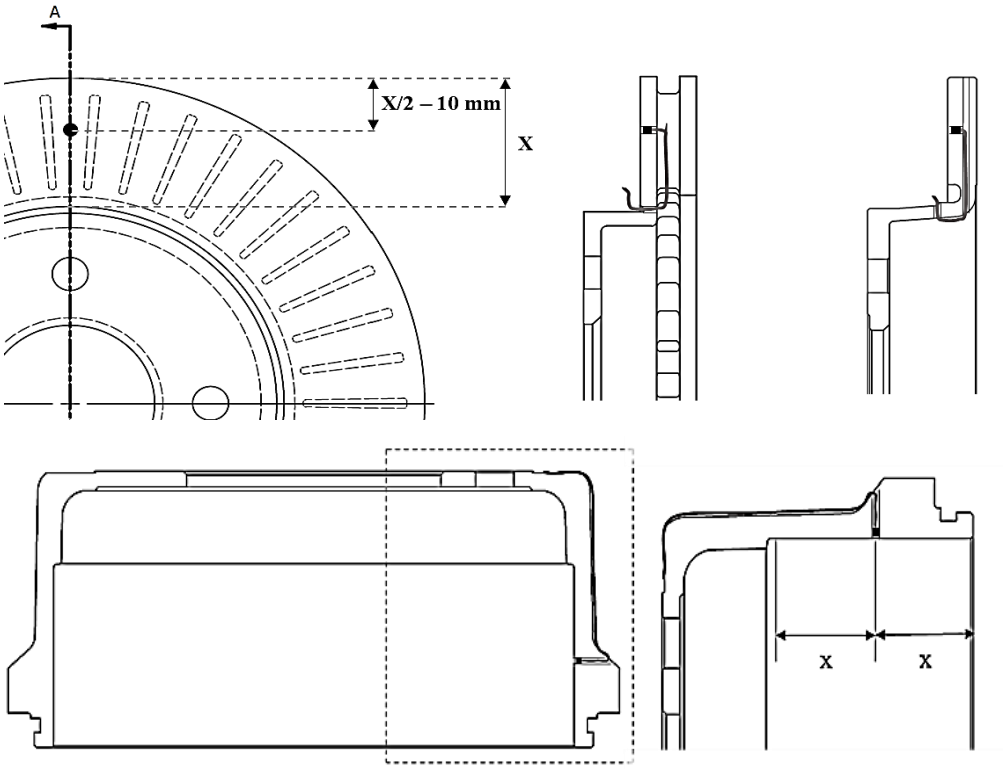

6. Sampling tunnel

25. The sampling tunnel is defined as the part between the outlet of the brake enclosure and the inlet of the sampling probes. During the ILS it was recommended to limit bends in the design of the sampling tunnel to a minimum – and when necessary – design them with a radius greater than 1.5 times the tunnel's inner diameter. It was requested to locate the sampling plane at least 5 hydraulic diameters downstream and at least 2 hydraulic diameters upstream of the last flow disturbance. The use of flow splitters for PM measurements was discouraged. There was no limitation regarding the sampling tunnel's inner diameter. Table 4 provides an overview of the sampling tunnel's inner diameter, bending radius, and the distances of the sampling plane from the last flow disturbances during the ILS.

Table 4
Overview of the sampling tunnel's inner diameter (d_i), bending radius, and the distances of the sampling plane from the last flow disturbances (upstream and downstream). White and grey cells denote labs that performed successful and questionable PM measurements, respectively [1].

	Lab B	*Lab C*	*Lab D*	*Lab F*	*Lab G*	*Lab H*	*Lab J*	*Lab K*	*Lab L*	*Lab M*	*Lab N*	*Lab P*	*Lab Q*	*Lab R*	*Lab S*	*Lab T*
Bending radius	$6d_i$	$2d_i$	$4d_i$	$10d_i$	$2d_i$	$1.5d_i$	$1.5d_i$	$2d_i$	$>1.5d_i$	$2d_i$	$2d_i$	$1.7d_i$	$3d_i$	$2d_i$	$2d_i$	$1.5d_i$
Tunnel inner diameter	160	355	253	108	150	125	150	300	175	150	150	150	148	150	219	160
Distance in diameters Downstream	$8d_i$	$5d_i$	$4d_i$	$5.5d_i$	$5d_i$	$6d_i$	$5d_i$	$0d_i$	$4d_i$	$5d_i$	$8d_i$	$5d_i$	$6d_i$	$8d_i$	$7d_i$	$6.5d_i$

	Lab B	*Lab C*	*Lab D*	*Lab F*	*Lab G*	*Lab H*	*Lab J*	*Lab K*	*Lab L*	*Lab M*	*Lab N*	*Lab P*	*Lab Q*	*Lab R*	*Lab S*	*Lab T*
Distance in diameters Upstream	$6d_i$	$5d_i$	N/A	$2d_i$	N/A	$2d_i$	$2d_i$	$0d_i$	$1.7d_i$	$2d_i$	$2d_i$	$2d_i$	$2d_i$	$2d_i$	$2.3d_i$	$2d_i$

26. Ford carried out an analysis to investigate particle losses in the tunnel under the ILS conditions. The analysis was presented in the TF2. Three different layouts were investigated: a 5 diameters straight sampling tunnel between the enclosure's outlet and the sampling plane's inlets, a 90° bend layout with a 5 diameters straight part between the enclosure's outlet and the sampling plane's inlets, and a 180° bend layout with a 5 diameters straight part between the enclosure's outlet and the sampling plane's inlets as shown in Figure 8 (upper part). Different tunnel diameters and air flows were examined taking into consideration the typical ILS testing conditions. The different scenarios were examined for diffusional, gravitational, and inertial losses. As shown in Figure 8, larger duct diameters show higher penetration; however, the difference is very low for 10.7 μm diameter particles. Similarly, high air velocity scenarios show lower penetration than low air velocity scenarios with the difference being not important. Overall, the tunnel losses for the three configurations are low (e.g., for 5 μm particles worst case is approximately 1.5%) for the typical air velocities of the ILS. Ford concluded that even for the worst-case assumptions from the ILS the expected difference in the overall PM10 range is low (about 2.5%). Similar conclusions were drawn from the JRC analysis presented later in the PM measurement section.

Figure 8

Penetration at a particle diameter of 10.7 μm at different ILS scenarios for three different tunnel layouts. Tunnel air flows of 110 m^3/h and 350 m^3/h are examined.

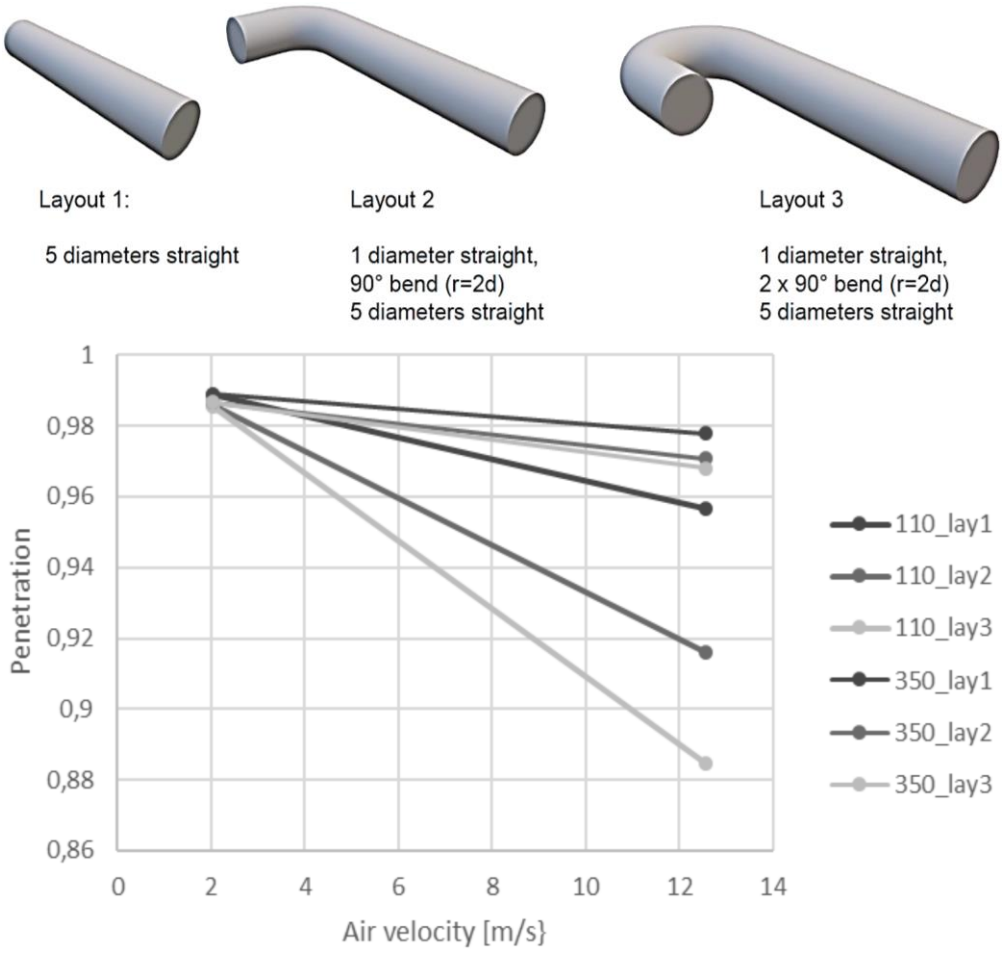

27. Based on the analysis presented above, the UN GTR allows for two possible designs of the sampling tunnel: a layout without a bend and a layout with one bend. The two layouts are not expected to result in significantly different PM and PN measurements. However, the testing facility shall ensure the design of the sampling tunnel meets the following requirements: (a) A maximum of one bend of 90° or less may be applied in the sampling tunnel provided that the bending radius is at least two times the duct inner diameter ($2 \cdot d_i$). The bending radius of two diameters has been selected over 1.5 diameters to minimize inertial losses. Additionally, a straight duct with a length of at least six times the duct diameter ($6 \cdot d_i$) shall follow the bend before locating the sampling plane (ISO 9096). Finally, a straight duct with a length of at least two times the duct diameter ($2 \cdot d_i$) shall follow the sampling plane before placing any flow disturbance (ISO 9096); (b) If there is no bend in the sampling tunnel, a straight duct with a length of at least six times the duct diameter ($6 \cdot d_i$) shall follow the exit of the enclosure before locating the sampling plane (ISO 9096). Additionally, a straight duct with a length of at least two times the duct diameter ($2 \cdot d_i$) shall follow the sampling plane before placing any flow disturbance (ISO 9096).

28. As shown in Table 4, all testing facilities that carried out acceptable PM measurements respected the requirements for the distancing to the flow disturbances except for Lab L which declared a distance of four tunnel diameters downstream of the enclosure instead of the requested five. Based on the submitted PM measurements this difference does not seem to be important. It is noteworthy that Lab K followed most of the requirements defined by the TF2; however, located the sampling plane directly at the outlet of the enclosure. This is not a viable setup since it may trigger significant streamlines moving across the nozzle resulting in high losses of bigger particles. According to Lab K, one additional reason for the higher PM losses may relate to the rectangular cross-section change from the outlet of the box to the outlet tube. Nevertheless, the potential effects cannot be quantified and finally assessed based on the available data. In any case, in the UN GTR it is mandated that the testing facilities shall ensure the design of round ducts with no variations in the cross-section between the enclosure exit and the sampling plane.

29. Layouts featuring a wide variety of tunnel inner diameters were used during the ILS (Table 4). Figure 9 illustrates the tunnel air speed applied by the laboratories when testing Br1, Br2, Br3, and Br5 (where applicable).

Figure 9
Tunnel air speed applied by the testing facilities when testing the different brakes during the ILS.

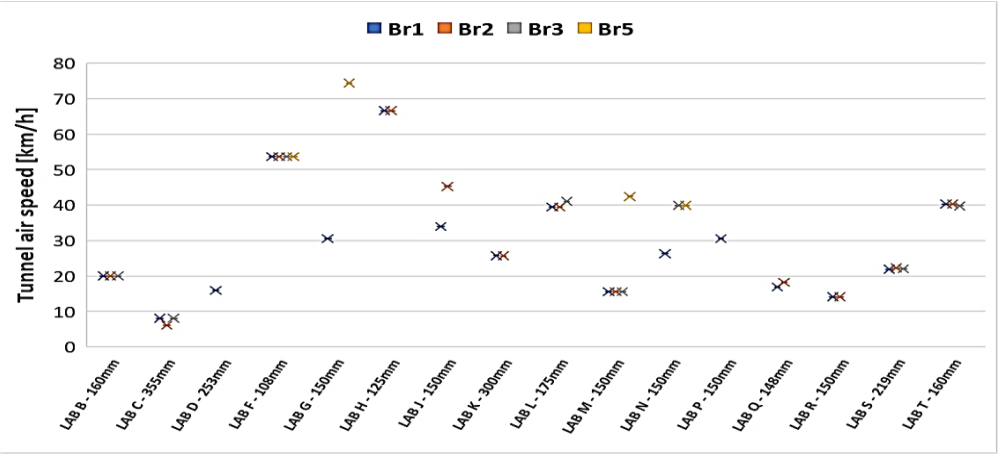

30. Typical tunnel speeds observed at the ILS vary between 15-45 km/h and cover all tested brakes (Br4 was tested using the same air flow rate as Br1). Labs F and H carried out all tests at high air speeds due to low duct diameters (108 mm and 125 mm, respectively). Such low duct diameters may lead to relatively high inertial losses when there are bends and depending on the setup; however, this was not confirmed for Lab F (analysis shown later in the document in the PM measurement paragraph). On the other hand, Lab C carried out all tests at a very low tunnel air speed (< 10 km/h) due to a very high duct diameter (355 mm). Testing at such a low tunnel air speed is not recommended as gravitational losses increase.

Additionally, high duct diameters imply also larger space requirements for installation. Overall, it has been decided that the sampling tunnel duct shall have a constant inner diameter of at least 175 mm and a maximum of 225 mm (175 mm ≤ d_i ≤ 225 mm). A request to mandate a fixed sampling tunnel diameter for all layouts was submitted (i.e., 200 mm); however, the vast majority of the group did not agree with this proposal and opted for allowing some flexibility to the testing facilities to design the layout based on their needs. Mandating a fixed diameter would have been a significant restriction compared to the range of diameters used in the ILS (108-355 mm).

7. Sampling plane

31. The sampling plane is the vertical plane in the sampling tunnel where the inlet of the sampling probes is placed. All extraction points shall be in the same cross-section area in-line with the specifications described in UN GTR No. 15 (exhaust emissions). It was explained earlier that it was decided to place the sampling plane at least 6 hydraulic diameters downstream and 2 hydraulic diameters upstream of the last flow disturbance. More details about the distancing in relation to the sampling tunnel design are discussed in the previous paragraph.

32. There are two possibilities for the design of the sampling plane: a layout with three sampling probes and a layout with four sampling probes. During the ILS, it was recommended not to use flow splitting devices for the PM measurements to avoid possible losses mainly of the coarse-size fraction particles. If a flow splitter was used, it was recommended to keep the change in the flow angle to less than or equal to 20º for each outlet to minimize particle losses. In any case, most of the testing facilities did not use flow-splitting devices; therefore, it was not possible to extract a solid conclusion regarding their feasibility for PM measurements. On the other hand, flow-splitting for PN measurement was advised to be allowed following certain requirements for the flow. Losses for lower-size particles which are of interest for PN measurement are expected to be negligible when the two branches of the splitter operate at the same flow. This has been confirmed in calibration of exhaust particle number systems.

33. Based on these requirements, it was decided to allow for certain flexibility when designing the sampling plane. More specifically, it was decided to allow for a minimum of three and a maximum of four extraction points (with corresponding sampling probes) depending on the tunnel's inner diameter. Two extraction points shall always be dedicated to PM measurements – one for PM2.5 and one for PM10. Additionally, one (for a three-probe setup) or two (for a four-probe setup) extraction points shall be dedicated to PN measurements (TPN10 and SPN10). This will allow for a sampling probe to be used for measuring other parameters than the regulated (e.g. particle size distribution). Independently of a three-probe or a four-probe setup, the probes shall be equally spaced around the central longitudinal axis of the dilution tunnel with the spacing between them being at least 47.5 mm. In addition, the probe-to-duct wall distance shall also remain at least 47.5 mm. In both cases, the probe-to-duct distance shall be measured using the outer diameter of the sampling probes. Initially, the distances were defined to a minimum of 50 mm according to ISO 9096; however, a flexibility of ±5% was allowed to enable the design of 175 mm tunnels for the three-probe setup. As a result, the three-probe setup requires a minimum duct diameter of 175 mm, while the four-probe setup requires a minimum duct diameter of 190 mm. Finally, it was decided to place the two PM probes at the same horizontal level (i.e., lower part of the vertical cross-section area) as it is shown in Fig. 10 to avoid improper mixing especially at lower cooling speeds (a detailed explanation is provided in the PM measurement section).

Figure 10 illustrates the proper positioning of the PM and PN sampling probes for both the three- and four-sampling probes layout.

Figure 10
Positioning of the PM and PN sampling probes for the three and the four sampling probes layout.

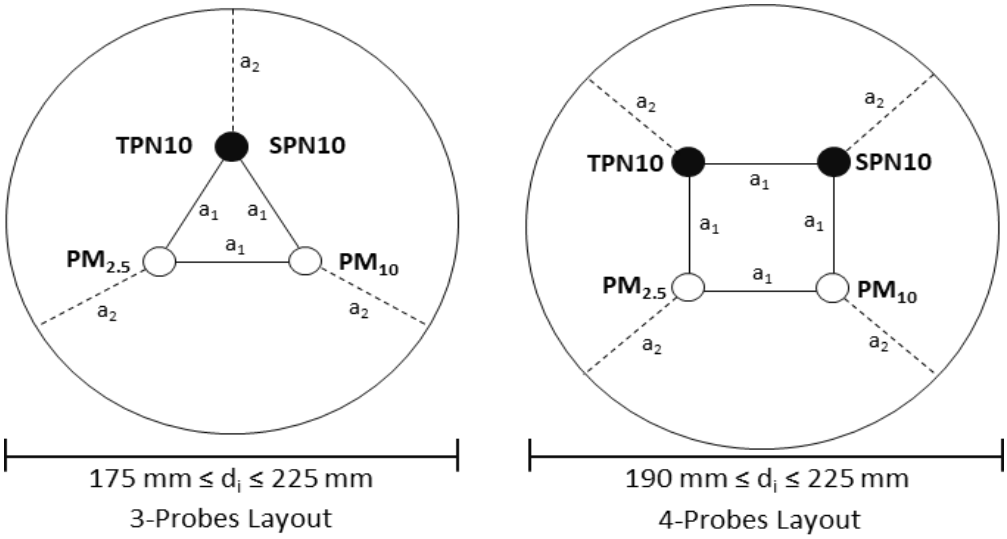

B. Test Cycle (WLTP-Brake Cycle)

1. General information

34. The testing cycle for performing a brake emissions test is the time-based Worldwide Harmonized Light-Duty vehicles Test Procedure (WLTP)-Brake Cycle profile. Legacy cycles for dynamometer testing address performance, endurance, and noise test purposes (i.e., SAE J2522 for the AK Master). These cycles provide useful information regarding brake emissions; however, they do not cover the full range of typical driving/braking conditions as defined in [3]. The dedicated Task Force (TF1) worked on the development of a novel brake cycle which would be representative of real-world brake applications. The WLTP–brake cycle was developed and validated at the vehicle and brake-dyno level and became available to the PMP IWG and the research community in 2018 [4].

35. The WLTP reference database was used for the development of the WLTP-Brake Cycle profile. The WLTP database consists of in-use driving data from five different regions (EU, USA, India, Korea, and Japan) with a total mileage of 743,694 km. The WLTP data consists of vehicle speed, engine speed (for most vehicles), date and time of the day, and trip number. The database lacks any brake-related information. Vehicle speed and deceleration-dependent threshold curves were introduced to differentiate between decelerations with and without brakes applied [4]. The WLTP data was separated into short trips and stop phases for further analysis. A short trip is a connected time sequence with vehicle speeds ≥ 1 km/h. Short trips are binned into four classes according to their maximum speed: Low: $V_{max} \leq 60$ km/h, Medium: 60 km/h < $V_{max} \leq 80$ km/h, High: 80 km/h < $V_{max} \leq 110$ km/h, Extra high: $V_{max} > 110$ km/h.

36. Distributions of certain driving parameters were used for the development of the WLTP-Brake Cycle. These are the brake phase duration, brake phase distance, number of brake phases per distance driven, initial braking velocity, average deceleration rate, and the time interval between brake applications. To get the reference distributions for the brake cycle development the following approach was used: The start speed distributions for brake phases from the European part of the WLTP database were calculated for short trips separately in the four different speed classes of the WLTP: low, medium, high and extra high. The timeshares for the speed classes in the European part of the database were then compared to the timeshares for the speed classes of the WLTP (without stop phases). Correction factors were derived to calculate a weighted overall distribution, which builds the reference for the brake cycle. More details are provided in [4].

37. The cycle development work was divided into five steps: (1.) The analysis of the joint frequency distributions of brake phases with regards to initial braking velocity, duration, and average deceleration per short trip speed class. These classes were combined into three-dimensional bins (velocity, stop duration, acceleration). The bins for the four different speed classes were then merged into a weighted final bin table; (2.) Candidate short trips from the whole WLTP in-use database were selected, whose brake events would match the derived joint frequency distribution of brake phases with regard to initial braking velocity, duration, and average deceleration. These short trips were then put together into a cycle with shortstop phases (3–5 s) to keep the driving time reasonably short; (3.) To match the distribution of time between stops, stop phases or constant speed phases within the cycle were inserted or prolonged to fit the distribution of periods between consecutive brake phases; (4.) Fine-tuning was performed to achieve a better fit for the database distributions. In addition to that, all deceleration phases without brake engagement were replaced with constant velocity segments to avoid any confusion between coast-down and braking decelerations. Finally, all acceleration and deceleration phases were modified to linear increase/decrease of the vehicle speed (constant acceleration values); (5.) The cycle was further subdivided into 10 trips with 9 in-cycle breaks (soakings) to account for the fact that the average trip length in the WLTP is much shorter than the whole novel cycle length.

Figure 11
Time-resolved vehicle speed for the WLTP-Brake cycle and classification of trip numbers.

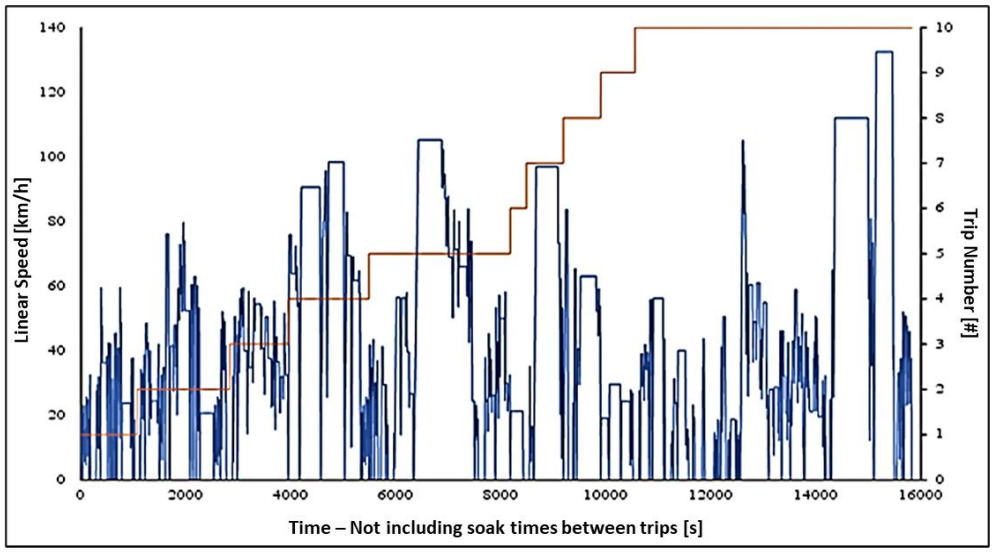

38. The WLTP-Brake Cycle is shown in Figure 11. It consists of 303 deceleration events at a distance of 192 km and a net duration of approximately 4½ h (15826 seconds of active speed control without including the cooling sections between the individual trips of the cycle). This results in an average speed of 43.7 km/h (disregarding trip breaks) which is reasonably close to the average speed of the WLTP database (46.5 km/h). The maximum speed is 132.5 km/h and the brake deceleration varies between 0.5 m/s^2 and 2.2 m/s^2 with a mean of 0.97 m/s^2. The stop phase percentage is 12.9% compared to the target of 13.5% in the WLTP EU database. The number of brake phases per km is 1.56 with the target value being 1.58. The entire cycle is published under a free license [5], whereas a detailed description of the different cycle events is provided in Annex A of the UN GTR.

2. Quality checks

39. Specifications for checking the correct execution of the WLTP-Brake cycle were provided in the GRPE-81-12 and the TF2 protocol for all sections of the brake emissions test: i) Cooling air adjustment; ii) Bedding procedure; iii) Emissions measurement. Two different checks were specified:

– A maximum of 10% of speed violations are allowed during the execution of the WLTP-Brake Cycle. A speed violation occurs whenever the actual speed of the dynamometer exceeds the upper or lower speed trace tolerance compared to the nominal speed (±2 km/h).

– Speed error as RMSSE (Root Mean Sum Square Error) during the execution of the WLTP-Brake Cycle – Recommendation for not exceeding an RMSSE of 1.6 km/h. The specification defines that RMSSE >3.2 km/h results in a non-valid test.

40. The ILS data revealed problems for certain testing facilities to follow the correct WLTP-Brake cycle script (Figure 12). As a consequence, the aforementioned criteria alone were not enough to identify these issues. For this reason, additional parameters have been considered for the quality check of the correct execution of the WLTP-Brake cycle. These include:

Figure 12

Accumulated speed and RMSSE violation data from all testing facilities and brakes for standard emission tests. Data from Labs B and D were not included due to severe problems with the time-base files.

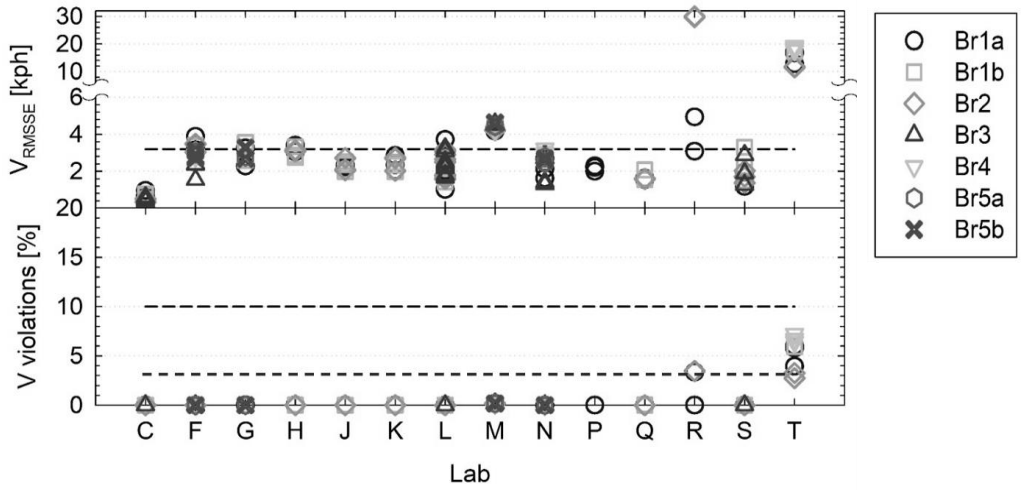

i. Speed violations check: The execution of the WLTP-Brake Cycle allows for a maximum of 3% of speed violations to ensure a repeatable and reproducible test. There was a suggestion to further reduce the maximum allowed violations as defined in the UN GTR to 3% (from 10%). This quality criterion is similar to the one applied in GTR 15; however, since the speed is controlled by the dynamometer (and not by the driver on the chassis dyno as in the UN GTR 15) it is expected to be fulfilled with the appropriate dynamometer controls. Finally, it was suggested to remove the RMSSE violations specification.

ii. Number of deceleration events: The ILS data revealed a problem in some tests and for certain testing facilities to apply the correct number of brake events while executing the WLTP-Brake cycle script. This indicates a systematic error in the script and is a problem when certain brake applications – i.e., high-energy applications – are omitted. For this reason, it was suggested to introduce a quality check that examines the number of executed brake events. It is necessary to ensure that all brake events of the WLTP-Brake cycle are applied. A violation of this criterion occurs whenever the actual number of applied brake events is not equal to the nominal value (i.e., 303). The number of brake events shall be verified using the submitted event-based files. The parameters "Stop Duration" and "Deceleration Rate - Distance Averaged" shall be cross-checked and verified that include 303 numerical and non-zero values that correspond to all brake events of the WLTP-Brake cycle.

iii. Kinetic Energy Dissipation: ILS data revealed a problem for certain testing facilities to apply the nominal WLTP-Brake cycle friction work (15983 J/kg) while executing the WLTP-Brake cycle script (Fig. 13). More specifically, testing facilities that exhibited higher than 10% deviation from the nominal friction work (Labs C, P, Q, H, R) all reported significantly reduced PM emissions compared to the unfiltered (and filtered) average of all labs. As a result, it was suggested to introduce a provision for the total friction work to be within ±5%

of the nominal value during emissions tests. The kinetic energy dissipation quality check is necessary to ensure the application of the correct amount of specific friction work (W_f) during the execution of the WLTP-Brake cycle. It is also an additional quality check that other input parameters (e.g. brake test inertia) have been calculated and applied correctly.

Figure 13
Accumulated bedding and emissions data from all testing facilities and brakes for standard emission tests. The nominal WLTP-Brake cycle friction work is 15983 J/kg. Analysis was performed using the event-based files.

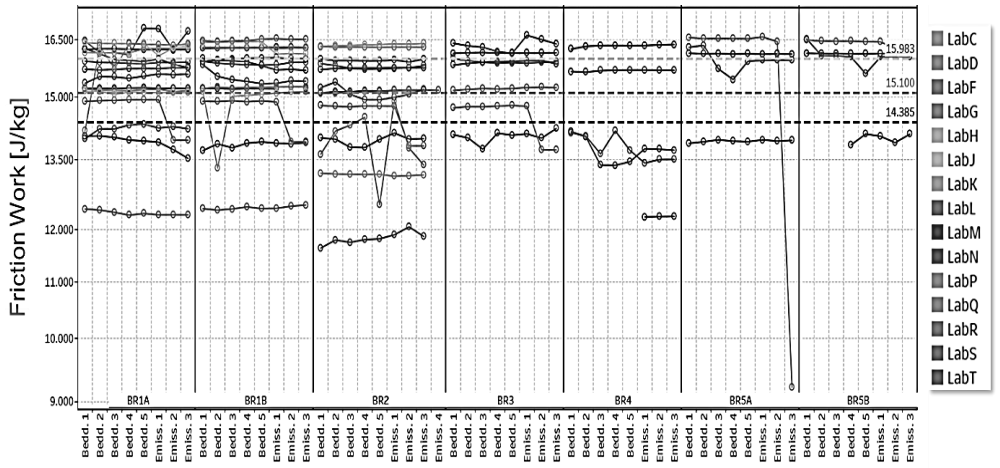

3. Temperature specifications

41. Specifications for the brake temperature at the beginning of each trip over the WLTP-Brake cycle were provided in the GRPE-81-12 and the TF2 protocol for all brake emissions test sections. More specifically, it was foreseen that Trip #1 of the WLTP-Brake cycle shall commence at ambient temperature (23±5°C). For all subsequent trips, the testing facility shall have waited until the brake reached exactly 40°C. For multiple consecutive emission tests, Trip #1 of the second – and all additional cycles – shall have commenced at 40°C.

42. ILS data revealed some non-compliances; however, the vast majority of the tests were conducted according to the defined specifications for the initial brake temperature (Table 5). More specifically, some non-compliances with the specification for the initial temperature of Trip #1 were observed. These mostly relate to testing facilities running emission tests #2 and #3 right after the 1st emissions test – 75% of the 221 data points within the specification. Very few non-compliances with the specification for the initial temperature of Trips #2-10 were observed with 95% of the 221 data points being within the specification. Most probably these non-compliances relate to the controls of the dyno that start the cycle at <40.5°C instead of sharp 40°C.

Table 5
High-level statistics of the initial brake temperature from all testing facilities and brakes for standard emission tests. Cells in white indicate compliance with the initial specification. Cells in grey indicate violations of the specification.

Initial Temperature	*Trip #1 [˚C]*	*Trip #2 [˚C]*	*Trip #3 [˚C]*	*Trip #4 [˚C]*	*Trip #5 [˚C]*	*Trip #6 [˚C]*	*Trip #7 [˚C]*	*Trip #8 [˚C]*	*Trip #9 [˚C]*	*Trip #10 [˚C]*
Average (Spec.)	24.8 (20±5)	38.9 (<40)	38.8 (<40)	38.7 (<40)	38.8 (<40)	38.9 (<40)	34.0 (<40)	38.8 (<40)	38.9 (<40)	37.3 (<40)
Minimum Temp.	17.7	27.3	27.3	27.1	27.1	27.1	25.2	27.1	26.2	26.0
5th Percentile	19.4	34.1	33.0	33.4	32.8	33.8	28.7	33.2	34.0	28.8
50th Percentile	22.9	39.7	39.7	39.7	39.7	39.7	33.9	39.7	39.7	39.1

Initial Temperature	*Trip #1 [˚C]*	*Trip #2 [˚C]*	*Trip #3 [˚C]*	*Trip #4 [˚C]*	*Trip #5 [˚C]*	*Trip #6 [˚C]*	*Trip #7 [˚C]*	*Trip #8 [˚C]*	*Trip #9 [˚C]*	*Trip #10 [˚C]*
95th Percentile	32.6	40.4	40.5	40.3	40.4	40.5	39.2	40.5	40.4	40.4
Maximum Temp.	122.1	41.2	41.4	41.2	42.2	42.3	40.5	41.6	41.5	41.9

43. Based on this data, a proposal was submitted for the three individual sections of the brake emissions test:

(a) Cooling adjustment section: Specific provisions related to the brake temperature at the beginning of Trip #10 apply to the cooling adjustment section. The proposal is to set the specification for the initial temperature of Trip #10 of the WLTP-Brake cycle at 40°C. This is to render the cooling adjustment procedure comparable for all testing facilities and brakes. It is proposed to warm the brake to 40°C following a sequence of brake events #1 to #7 of Trip #10 (brake events #190 to #196 when the entire WLTP-Brake cycle is considered). The method has been applied successfully during the ILS.

(b) Bedding section: Specific provisions related to the brake temperature at the beginning of each WLTP-Brake cycle apply during the bedding section. The initial temperature of Trip #1 of the 1st WLTP-Brake cycle has been set at 23±5°C. The testing facility shall not apply soakings between the individual trips of the WLTP-Brake cycle during the bedding procedure to reduce testing time. The ILS did not reveal any significant problem of overheating the brakes with this method. On the other hand, soaking shall apply between the five repetitions of the WLTP-Brake cycle. The subsequent four WLTP-Brake cycles (2nd to 5th) shall commence when the brake temperature reaches 40°C. Finally, a specification for the minimum initial temperature of WLTP-Brake cycles 2-5 has been set at 30°C to avoid running the emissions test at extremely low temperatures.

(c) Emissions measurement section: Specific provisions related to the brake temperature at the beginning of Trip #10 apply to the emissions measurement section. The proposal is to leave the specification for the initial temperature of Trip #1 as is; however, adjusted to the 23°C of the incoming cooling air temperature has been submitted (23±5°C). It was also proposed to leave the target for the initial temperature of Trips #2-10 at 40°C taking into account that testing of all brakes shall be carried out assuming the full-friction protocol. Finally, a specification for the minimum initial temperature of Trips #2-10 has been set at 30°C to avoid running the emissions measurement section at extremely low temperatures.

C. Cooling air conditioning

44. The conditioned cooling air a) provides clean and continuous cooling to the brake assembly and b) transports the aerosol from the enclosure into the sampling tunnel and the PM/PN sampling probes. The cooling air needs to be: (i) at a constant flow to ensure repeatable and reproducible testing conditions; (ii) under stable conditions for temperature and humidity, and (iii) clean with low background particle number concentration values.

1. Cooling air flow measurement

45. The TF2 did not provide specific requirements for the position of the flow/speed measurement location relative to the enclosure and the sampling plane(s). It was only recommended to measure either upstream of the enclosure or downstream of the sampling point. When measuring the flow/speed upstream of the enclosure, it was recommended to locate the flow element at the centre of the duct at least 8 hydraulic diameters downstream and at least 2 hydraulic diameters upstream of any flow disturbance. When measuring the flow/speed downstream of the sampling point, it was recommended to locate the flow element at the centre of the duct at least 8 hydraulic diameters downstream and at least 2 hydraulic diameters upstream of any flow disturbance. Volume flow was requested to be constant throughout the entire brake emissions test.

46. During the ILS, eight testing facilities measured cooling air speed, while eight testing facilities measured the cooling air flow rate. Five testing facilities measured the cooling air speed/flow only upstream of the enclosure. Six testing facilities measured the cooling air speed/flow only downstream of the enclosure. Finally, five testing facilities measured the cooling air speed/flow both upstream and downstream of the enclosure. Certain problems were identified when measuring the cooling air speed/flow upstream of the enclosure. These relate mostly to inaccurate measurements due to changes in the duct dimensions which do not allow for calculating the flow accurately at the sampling plane. Additionally, a measurement upstream of the enclosure cannot identify possible leaks in or downstream of the enclosure which may compromise the emissions measurement.

47. Since the volume flow is one of the most critical parameters for correctly calculating PM and PN emissions, it was agreed to harmonize its measurement to the extent possible. For this reason, it was agreed to allow only measuring the air flow rate (and not the air speed). Additionally, the measurement shall be performed downstream of the sampling plane. More specifically, it was mandated to locate the flow measurement element at the centre of the duct at least five inner diameters downstream and two inner diameters upstream of any flow disturbance. Since volumetric flow can change with the actual temperature and pressure, it was agreed that the air flow shall be also normalized and reported to a common reference condition (273.15 K and 101.325 kPa). Certain specifications and accuracy requirements for the flow measurement instrumentation were proposed following UN GTR No. 15 and the recommendations of the TF2 and the PMP members. Finally, distancing specifications were proposed for air flow rate measurement elements that use air filters to protect the device from contamination. Some stakeholders commented that the usage of these filters may affect the air flow measurement accuracy; however, TF2 experts pointed out that following the specifications defined by the manufacturer would eliminate such a possibility.

48. Figure 14 illustrates the range of the cooling air flow rates applied by the testing facilities when testing the different brakes during the ILS. A wide range of flow rates have been applied by the different labs; however, most of the tests were carried out with flow rates between 500-1000 m^3/h. Overall, it was observed that there is no need for very high flow rates variations to test the different brakes. The entire range of the applied tunnel air flow rates corresponded to air speeds of <5 km/h to almost 45 km/h. Very low speeds have been linked to high background concentrations (Lab Q) and high losses, particularly of bigger particles (Lab C). Therefore, it was agreed to limit the lower allowed tunnel operational air flow rate to 100 m^3/h and at the same time not allow for duct inner diameters higher than 225 mm. Specifications for the maximum operational air flow rate capacity relative to the minimum operational air flow rate were also introduced to ensure that the testing facility will have the capacity to correctly test different brakes and reproduce their temperature regimes. More specifically, the maximum operational flow shall be at least 5 times the minimum operational flow and at least 1000 m^3/h greater than the minimum operational flow.

Figure 14
Cooling air flow rate and air speed range applied by the testing facilities during the ILS.

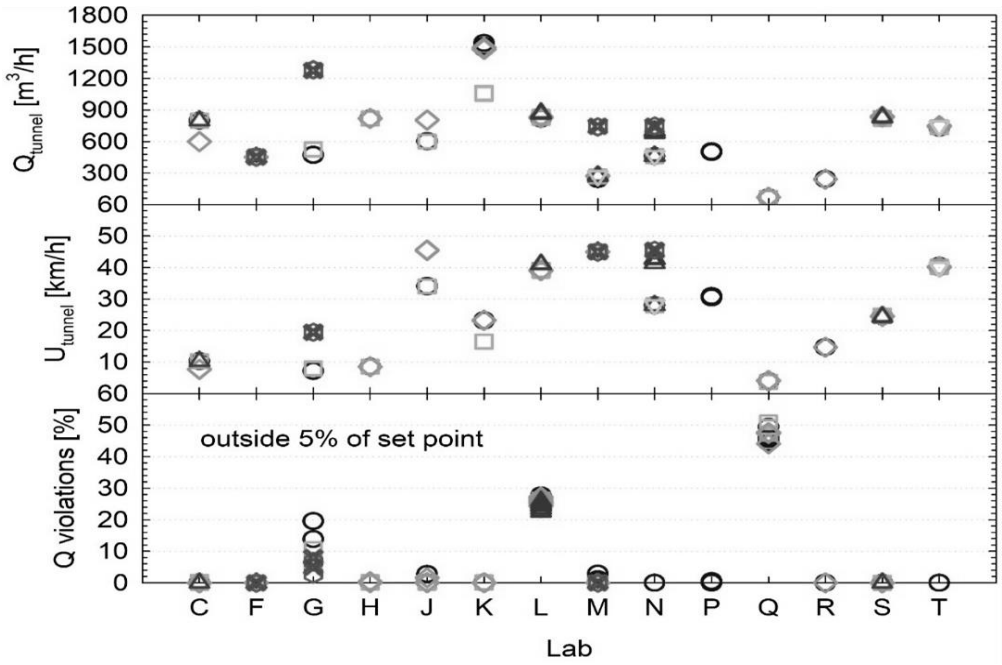

Figure 15
Percent violations of the cooling air flow recorded by the different testing facilities during the ILS.

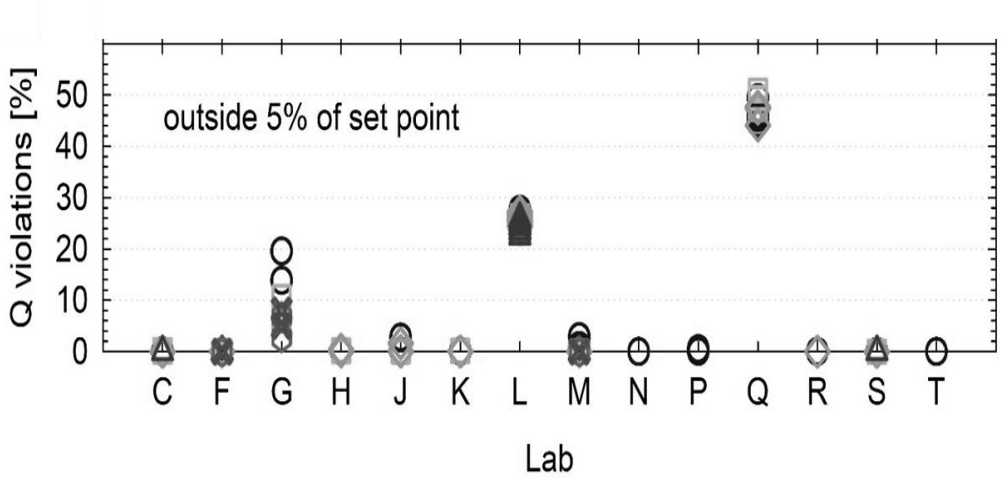

49. Figure 15 illustrates the percent violations of the cooling air flow recorded by the different testing facilities during the ILS. The percent violations were calculated using the 1 Hz data from the Time-Based files. Each second that the air flow rate was outside ±5% of the nominal value was considered a violation. A 10% violation means that the testing facility was outside the ±5% of the nominal flow for 10% of the cycle duration. Ten testing facilities reported violations of less than 1.0% with most of the cases being at 0.0% (56%). Only three testing facilities reported violations higher than the maximum allowed.

50. Table 6 provides some theoretical examples of how the air flow rate fluctuation might influence the isokinetic sampling ratio based on the ILS data. Different scenarios are given by applying a wide range of tunnel (275-800 m^3/h) and sampling (10-65 l/min) flow rates.

Table 6
Theoretical examples of how air flow rate fluctuation influences the isokinetic sampling ratio. White cells indicate actual measurements. Grey cells indicate a theoretical scenario.

Lab	*Tunnel Flow (m^3/h)*	*Deviation from nominal (%)*	*PM Sample Flow (lpm)*	*Isokinetic Ratio (-)*
Lab-C	800.0	-	65.0	1.11
Lab-C	760.0	-5%	65.0	1.17
Lab-C	720.0	-10%	65.0	1.24
Lab-C	840.0	+5%	65.0	1.06
Lab-C	880.0	+10%	65.0	1.01
Lab-G	474.0	-	33.4	1.05
Lab-G	450.3	-5%	33.4	1.11
Lab-G	426.6	-10%	33.4	1.17
Lab-G	497.7	+5%	33.4	1.00
Lab-G	521.4	+10%	33.4	0.96
Lab-M	275.0	-	10.0	1.09
Lab-M	261.3	-5%	10.0	1.15
Lab-M	247.5	-10%	10.0	1.21
Lab-M	288.8	+5%	10.0	1.04
Lab-M	302.5	+10%	10.0	0.99

51. It is demonstrated that potential issues might occur at all levels of tunnel flows with average deviations higher than 5% of the nominal. As an example, Lab C might violate the target isokinetic ratio of 0.9-1.15 with only a 5% deviation from the nominal air flow rate. Labs G and M would need slightly higher average deviations to violate the target isokinetic ratio. In any case, there is a need to restrict tunnel flow violations both at average and instantaneous flow levels. The performance of most testing facilities during the ILS showed that this combination is possible.

52. Based on the data presented in the last two paragraphs, it was agreed that the average measured cooling air flow rate shall be within ±5 percent of the nominal value during the entire emissions test. Specifications for the instantaneous cooling air flow rate have also been introduced to minimize the fluctuation of the isokinetic ratio.

2. Cooling air flow conditioning

53. According to the TF2 specifications, the incoming cooling air temperature and relative humidity shall be set to 20°C and 50%, respectively. Emission tests during the ILS were considered successful when the average temperature of the incoming cooling air was within ±2°C with respect to the target value (i.e., 20±2°C) and when the average relative humidity was within ±5% of the target value (i.e., 50±5%). Provisions for the instantaneous temperature and relative humidity were also defined.

54. Figure 16 illustrates the percent violations of the average temperature recorded by the different testing facilities during the ILS. Additionally, the minimum and maximum instantaneous temperature values are plotted.

Figure 16

Percent violations of the average temperature recorded by the different testing facilities during the ILS. Minimum and maximum instantaneous temperature values are also plotted.

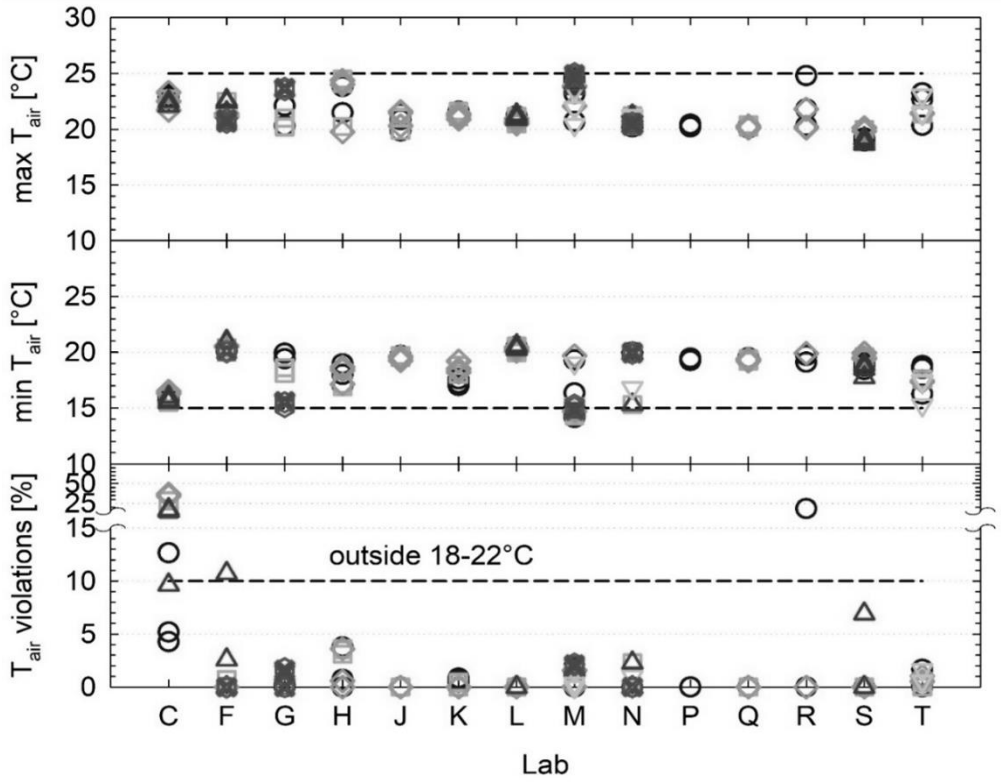

55. The percent violations were calculated using the 1 Hz data from the Time-Based files. Each second that the air flow was outside ±2°C of the nominal value was considered a violation. A total of seven non-compliances to the target average temperature of 20±2°C were reported in 155 tests (4.5%). It is noteworthy that Lab-D's data are not plotted since the testing facility did not have the capacity to control the cooling air temperature and humidity. Regarding the instantaneous temperature, a total of 20 non-compliances to the target temperature of 20±5°C for no longer than 10% of the WLTP-Brake cycle were reported in 155 tests (12.9%).

56. Figure 17 illustrates the percent violations of the average relative humidity recorded by the different testing facilities during the ILS. Additionally, the minimum and maximum instantaneous relative humidity values are plotted. The percent violations were calculated using the 1 Hz data from the Time-Based files. Each second that the air flow humidity was outside ±5% of the nominal value was considered a violation. A total of nine non-compliances to the target average relative humidity of 50±5% were reported in 155 tests (5.8%). 118 tests were completed with average relative humidity deviations lower than 1% (76.1%). Lab-D's data are not plotted since the testing facility did not have the capacity to control the cooling air temperature and humidity. Regarding the instantaneous relative humidity, a total of 30 non-compliances to the target relative humidity of 50±5% for no longer than 10% of the WLTP-Brake cycle were reported in 155 tests (19.4%). 66 tests were completed with instantaneous relative humidity deviations lower than 1% (42.6%). It is noteworthy that Lab-C reported an issue with the climatic controls that resulted in 12 non-compliances.

Figure 17

Percent violations of the average relative humidity recorded by the different testing facilities during the ILS. Minimum and maximum instantaneous relative humidity values are also plotted.

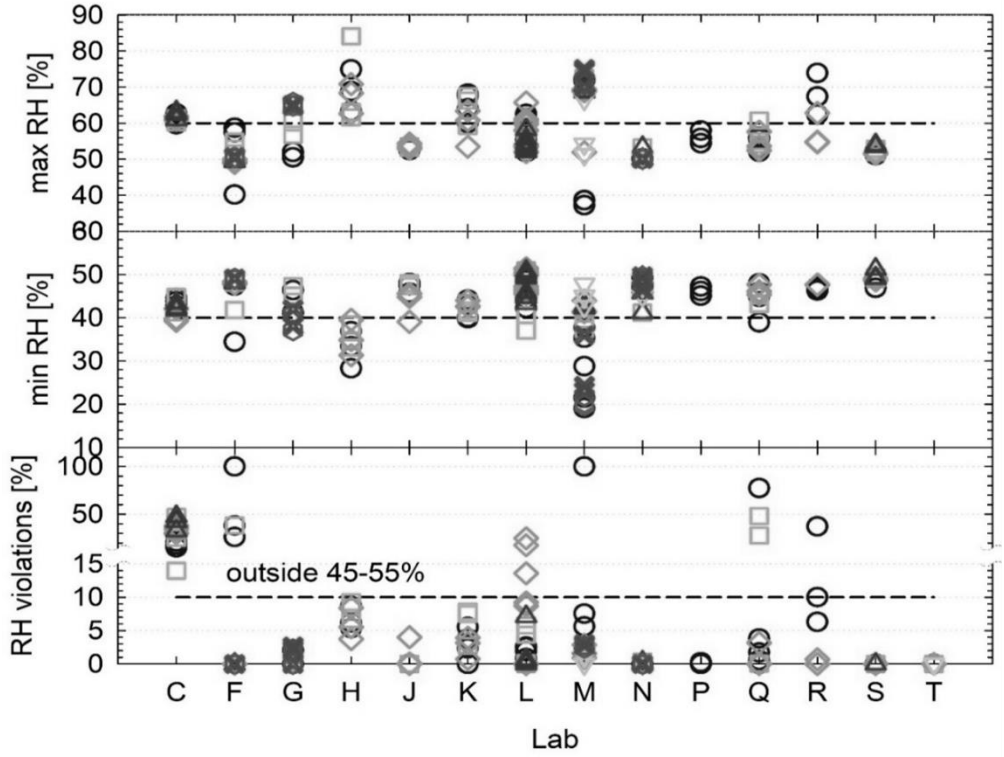

57. Based on the data presented, it was agreed to maintain the same requirements for the cooling air temperature both at average and instantaneous values levels (20±2°C and 20±5°C for no longer than 10% of the duration of the test). However, it was requested by some stakeholders to adjust the cooling air flow temperature to 23°C instead of 20°C to match the vehicle testing conditions defined in the UN GTR 15. Therefore, the agreed values are 23±2°C for the average temperature and 23±5°C for no longer than 10% of the duration of the test for the instantaneous temperature. Regarding the cooling air relative humidity, it was agreed to maintain the same requirement for the average value (50±5%) and adjust the instantaneous value at 50±30% for no longer than 10% of the duration of the test. In addition to the specifications defined for the relative humidity, the testing facility shall ensure that the average absolute humidity of the cooling air is kept between 6 and 11 gH2O/kg dry air throughout the entire brake emissions test.

3. Cooling air cleaning

58. The cooling air entering the test system shall pass through a medium capable of reducing particles of the most penetrating particle size in the filter material by at least 99.95% or through a filter of at least class H13 as specified in EN 1822. Any other type of filter applied to remove volatile organic species (charcoal, activated carbon, or equivalent) shall be installed upstream of the H13 (or equivalent) filter.

59. During the ILS, it was requested to define the background concentration at two levels. The first level concerned the system background upon installation (or when there are indications of system malfunction) and was carried out without the brake assembly or fixture. The second level concerned regular background checks before and after the execution of a brake emissions test at the air flow setting of the emissions test. 10 testing facilities out of 16 completed the system background check successfully (63%). On the other hand, 173 regular background checks were reported in 222 completed emission tests (78%).

60. The background concentration is defined on a PN basis (the symbol # is used for particles). Background PN concentrations shall be measured in (#/cm^3) and expressed in

(#/km) to reflect the changes in the cooling air flow when testing different brakes. During the ILS, there was no limit for the background concentration; however, it was agreed to define it after the ILS. Figure 18 illustrates the PN concentrations (coloured) and the PN background (grey) reported by the testing facilities with Br1a, Br1b, and Br2 during the ILS. It is observed that background PN concentrations in the tunnel were at least one order of magnitude below the cycle-average tunnel concentrations. However, Labs D, H, and R reported background levels similar to measured emission levels; therefore, PN results from these specific labs are not reliable.

Figure 18
PN (dark) and the PN background (grey) concentrations reported by the testing facilities with Br1a, Br1b, and Br2 during the ILS.

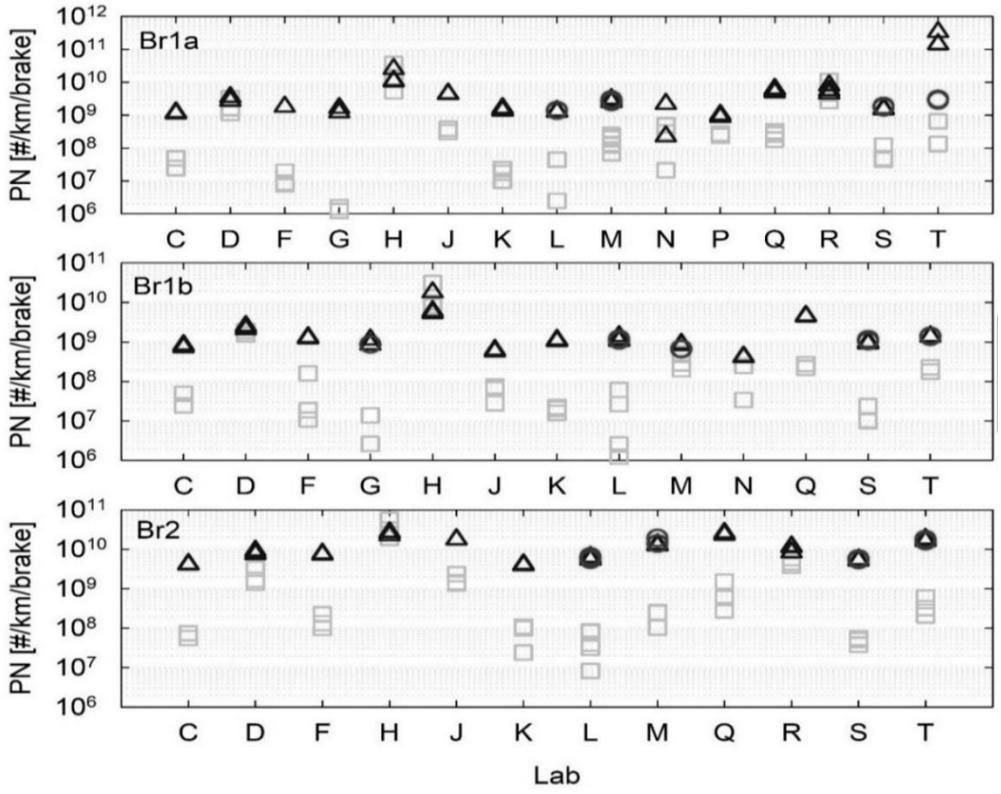

61. Table 7 provides some theoretical examples of how the background concentration might influence the PN concentration measurements based on the ILS data. Different scenarios are given by applying different tunnel flows (250-850 m^3/h). It is demonstrated that potential issues (i.e., background levels >5E+08 #/km) might occur at all levels of tunnel flows when the background concentration is higher than 10 #/cm^3. It is also observed that increasing the tunnel air flow rate results in a higher background in terms of the number of particles per distance driven. As a result, it was agreed that the average background concentration in the tunnel shall not exceed the maximum limit of 20 #/cm^3 for each Total PN (TPN10) and Solid PN (SPN10). The limit of 20 #/cm^3 was decided also taking into account the capabilities of the PN measurement devices. The limit of 20 #/cm^3 applies to the background concentration at both system and test levels. The measurement shall be carried out with nozzles of any diameter since isokinetic sampling and minimization of bigger fine particle losses is relevant only during brake emissions testing and not during the background measurement. Finally, it was decided not to apply background subtraction/correction for reporting actual TPN10 and SPN10 concentrations.

Table 7
Theoretical examples of how background concentration influences the PN concentration measurements. White cells indicate low and thus acceptable background levels. Grey cells indicate high and thus non-acceptable background levels.

Lab	*Tunnel Flow (m^3/h)*	*BG Concentration ($\#/cm^3$)*	*Background Levels (#/km)*
Lab-X	250	10	5.7E+07
Lab-X	250	50	2.9E+08
Lab-X	250	100	5.7E+08
Lab-Y	550	10	1.3E+08
Lab-Y	550	50	6.3E+08
Lab-Y	550	100	1.3E+09
Lab-Z	850	10	1.9E+08
Lab-Z	850	50	9.7E+08
Lab-Z	850	100	1.9E+09

62. Table 8 summarises the requirements for the cooling air's temperature, humidity, and flow defined in the UN GTR.

Table 8
Summary of the cooling air temperature, humidity, and flow requirements as defined in the UN GTR.

Parameter	*Cooling air temperature*	*Cooling air relative humidity*	*Cooling airflow*
Nominal value	23 ºC	50 %	Set value (Q_{set}) per paragraph 10.
Average value: Maximum permissible tolerance	±2 ºC	±5 %	±5 % of Q_{set}
Instantaneous values (1Hz): Maximum permissible tolerance	±5 ºC	±30 %	±5 % of Q_{set}
Instantaneous values (1Hz): Permissible deviation beyond the maximum permissible tolerance	Not defined	Not defined	±10 % of Q_{set}
Instantaneous values (1Hz): Maximum time exceeding the maximum permissible tolerance	10 % of each test section's duration	10 % of each test section's duration	5 % of each test section's duration

D. Cooling adjustment section

63. Testing facilities have been performing emissions measurements on dynamometers with different design characteristics. Until the publication of the GRPE-81-12, there was no commonly accepted method for adjusting the incoming cooling air flow. This resulted in substantial differences in the observed temperature regimes among the testing facilities for the same brake applications. Table 9 summarises the proposed target parameters defined in the GRPE-81-12 to overcome this problem. Seven vehicles were tested over trip #10 of the

WLTP-Brake cycle on a test track to derive the proposed values. More details regarding the initial proposal can be found in [6].

64. The development of the cooling adjustment method in GRPE-81-12 was based on real-world vehicle data tested under the WLTP-Brake cycle. Laboratory data demonstrated that a common air flow would not provide realistic temperature regimes for all brake applications. This is why TF1 proposed and adopted the different Nominal Wheel Load to Disc Mass ($WL_{n\text{-}f}$/DM) groups (following the industry's suggestion) and elaborated on the target temperatures for every group always allowing for some flexibility to account for different designs, properties, and uncertainty. The GRPE-81-12 adopted a similar approach which was further elaborated and refined to include more experimental data submitted at the TF and PMP level. Any simplification step in future versions of the UN GTR will need to be tested, verified, and proven robust with experimental data.

Table 9
Default temperature limits for brake discs and brake drums during trip #10 per GRPE-81-12.

Axle *[-]*	*Disc type* *[-]*	*Average Temperature* *[˚C]*	*Average Top 5% IBT* *[˚C]*	*Average Top 5% FBT* *[˚C]*	*Maximum Temperature* *[˚C]*
Front	Vented	85	85	135	170
Rear	Vented	65	65	95	115
Rear	Solid	80	85	135	180
Tolerance		±10	±15	±25	±25

65. Figure 19 shows a clear tendency for reduced average brake temperatures with reduced $WL_{n\text{-}f}$/DM ratios. Similar trends were observed for the other three parameters included in the GRPE-81-12 (i.e., average top 5% initial brake temperature, average top 5% final brake temperature, and maximum brake temperature). These trends were observed and demonstrated on brake dynamometer tests and not on proving ground or on-road vehicle tests. It was concluded that the proposed PMP protocol seemed not applicable as it was for the entire range of brake applications and a separation in the target temperatures based on the $WL_{n\text{-}f}$/DM ratio was required.

Figure 19
Average brake temperature during Trip #10 of the WLTP-Brake cycle from different brakes as a function of the WL_{n-f}/DM ratio. Data from six labs are plotted. Vehicle data (grey circles) show the proving ground values.

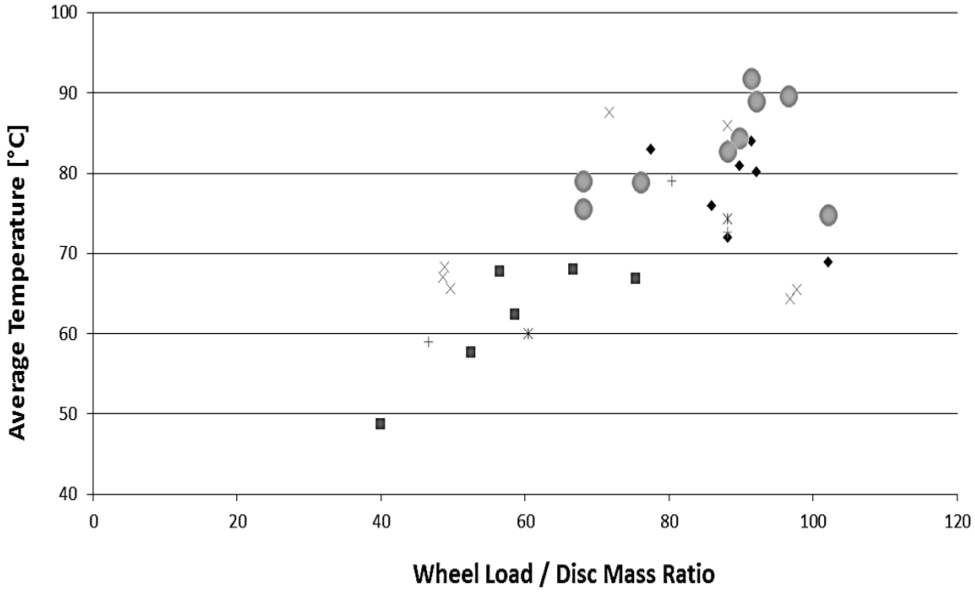

66. Three possible solutions were discussed to overcome the problem. The first was to keep the method as in GRPE-81-12 with some minor modifications that included: (i) removing the peak temperature as it seemed to be the less reproducible and (ii) further relaxing existing threshold values for the other three parameters. This option was rejected because it would allow the testing facilities to run brake emissions tests cooler to much cooler for a very broad range of brake applications. As a result, this would compromise PM and PN measurements and allow for significant variations among labs. The second option was to change the philosophy by: (i) setting a minimum acceptable average temperature to ensure that labs do not run very cool and (ii) defining Initial Brake Temperature (IBT) and Final Brake Temperature (FBT) based on vehicle data similarly to the original proposal. This option was rejected because keeping the peak temperature value would not ensure the proper emissions characterization of low-quality brakes. The third – and selected option – was to keep the same philosophy but define the threshold values for the parameters based on four different WL_{n-f}/DM bins. Additionally, it was suggested to remove the peak temperature from the list of target parameters.

67. As a result, four different target temperatures were defined for IBT and FBT, respectively, representing different WL_{n-f}/DM classes. Target values were adjusted based on the available vehicle and dyno data. Additionally, lower threshold values for the average temperature were defined to ensure that the testing facilities would not run tests much cooler. Peak temperature was removed from the target parameters since it is not measured in a repeatable and reproducible manner. Table 10 summarises the proposal which was applied during the ILS and Figure 20 shows the data that supported the formulation of this proposal.

Table 10
Temperature metrics and limits for brakes during Trip #10 of the WLTP-Brake cycle.

WL_{n-f}/DM	*Average Temperature [˚C]*	*Average 5% IBT [˚C]*	*Average 5% FBT [˚C]*
≤ 45	> 50 °C	55 ± 15 °C	85 ± 25 °C
>45 & ≤ 65	> 55 °C	65 ± 15 °C	105 ± 25 °C
>65 & ≤ 85	> 60 °C	75 ± 15 °C	120 ± 25 °C
> 85	> 65 °C	85 ± 15 °C	140 ± 25 °C

68. According to the proposed method which was applied in the ILS, in order to determine the appropriate cooling air flow for a given brake the testing facility shall first classify the tested brake into a $WL_{n\text{-}f}$/DM Group. The "Nominal Wheel Load" is defined in the UN GTR based on the vehicle characteristics both for the M1 and N1 vehicle categories. The "Nominal Wheel Load" differs from the "Actual Wheel Load" which is reduced by 13% and is applied during emissions testing. Four different groups have been identified based on the $WL_{n\text{-}f}$/DM ratio: 1st Group: $WL_{n\text{-}f}/DM \leq 45$; 2nd Group: $WL_{n\text{-}f}/DM > 45 \,\&\, \leq 65$; 3rd Group: $WL_{n\text{-}f}/DM > 65 \,\&\, \leq 85$; 4th Group: $WL_{n\text{-}f}/DM > 85$.

69. After having classified the brake to a $WL_{n\text{-}f}$/DM Group, the testing facilities shall run Trip #10 of the WLTP-Brake cycle with new brake parts to obtain the target temperature parameters and compare them to the limits described in Table 10. The following target parameters shall be used as a reference against which the cooling adjustment results shall be compared: (i) Average brake temperature over the entire Trip #10 of the WLTP-Brake Cycle; (ii) Average IBT of events #46, #101, #102, #103, #104, and #106 from Trip #10 of the WLTP-Brake Cycle; and (iii) Average FBT of events #46, #101, #102, #103, #104, and #106 from Trip #10 of the WLTP-Brake Cycle. All three criteria shall be fulfilled for a successful adjustment of the cooling air speed.

Figure 20
Trip #10 temperature parameters from different brakes as a function of the $WL_{n\text{-}f}$/DM ratio. Data from six labs are plotted.

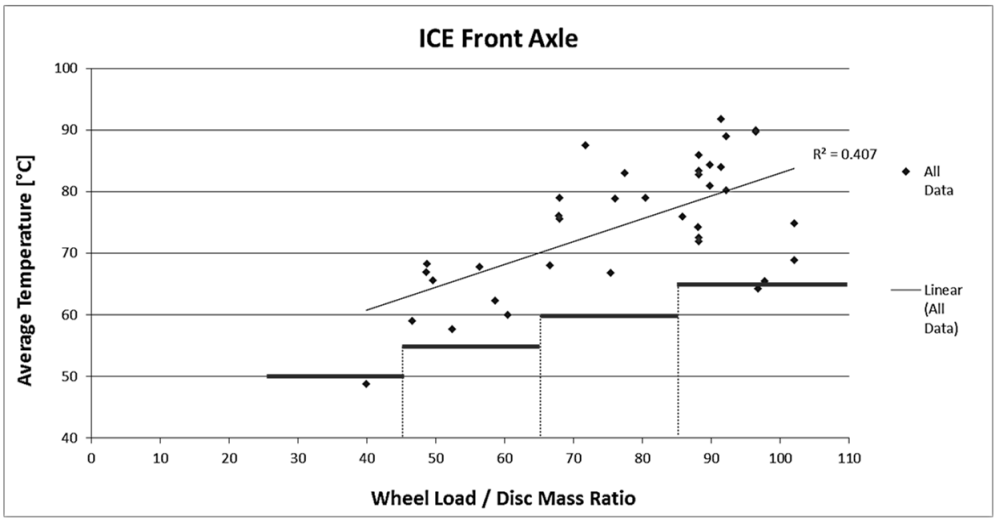

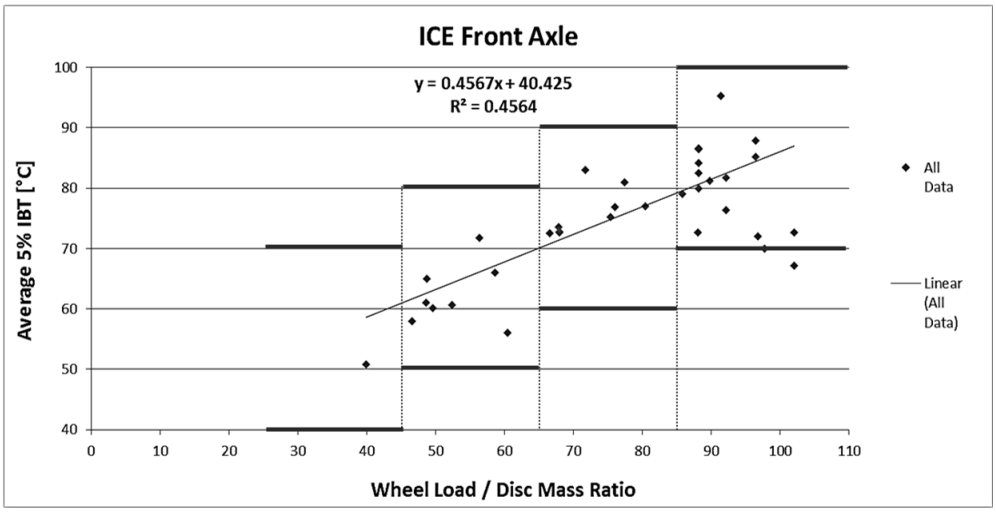

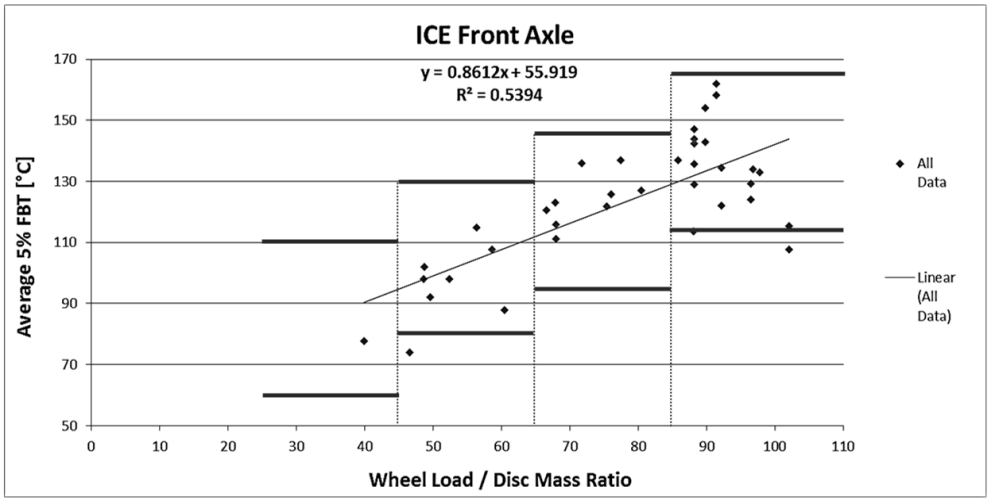

70. ILS data (crosschecked through temperature measurements over Trip #10 of the WLTP-Brake Cycle during emissions measurement – actual cooling adjustment data was not available) showed that the specification for the average Trip #10 temperature was successfully applied (Fig. 21 – upper part). As an example, for the reference brake (Br1a) only 5 "non-compliances" to the minimum target average temperature value were recorded in 93 completed emissions measurement tests. Similarly, 3 "non-compliances" were observed in 40 completed emissions measurement tests with Br2.

71. Regarding the average IBT (Fig. 21 – middle part), the defined specification was also generally successfully followed during the ILS. Some non-compliances were observed for the maximum threshold IBT for the 4th Group ($WL_{n\text{-}f}/DM > 85$) and this has been taken into account and adjusted in the final proposal. As an example, for the reference brake, only 4 "non-compliances" to the maximum target average IBT values were recorded in 108 completed emissions measurement tests. Similarly, only 1 "non-compliance" to the maximum target average IBT value was recorded in 43 completed emissions measurement tests for Br2, whereas for Br5a there were 6 "non-compliances" out of 12 completed measurements.

72. Finally, regarding average FBT (Fig. 21 – bottom part), again the defined specification was also generally successfully followed during the ILS. Some non-compliances were observed for the maximum threshold FBT for the 4th Group ($WL_{n\text{-}f}/DM > 85$) and this has been taken into account in the final proposal. As an example, for the reference brake, only 2 "non-compliances" to the maximum target average temperature value were recorded in 108 completed emissions measurement tests, whereas for Br5a there were 8 "non-compliances" out of 12 completed measurements. Zero "non-compliances" with the target values were observed for Br2 and Br3.

Figure 21

Trip #10 temperature parameters from the different brakes tested during the ILS as a function of the $WL_{n\text{-}f}$/DM ratio.

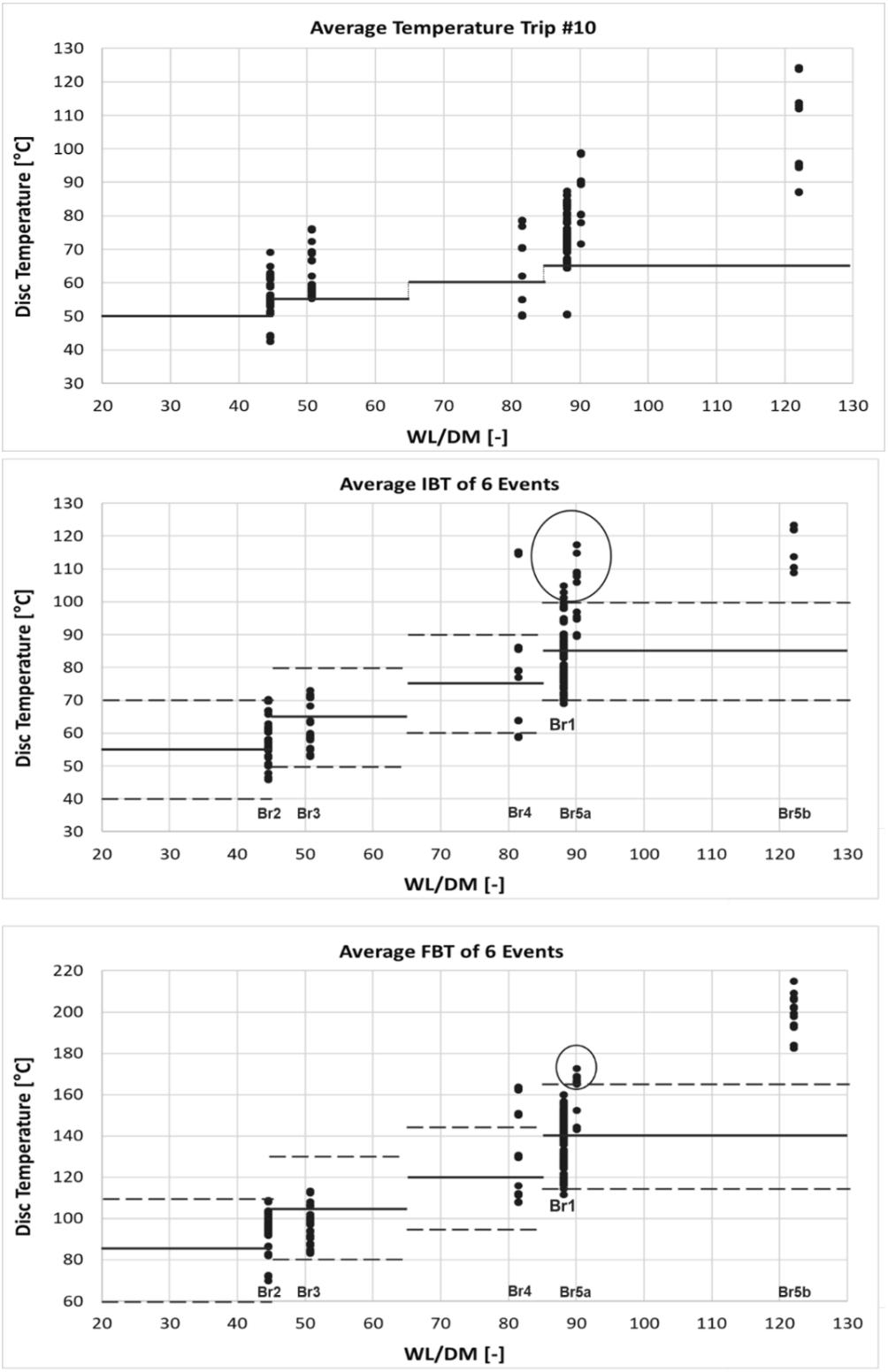

73. After performing the analysis of the ILS results, the TF2 decided to resolve the problems described previously by adjusting the target average IBT and FBT. As a result, it has been proposed to increase the average target IBT and FBT by 5°C and further relax the maximum allowed deviations by 10°C. This would allow for having the same minimum allowed IBT and FBT, while it would be possible to run tests slightly hotter. An additional adjustment to account for the increase of the cooling air flow temperature from 20°C to 23°C

was also performed by increasing the average target IBT and FBT by another 5°C. This increase is very well supported by data published in [7]. Table 11 summarises the final proposal for the target temperatures submitted in the UN GTR.

Table 11
Temperature metrics and limits for brakes during Trip #10 of the WLTP-Brake cycle as given in the UN GTR.

$WL_{n\text{-}f}$/DM	*Average Temperature [˚C]*	*Average 5% IBT [˚C]*	*Average 5% FBT [˚C]*
≤ 45	≥ 50 °C	65 ± 25 °C	95 ± 35 °C
>45 & ≤ 65	≥ 55 °C	75 ± 25 °C	115 ± 35 °C
>65 & ≤ 85	≥ 60 °C	85 ± 25 °C	130 ± 35 °C
> 85	≥ 65 °C	95 ± 25 °C	150 ± 35 °C

74. ILS data demonstrated that NAO and ECE pads have a similar temperature effect on Br1 (Br1a vs. Br1b). More specifically, the average brake temperature over Trip #10 of the WLTP-Brake cycle was 72.4°C and 76.1°C for Br1a and Br1b, respectively. The average IBT was 82.0°C and 84.8°C for Br1a and Br1b, respectively. Finally, the average FBT was 136.8°C and 136.5°C for Br1a and Br1b, respectively. Therefore, there seems not to be a need for introducing specific provisions for different pad materials taking also into account the flexibility of the method and the proposed relatively wide threshold temperature values for IBT and FBT.

75. The development of the cooling air adjustment method relied mainly on data from front conventional brake systems (Vented Gray Cast Iron - GCI). It was recommended to apply this method also to other types of available discs in the market (e.g., Solid Gray Cast Iron, Coated Discs (CD), Carbon Ceramic Discs (CCD), etc.). In fact, the method development took into account some data points also with other brake disc materials. Figure 22 shows the data that supported the formulation of this proposal (Figure 20); however, highlighting the different types of discs tested and adjusting the lower and higher temperature threshold values to the final proposal. Some stakeholders expressed reservations regarding the cooling adjustment of coated discs, carbon ceramic discs, and light-material discs (e.g., aluminium discs). Indeed, it has been demonstrated that particularly FBT can be lower with these discs compared to conventional cast iron discs [8]. For this reason, the PMP IWG considered a relaxation of the target temperatures for carbon-ceramic disc brakes with the first amendment. More specifically, for these brakes the default temperature metrics apply; however, the ABT temperature metrics are lowered by 15 °C and the tolerances to the low end of the temperature regime for the IBT and FBT are further relaxed by 15 °C. Target values for these types of discs might be revised in the next amendment of the UN GTR when more data become available.

76. The cooling adjustment method relies on testing the front axle brake following the described protocol. It was recommended to perform the cooling adjustment of rear brake systems by applying the cooling air flowrate obtained for the corresponding front brake application (i.e., same vehicle data). This was proposed mainly for harmonization and simplification purposes. At the moment, the PMP does not have enough data to elaborate on corresponding $WL_{n\text{-}f}$/DM classes for rear brakes. If this becomes the case in the future and the PMP identifies a need an amendment to the protocol could be proposed. All testing facilities will first test front brakes; therefore, the cooling flow will be already known and will not lead to an additional testing burden. Taking into account that rear brakes are tested under a much lower load, the temperature differences are not expected to be significant with the application of the front brake flow.

Figure 22

Trip #10 temperature parameters from different brakes as a function of the $WL_{n\text{-}f}$/DM ratio. Threshold temperatures (lines) are according to the UN GTR proposal.

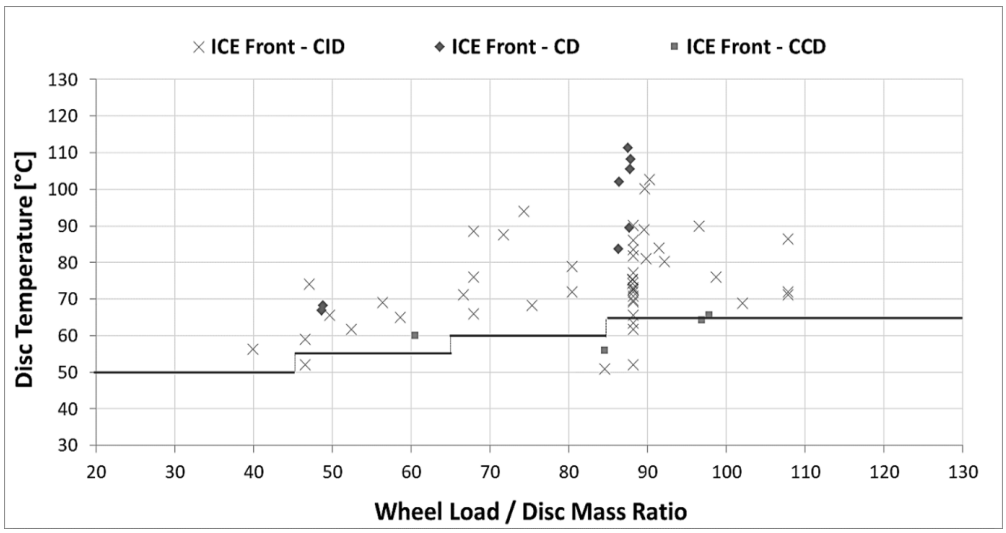

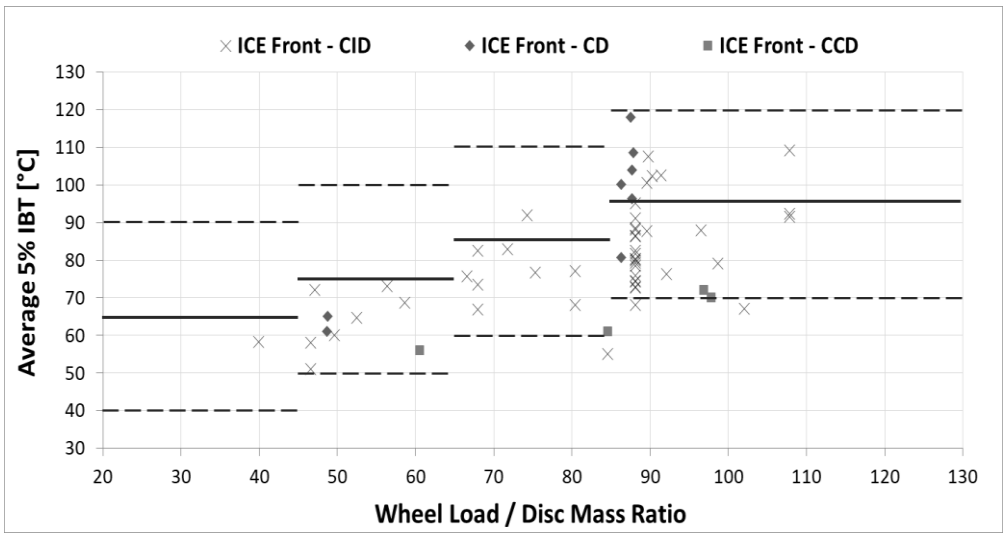

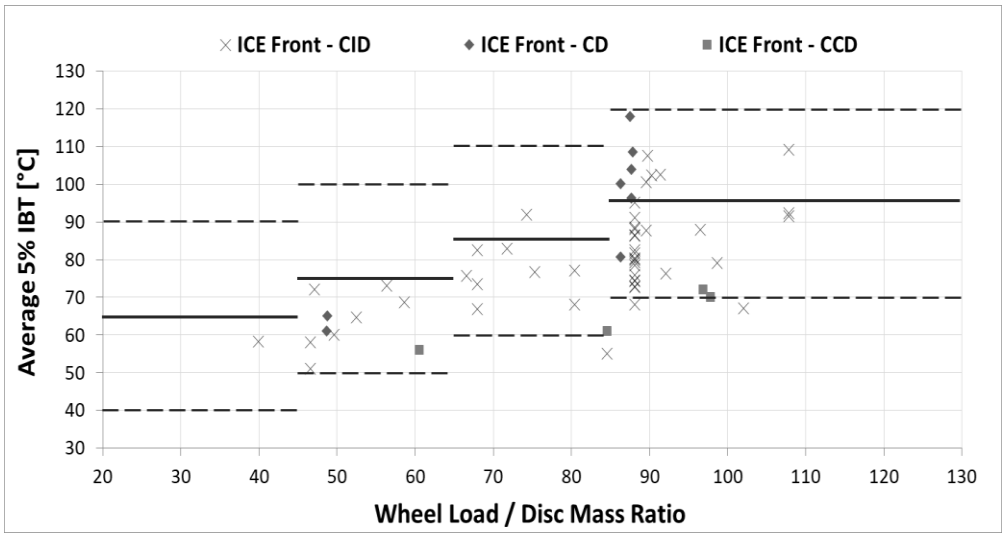

77. The proposed method was tested during the ILS (Br4 – drum brake). The ILS data did not show that the application of the cooling air flow obtained for the corresponding front brake application has a negative effect on the drum brake's emissions or temperatures. Figure 23 shows the target temperatures recorded by the testing facilities during the ILS. Some of

the differences are attributed to the wrong execution of the WLTP-Brake cycle (lower friction work). Target values for rear brakes might be revised when more data become available. Overall, it is shown that when non-valid tests are excluded (i.e., tests with lower friction work) the differences in the target parameters among the facilities are within acceptable thresholds.

Figure 23
Drum temperatures from the different labs during the ILS. Some tests were performed incorrectly by applying a lower total friction work.

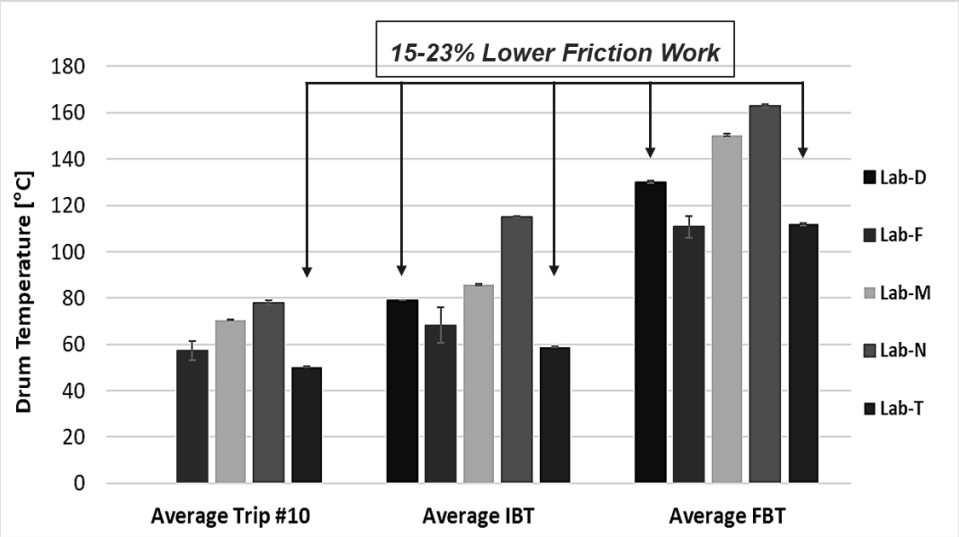

In the second amendment it was added that if multiple cooling airflows meet the requirements for all temperature metrics, the testing facility shall select the cooling airflow that is closest to 950 m^3/h and meets all requirements defined for isokinetic sampling. Although the experimental results of the third interlaboratory study did not show a clear positive impact, it was considered important to narrow the range of flow rates.

E. Bedding section

78. The bedding procedure is important to precondition the brake couple and stabilize its emission behaviour prior to performing an emission measurement test. On one hand, bedding should be long enough to ensure the stabilization of the friction couple's emissions behaviour. On the other hand, there needs to be a compromise in terms of the bedding duration to ensure a reasonable overall testing time.

79. For the ILS, the testing facilities were requested to apply 5 WLTP-Brake cycles for bedding the tested brakes. The testing facilities were instructed not to apply soak times between individual trips. Each one of the 5 WLTP-Brake cycles should have commenced at 40°C (1st repetition shall have commenced at ambient temperature). It was recommended to record PN emissions during bedding but not use the values for emission calculation purposes as concentrations might be artificially increased. Labs were invited to run an additional testing campaign to compare the bedding of brakes with the application 10 Trips #10 of the WLTP-Brake cycle against the default method. Due to the complete absence of relevant data, it was agreed that the number of WLTP-Brake cycles required for the proper bedding of drum brakes would be discussed and agreed upon after the ILS.

1. Disk brakes

80. 174 standard emission WLTP-Brake cycles were completed with all brakes by all testing facilities. This translates to 277 completed bedding WLTP-Brake cycles. Additionally, 16 alternative bedding emission WLTP-Brake cycles were completed with Br1, Br2, and Br3 – these were associated with 60 completed bedding Trips #10. Some testing facilities faced problems completing the bedding procedure successfully (12% of all emissions tests), whereas in most cases the testing facilities realized the problems only after

registering the bedding data. Table 12 summarises the average temperature data for Br1a. Overall, the average temperature of the WLTP-Brake cycle seems to decrease on average by 5-10°C when shifting from bedding to emission cycles. The average brake temperature during the five bedding WLTP-Brake cycles is close to 75°C, while the corresponding temperature during the three emission cycles is close to 68°C. The decrease would have been lower (if any); however, the absence of cooling sections in bedding cycles results in overall higher average temperatures over this section.

Table 12
Average temperature data for Br1a for 13 testing facilities. Data from three labs are not available due to problems with the Time-Based files or missing bedding data (Lab C).

	Bed-1 [C°]	*Bed-2 [C°]*	*Bed-3 [C°]*	*Bed-4 [C°]*	*Bed-5 [C°]*	*Emis-1 [C°]*	*Emis-2 [C°]*	*Emis-3 [C°]*
Lab-F	84.6	76.3	71.1	71.4	72.0	72.4	73.1	73.6
Lab-G	78.5	N/A	N/A	80.1	82.3	71.5	N/A	71.8
Lab-H	75.9	75.2	74.0	73.7	73.5	64.4	64.7	65.4
Lab-J	74.1	75.0	75.2	75.3	75.3	66.8	69.7	67.1
Lab-K	75.2	75.5	75.9	75.8	76.0	68.0	71.8	72.2
Lab-L	73.8	72.8	72.4	71.6	72.4	65.2	65.1	65.3
Lab-M	91.1	89.5	89.1	90.1	88.9	76.1	75.5	75.3
Lab-N	81.4	75.4	74.7	74.7	74.6	67.0	67.1	67.1
Lab-P	69.7	70.1	70.6	71.3	71.0	61.6	61.5	60.9
Lab-Q	79.3	79.5	79.6	79.9	79.9	67.4	66.5	66.2
Lab-R	63.5	62.0	59.5	58.9	64.0	64.3	56.4	63.5
Lab-S	83.9	74.1	72.9	73.6	73.0	69.1	67.2	66.7
Lab-T	75.4	75.3	75.6	75.8	76.0	75.3	75.5	75.3
AVG	**77.4**	**75.1**	**74.2**	**74.8**	**75.3**	**68.4**	**67.8**	**68.5**

81. Table 12 shows that bedding cycles come with higher average temperature fluctuations compared to emission cycles which seem to give more stabilized average temperatures. This is better depicted in Figure 24 where it seems that only Labs R and T did not exhibit a stabilized temperature behaviour for the reference brake during the emissions repetitions. A more careful look into the data of these two testing facilities revealed that they did not apply the suggested bedding protocol successfully. In fact, these two labs cooled down the brake to 40°C in all WLTP-Brake cycle trips; thus, resulting in a less intensively preconditioned brake couple compared to that of the other testing facilities. Due to very few data points, it is not possible to investigate the influence of the different bedding on PM/PN emissions; however, it shall be noted that Lab T was the only facility that reported the emission of volatile particles. Overall, it can be assumed that the application of a 25h test at constantly lower temperatures might influence the emissions behaviour of the brake. Similar conclusions were drawn also for the other tested disc brakes.

Figure 24
Average brake temperature for each WLTP-Brake cycle for all testing facilities (Br1a)

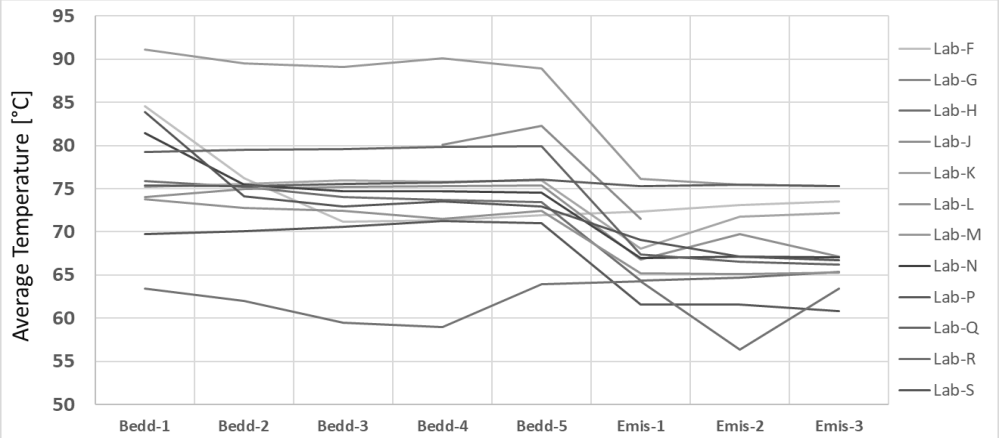

82. The stability of PM and PN measurements over the three repetitions was used to investigate the effectiveness of the proposed bedding protocol (Table 13).

Table 13
PM10 emissions per brake for the reference brake. Data from three repetitions are given. The variability of the measurement for each testing facility is also given.

	Emissions-1 [mg/km]]	*Emissions-2 [mg/km]]*	*Emissions-3 [mg/km]]*	*Variability [%]*
Lab-F	7.2	7.2	7.6	3.1
Lab-G	6.5	6.3	6.2	2.4
Lab-H	1.7	3.5	4.1	40.3
Lab-J	6.1	5.9	5.7	3.4
Lab-K	2.7	2.8	2.8	2.1
Lab-L	5.6	5.7	5.8	1.8
Lab-M	7.3	7.8	7.9	4.2
Lab-N	4.0	4.2	4.1	2.4
Lab-P	N/A	3.0	2.6	10.1
Lab-Q	2.8	2.6	2.4	7.7
Lab-S	5.0	4.6	4.7	4.4
Lab-T	5.9	6.6	6.7	6.8
AVG	**5.0**	**5.0**	**5.1**	**0.7**

83. Table 13 shows that PM10 emission levels measured with Br1a over the three repetitions of the emission tests are very similar. Lab H had several problems with bigger particle losses; therefore, its PM measurements are not reliable. Labs C and R accumulated the three repetitions on one filter; therefore, there is no separate data for the three repetitions of the emissions measurement. It is concluded that the emissions behaviour of the brakes seems to be adequately stabilized with the execution of the default bedding schedule. The same applies to the rest of the disc brakes tested during the ILS (Figure 25). Br5 shows less stability due to much fewer data points compared to the other disc brakes.

Figure 25
Average PM10 emissions of all measurements carried out by the testing facilities for all disc brakes

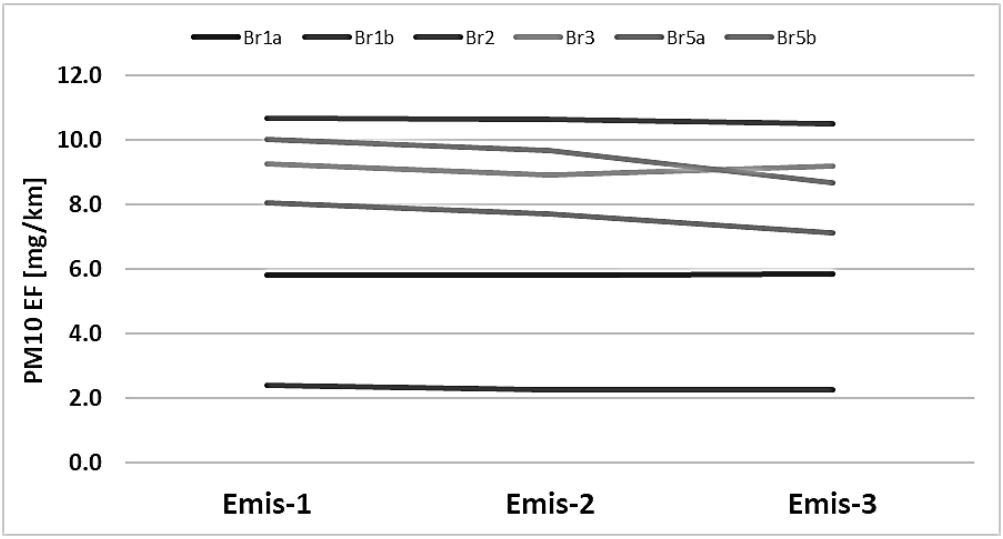

84. Figure 26 shows that TPN10 emission levels with all brakes seem to stabilize after the execution of 5 WLTP-Brake cycles. Only in the case of Br1a, there seems to be a decrease from the first emissions test to the second; however, this average is largely defined from one measurement that included volatile particle formation (Lab T). More specifically, the average TPN10 decreases from 3.6E+10 #/km (1st emissions measurement) to 2.0E+10 #/km (2nd emissions measurement) and 1.6E+10 #/km (3rd emissions measurement), while Lab T's corresponding emissions were 3.4E+11 #/km, 1.4E+11 #/km, and 1.5E+11 #/km, respectively. Overall, the PM and PN emission behaviour of the disc brakes seems to be adequately stabilized with the execution of the default bedding schedule.

Figure 26
Average TPN10 emissions of all measurements carried out by the testing facilities for all disc brakes

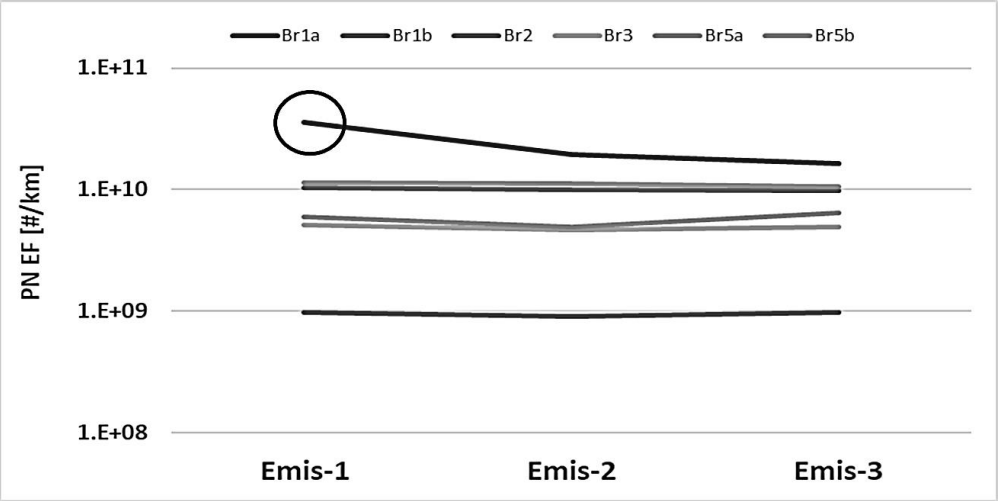

2. Drum brakes

85. Five testing facilities completed 15 standard emission WLTP-Brake cycles with the drum brake. These correspond to 25 bedding WLTP-Brake cycles. Two testing facilities encountered problems completing the bedding procedure successfully. Additionally, Lab D submitted incomplete bedding data in the Time-Based files. Despite the few valid data points, it is observed again that bedding cycles come with higher average temperature fluctuations compared to emission cycles. Figure 27 shows that the average brake temperatures during emission cycles are more stabilized compared to the bedding cycles. Overall, the average

temperature of the WLTP-Brake cycle seems to decrease on average by 15-25°C when shifting from bedding to emission cycles. Table 14 summarises the average temperature data for Br4.

Table 14
Average brake temperature data for Br4 over bedding and emission cycles. Data for 5 testing facilities are summarized

AVG. Temp.	*Bed-1 [C°]*	*Bed-2 [C°]*	*Bed-3 [C°]*	*Bed-4 [C°]*	*Bed-5 [C°]*	*Emis-1 [C°]*	*Emis-2 [C°]*	*Emis-3 [C°]*
Lab-D	55.1	54.8	54.8	55.2	56.3	61.2	61.9	61.8
Lab-F	72.8	73.5	73.4	73.4	73.3	65.6	65.5	65.1
Lab-M	93.7	96.8	88.3	87.6	86.3	71.3	71.1	72.2
Lab-N	77.7	78.1	70.8	61.8	60.4	58.4	52.3	52.1
Lab-T	N/A	N/A	N/A	N/A	N/A	48.4	48.7	48.9
AVG	**74.8**	**75.8**	**71.8**	**69.5**	**69.0**	**61.0**	**59.9**	**60.0**

Figure 27
Average brake temperature for each WLTP-Brake cycle for the drum brake. Lab T did not submit bedding data. Lab D's data indicate incomplete bedding cycles.

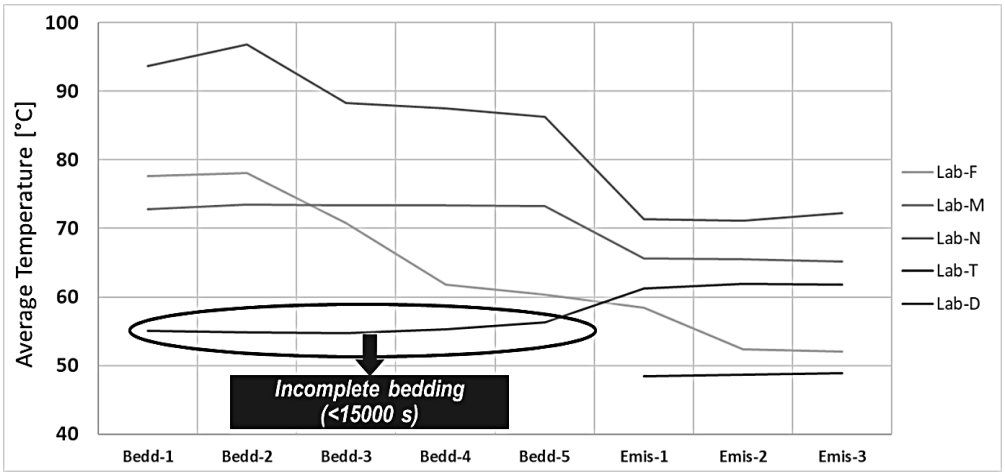

86. The stability of PM and PN measurements over the three repetitions was used to investigate the effectiveness of the proposed bedding protocol for adequately preconditioning the drum brake. Table 15 shows that PM emission levels measured with Br4 over the three repetitions of the emission tests are very similar. Lab D submitted problematic particle emissions data for this brake (explained later in the PM section); therefore, its PM measurements are not reliable. Labs F reported zero-emission levels for all three repetitions; however, data are presented for completeness. It is concluded that the emissions behaviour of the brakes seems to be satisfactorily stabilized with the execution of the default bedding schedule. In any case, PM emissions levels are very low and the observed variabilities are within the method's uncertainty.

Table 15
PM10 and PM2.5 emissions per brake for the drum brake (Br4). Data and their variability from three repetitions are given.

PM10	*Emis.-1 [mg/km]]*	*Emis.-2 [mg/km]]*	*Emis.-3 [mg/km]]*	*Variability [%]*	*PM2.5*	*Emis.-1 [mg/km]]*	*Emis.-2 [mg/km]]*	*Emis.-3 [mg/km]]*	*Variability [%]*
Lab-D	1.4	0.6	0.0	105	Lab-D	N/A	N/A	N/A	N/A
Lab-F	0.0	0.0	0.0	N/A	Lab-F	0.0	0.0	0.0	N/A
Lab-M	0.4	0.3	0.3	17.3	Lab-M	0.2	0.2	0.2	0.0
Lab-N	0.6	0.7	0.7	8.7	Lab-N	0.4	0.4	0.5	13.3
Lab-T	0.5	0.7	0.7	18.2	Lab-T	0.3	0.4	0.4	15.7
AVG	**0.6**	**0.5**	**0.4**	**7.1**	AVG	**0.2**	**0.3**	**0.3**	**10.0**

87. Figure 28 shows that TPN10 seems to stabilize at very low levels after the execution of 5 WLTP-Brake cycles. There is a tendency to further reduce TPN10 between the 7th and the 8th WLTP-Brake cycle repetition but is not confirmed for all testing facilities. Moreover, the emission levels are very low; therefore, it is not easy to draw solid conclusions. Lab F's measurements correspond to emission levels much lower than the background; therefore, are not considered reliable.

Figure 28
Average TPN10 emissions of all measurements carried out by the four testing facilities with the drum brake. Lab D did not submit PN measurements.

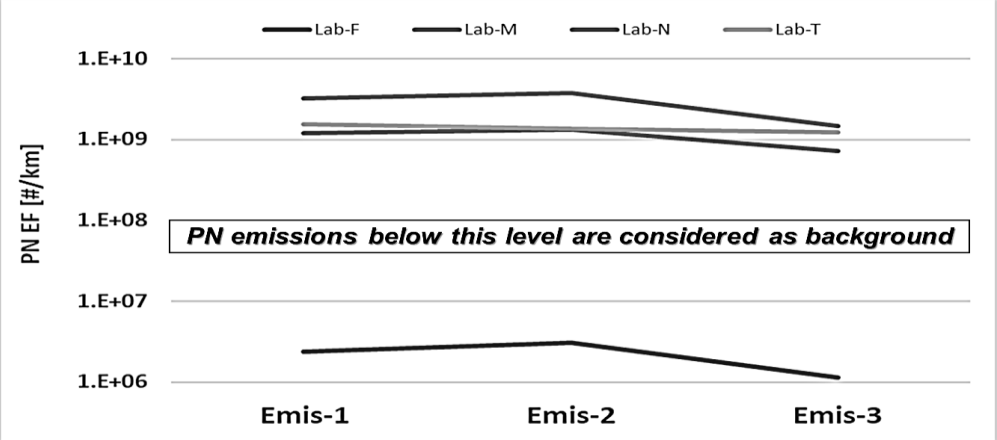

88. Overall, the PM and PN emission behaviour of the drum brake seems to be adequately stabilized with the execution of the default bedding schedule. However, due to very few data points, it is not possible to reach a solid conclusion and further investigations might help to further improve the procedure in the future always keeping in mind practical aspects. Some stakeholders suggested carrying out the drum bedding by applying a higher payload. However, imposing an excessive load on rear brakes can be questionable. Brake force distribution for M1 vehicles is nominally 70:30 and for N1 vehicles is 60:40 or similar. So, using a two- or three-times higher front brake load on a rear brake can change the friction behaviour during bedding and emission particle properties in the subsequent test cycles.

3. Alternative bedding

89. Some stakeholders proposed investigating the possibility of applying a different protocol for preconditioning the brakes. For this reason, it was suggested to run some additional tests to compare the bedding of brakes with the application of 10 Trips #10 of the WLTP-Brake cycle against the default method. Table 16 summarizes the main differences

between the two “protocols”. It is observed that the default method lasts 33% longer than the alternative method but also ensures 33% higher energy dissipation during the preconditioning of the brake.

Table 16
Main differences between the default and alternative bedding protocols. Duration, braking energy, number of events, and average deceleration are examined.

	Default Duration [h]	*Braking Energy [Wh]*	*Brake events number [#]*	*Average deceleration [m/s2]*
Default (5 x WLTP-Brake)	22.0	168.9	1515	0.97
Alternative (10 x Trip #10)	14.6	113.4	1140	0.93
Difference [%]	33%	33%	25%	4%

90. During the ILS, 3 testing facilities performed alternative bedding tests with several brakes (Br1, Br2, Br3). In principle, all bedding cycles were executed successfully. Labs L and N completed also the emission tests without problems. Emissions data from Lab B are not considered valid in the analysis following a request of the testing facility. It was discussed previously, that the default bedding method results in stabilized average temperature over the emission tests. A similar trend is observed with the alternative method. The average temperature of each WLTP-Brake cycle during emissions tests seems to be stable after the execution of the alternative bedding procedure – an exception is recorded with Lab N when testing Br3. Despite the few data points, the examination of the average temperature seems not to reveal inadequate preconditioning with the application of the alternative method.

91. The stability of PM and PN measurements over the three repetitions was used to investigate the effectiveness of the two bedding protocols. Table 17 shows that PM measurements with the alternative bedding method come with generally higher variability compared to the default method. Another observation is that the PM emission levels do not seem to be significantly affected by the bedding method except for tests with Br3. The alternative bedding method results in much lower PM10 emissions (4.7 mg/km vs. 6.9 mg/km). There is no obvious explanation for this phenomenon but could be due to the differences noticed in temperatures, as discussed previously. Overall, the emission behaviour seems to be more stabilized when the default method is applied; however, there are only very few data points to reach a safe conclusion.

Table 17
PM10 emissions in mg/km per brake for the different brakes. Data from three repetitions are given. The variability of the measurement for each brake is also given.

Alternative Bedding PM10	*Emissions-1 [mg/km]*	*Emissions-2 [mg/km]*	*Emissions-3 [mg/km]*	*Average [mg/km]*	*Variability [%]*
Lab L - Br1a	6.7	5.7	5.5	6.0	11%
Lab L - Br1b	3.3	3.4	4.3	3.7	15%
Lab L - Br2	9.3	N/A	N/A	9.3	N/A
Lab L - Br3	9.5	9.4	9.2	9.4	2%
Lab N - Br3	5.2	4.6	4.4	4.7	9%

Default Bedding PM10	*Emissions-1 [mg/km]*	*Emissions-2 [mg/km]*	*Emissions-3 [mg/km]*	*Average [mg/km]*	*Variability [%]*
Lab L - Br1a	5.6	5.7	5.8	5.7	2%
Lab L - Br1b	3.4	3.4	3.8	3.5	7%
Lab L - Br2	9.6	9.3	9.6	9.5	2%
Lab L - Br3	8.5	8.6	8.6	8.6	1%
Lab N - Br3	7.6	7.1	6.1	6.9	11%

92. Table 18 shows that TPN10 measurements with the alternative bedding method come with a similar to slightly higher variability compared to the default method. In general, TPN10 emission levels do not seem to be affected by the bedding method – again an exception is observed in Lab N's tests with Br3 that exhibit a difference of an order of magnitude (4.2E+08 #/km vs. 5.2E+09 #/km), in line with the PM results. Overall, it is not possible to reach a sound conclusion about the emission behaviour with the two examined methods due to few data points. Overall, the PM and PN emission behaviour of the brake seems to be better stabilized with the execution of the default bedding schedule. However, due to very few data points, it is not possible to reach a solid conclusion and further investigations might help to further improve the procedure in the future.

Table 18
TPN10 emissions in #/km per brake for the different brakes. Data from three repetitions are given. The variability of the measurement for each brake is also given.

Alternative Bedding TPN10	*Emissions-1 [#/km]*	*Emissions-2 [#/km]*	*Emissions-3 [#/km]*	*Average [#/km]*	*Variability [%]*
Lab L - Br1a	1.3E+09	1.3E+09	1.3E+09	1.3E+09	2%
Lab L - Br1b	1.4E+09	1.2E+09	1.1E+09	1.2E+09	12%
Lab L - Br2	N/A	N/A	N/A	N/A	N/A
Lab L - Br3	3.1E+09	3.1E+09	3.1E+09	3.1E+09	1%
Lab N - Br3	4.3E+08	4.3E+08	4.1E+08	4.2E+08	3%

Default Bedding TPN10	*Emissions-1 [#/km]*	*Emissions-2 [#/km]*	*Emissions-3 [#/km]*	*Average [#/km]*	*Variability [%]*
Lab L - Br1a	1.4E+09	1.4E+09	1.4E+09	1.4E+09	0%
Lab L - Br1b	1.2E+09	1.1E+09	1.1E+09	1.1E+09	6%
Lab L - Br2	5.4E+09	5.7E+09	5.6E+09	5.6E+09	3%
Lab L - Br3	3.0E+09	3.0E+09	3.1E+09	3.1E+09	1%
Lab N - Br3	5.5E+09	5.0E+09	5.1E+09	5.2E+09	4%

F. Emissions measurement section

1. Measurement of PM mass concentration

93. The TF2 defined some high-level minimum specifications as guidelines for the PM mass measurement. The methodology relies on the gravimetrical measurement of PM10 and PM2.5 mass emissions. The TF2 defined minimum specifications regarding: (a) transport and extraction of the aerosol, (b) the PM sampling devices, (c) the sampling media, and (d) the weighing procedure. These are summarized to the following:

94. Transport and Extraction – It was recommended to limit bends to a minimum – and when necessary – design them with a radius greater than 1.5 times the duct/tube diameter. The sampling plane was located at least 5 hydraulic diameters downstream and at least 2 hydraulic diameters upstream of a flow disturbance element according to ISO 9096. Appropriate nozzles to ensure isokinetic sampling for both PM10 and PM2.5 were mandated. Some recommendations for the sampling nozzles according to ISO 9096 were provided. The isokinetic ratio shall have been kept between 0.9 and 1.15. The aspiration angle was restricted to ±15°. The use of flow splitters for PM measurements was discouraged.

95. PM Sampling Devices – Single- or multi-stage PM10 and PM2.5 cyclonic separators followed by gravimetrical filter holders were the primary choice for the collection of the PM10 and PM2.5 samples. Alternatively, single- or multi-stage inertial impactors were used. The separation efficiency specifications described in ISO 23210 and ISO 25597, respectively, were followed. When the testing facilities applied a pre-classifier before the PM collection device it should have a cut-off point ≥11.5 µm to avoid compromising the efficiency of the PM sampling device. The PM sample filter was located as short as possible without exceeding 1 m downstream of the pre-classifier's exit. The sampling flow was constant (i.e., within 5% of the set point throughout the test) not to compromise the associated collection efficiency curve.

96. Sampling media – The PM sampling filters complied with EN12341 regarding the following minimum requirements: Plane filter efficiency better than 99.5% on a test aerosol with an aerodynamic diameter of 0.3 µm at the maximum sampling flow rate or better than 99.9% on a test aerosol of 0.6 µm aerodynamic particle diameter. This efficiency was certified by the filter supplier. Teflon-coated Glass Fiber filters or PTFE 47 mm Membrane filters with polymer support or an appropriate impaction were used for the PM10 and PM2.5 mass measurements. For inertial impactors, it was recommended to use aluminium foils or polycarbonate film as an impaction substrate. The impaction substrate shall have been properly coated with a thin layer of adhesive collection substrate to eliminate the particle bounce and re-entrainment.

97. Weighing Procedure – The testing facilities were instructed to weigh only the filter – or the impaction substrate – and not any other part of the testing equipment. The filters or substrates were conditioned for a minimum of 24 h and a minimum of 1 h in standard temperature and humidity conditions (22±3°C and 50±10% RH per clause 1 of CFR 1065.190) before and after their use, respectively. The weighing room environmental conditions were regulated to ensure controlled conditions at 22±1°C and 50±5% RH. A charge neutralizer (radioactive or corona-based) was used to discharge the filters and avoid electrostatic forces interference. The weighing balance had a resolution of at least 1 µg and was isolated from vibrations, electrostatic forces, and air streams. PM data was validated using reference filters that matched each sampled filter media shall be selected. The PM filters were weighed twice. When the difference between the first and second measurements was higher than 30 µg the filter was measured for a third time. If the difference between the second and third measurements was higher than 30 µg the measurement was invalid. The value of 30 µg was revised to 10 µg in the first amendment of the GTR No. 24 to further reduce the method's uncertainty.

98. Following the ILS exercise, the TF2 elaborated on the results and used the lessons learnt to further restrict the PM measurement specifications in the final protocol. Figure 29 provides a general overview of the proposed layout. A detailed description of all elements in Figure 29 is provided in the UN GTR text. The positioning and dimensions of the different

elements are provided for illustrative purposes; therefore, exact conformance with the figure is not required. Five paragraphs have been introduced in the UN GTR:

12.1.1. Describes the general elements related to the aerosol extraction and defines the sampling plane;

12.1.2. Discusses the PM sampling including the separation device and the sampling lines. Specifications about the cyclone and the sampling tubes are discussed. Provisions regarding the sampling volumetric flow and the isokinetic ratio are discussed;

12.1.3. Describes the general specifications for the sampling media allowed for PM measurements. The paragraph heavily relies on UN GTR No. 15 – not many changes compared to the initial proposal have been applied;

12.1.4. Describes the general specifications for the weighing procedure. A slightly modified procedure has been introduced. The paragraph discusses also preconditioning as well as filter handling;

12.1.5. Describes the PM emissions calculation method taking into account the type of tested brake (full-friction braking vs. non-friction braking).

Figure 29
Indicative setup of the PM sampling unit

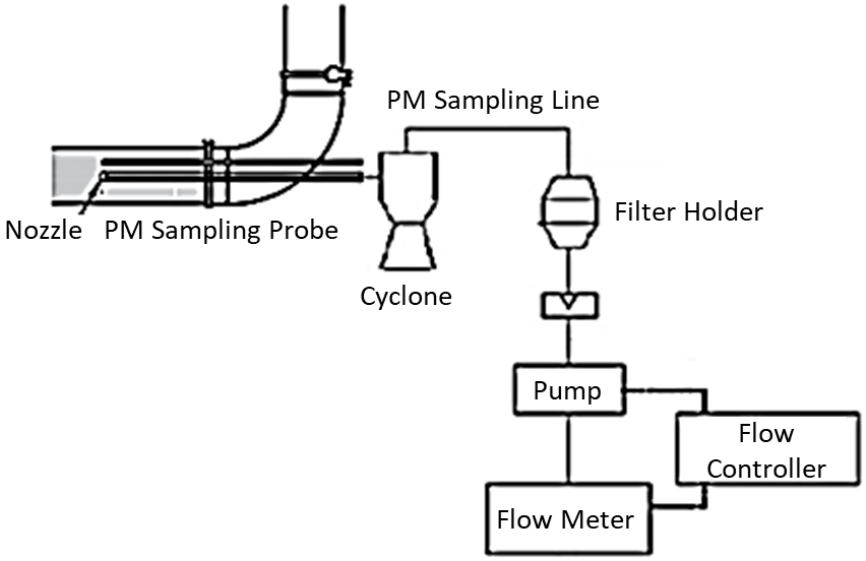

99. Transport and Extraction: The most important potential sources of error and losses during particle transport from the enclosure to the sampling plane as well as during their extraction at the PM sampling nozzle include: (i) anisokinetic sampling, (ii) anisoaxial sampling, (iii) inertial impaction, and (iv) gravitational deposition. The ILS data and results were used to investigate these sources of error. Figure 30 shows that anisokinetic sampling can have a strong effect on both PM fractions. For this reason, it was proposed to define an isokinetic ratio between 0.90-1.15 for the ILS following the requirement defined in ISO9096. Sampling is defined as isokinetic when the air speed in the sampling tunnel and the sampling nozzle is equal. The isokinetic ratio is defined as the ratio of the air speed in the sampling nozzle to the air speed in the sampling tunnel.

Figure 30
Percent error of PM2.5 and PM10 calculated for different values of the isokinetic ratio. Graph taken from AVL as presented in the 28th TF2 Meeting.

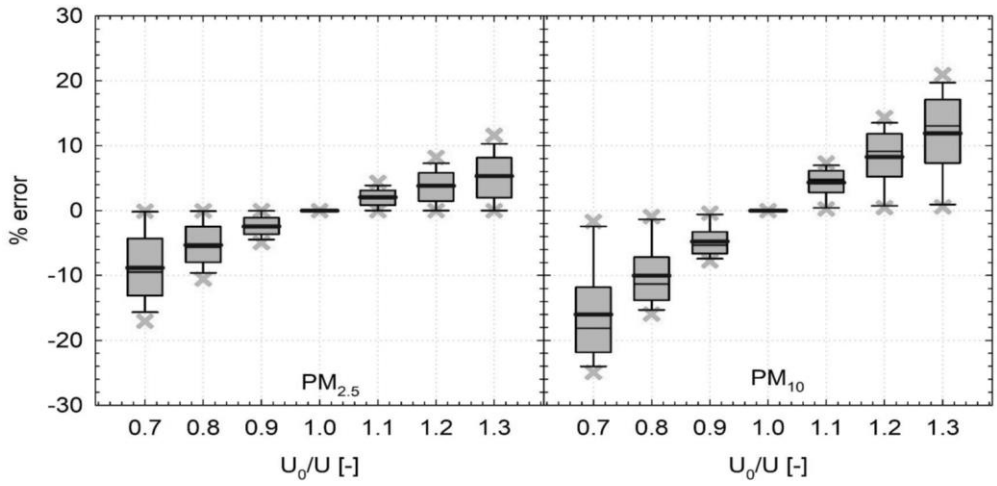

100. Figure 31 summarizes the average isokinetic ratio calculated over the emissions measurement section for the mandatory brakes (Br1a, Br1b, Br2) for all testing facilities. Equation 12.3 in the UN GTR was used to calculate the isokinetic ratio. The air flow rate values in the sampling tunnel and nozzle refer to the same temperature and pressure conditions; therefore, normalized values were used to ensure comparability between the testing facilities. The graph presents PM10 measurements; however, similar values were found for PM2.5 (not plotted here).

Figure 31
Average isokinetic ratio calculated over the emissions measurement section for Br1, Br2, and Br3 on the PM10 fraction.

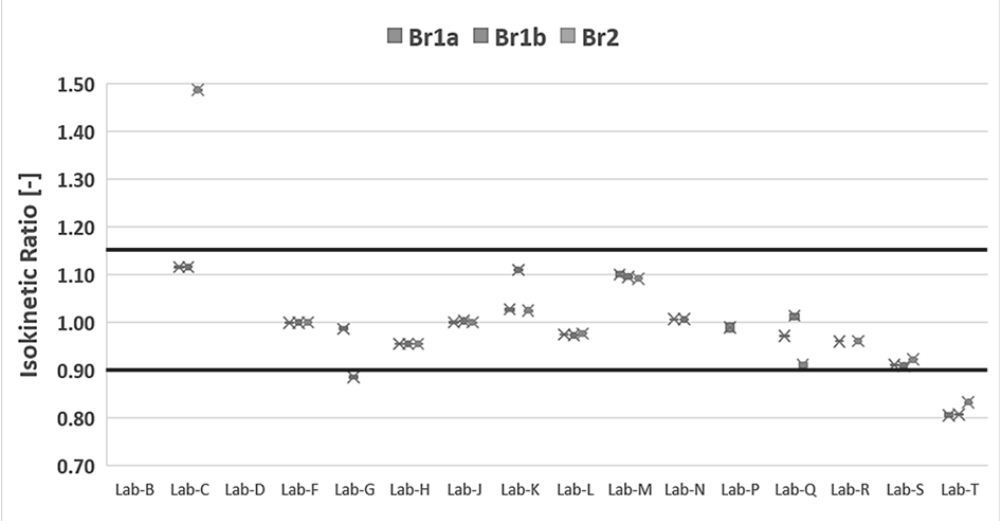

101. It is observed in Figure 31 that almost all testing facilities carried out emission tests with the mandatory brakes at optimal isokinetic ratio conditions. Lab T carried out all tests at a lower isokinetic ratio of 0.8 – this is expected to result in an underestimation of PM emissions for this testing facility of about 10%. Lab C carried out a measurement with an isokinetic ratio of 1.5 resulting in a significant overestimation of the PM10 for Br2. In all other cases, the threshold values of 0.9-1.15 were respected. This means that errors in the PM reported by the testing facilities cannot be attributed only to anisokinetic sampling. One should note that the calculation of the isokinetic ratio was carried out using the average cooling air flow rate over the tests calculated from the Time-Based file. However, the cooling air flow rate was not always measured correctly; therefore, there could be errors in the reported isokinetic ratio values. This was one of the reasons for restricting the measurement

of the cooling air flow as discussed previously in the report. Additionally, the calculation assumes a stable PM10 sampling flow which might have not always been the case. For this reason, a specification for the sampling air flow rate to be constant has been introduced in the UN GTR. More specifically, the isokinetic sampling shall be ensured through the accurate control of the cooling air flow and the PM sampling flow. For this reason, the actual flow rates shall be checked and verified post-test that are within ±5% of the nominal values. Finally, it was mandated to use appropriate nozzles for achieving an isokinetic ratio as close to 1.0 as possible.

102. Figure 32 shows that for an isokinetic sampling the effect of anisoaxial sampling is expected to be negligible for aspiration angles smaller than 15°. For this reason, it was proposed to define a maximum allowed aspiration angle of 15°. During the ILS, all testing facilities declared to have followed the specification for restricting the aspiration angle to a maximum of 15°. Therefore, it was not possible to extract any conclusion regarding this parameter and its influence on PM emissions from the ILS. The proposal for the UN GTR remains to keep the restriction of the angle as is to 15°.

Figure 32

Percent error of PM2.5 and PM10 calculated for different values of the aspiration angle. Graph taken from AVL as presented in the 28th TF2 Meeting.

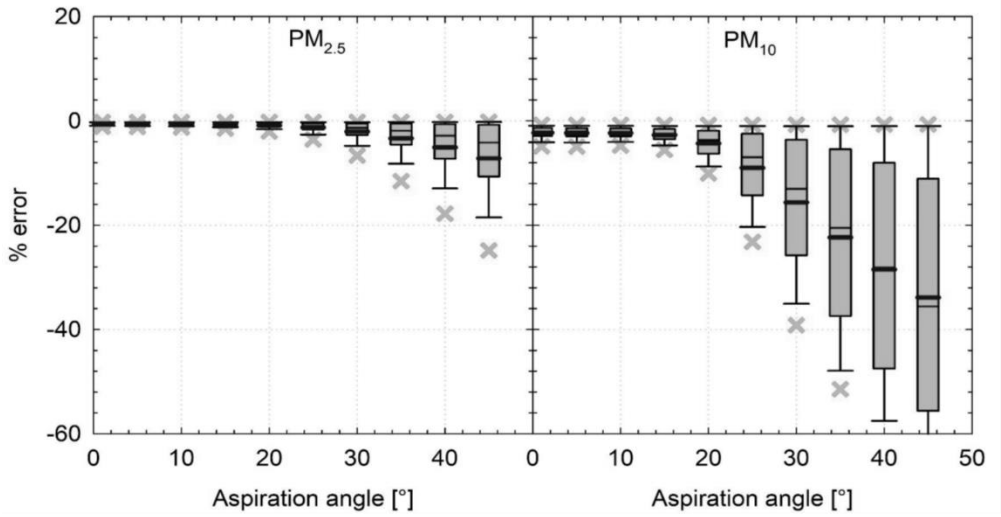

103. Figure 33 illustrates the theoretical percent error due to gravitational losses in the PM2.5 (left-hand side) and PM10 (right-hand side) measurement as a function of the sample flow/tunnel air speed and the tube/tunnel inner diameter for PM sampling tubes (upper part) and the sampling tunnel (lower part), respectively. From the graphs, it is apparent that gravitational losses on tunnel ducts are not typically critical. This has already been discussed earlier in Figure 8 and is demonstrated also in this paragraph. On the other hand, gravitational losses in horizontal tubing can be significant when large diameters are combined with small flows – this applies specifically to PM10 and to a lesser extent to PM2.5.

Figure 33

Percent error due to gravitational losses in the PM2.5 and PM10 measurement as a function of the sample flow/tunnel air speed and the tube/tunnel inner diameter for PM sampling tubes and the sampling tunnel.

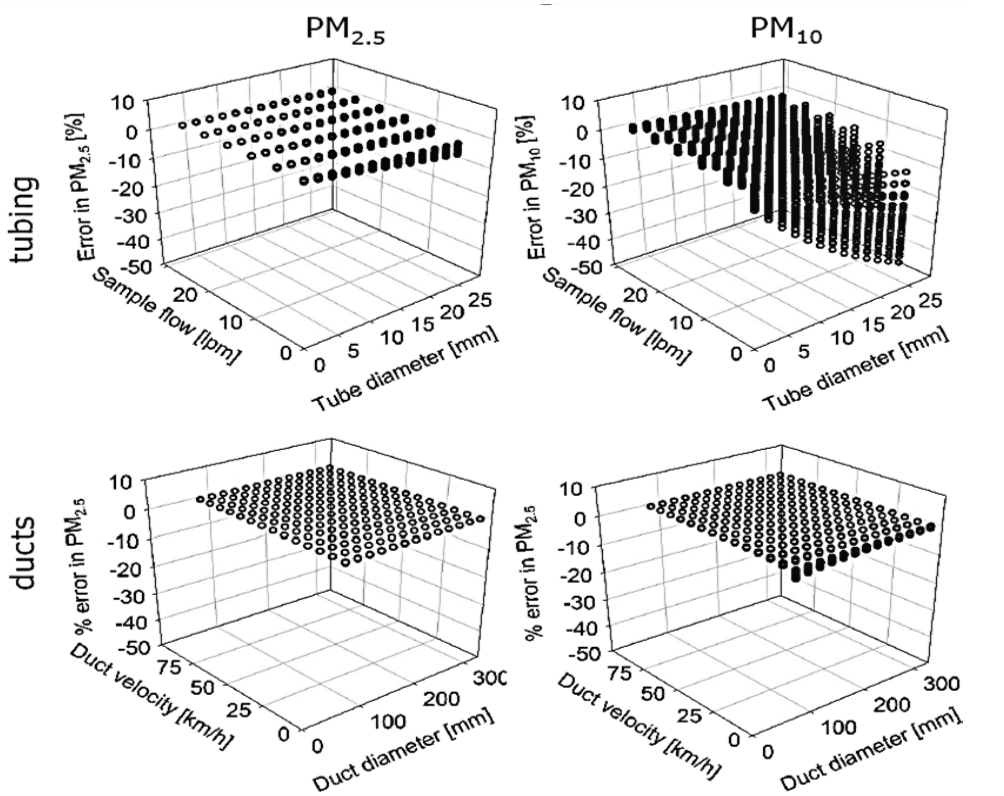

104. An attempt to calculate the gravitational losses for the 10 μm particles in the different setups during the ILS is given below. The calculations were performed for all applied flows taking into account the inner diameter of the sampling tunnel. A length of 1 m has been considered as typical for the sampling tunnel – results are very similar when a sampling length of 1.5 m is considered. As shown in Figure 34, the gravitational losses in the tunnel are expected to be very low under typical ILS operating conditions.

Figure 34

Percent error due to gravitational losses for 10 μm particles in the tunnel. The following assumptions have been considered: d_a=10 μm, $V_{settling}$=0.00304 m/s, pair=1.2 kg/m^3, μ=1.83E-05, L_{ref}=1 m.

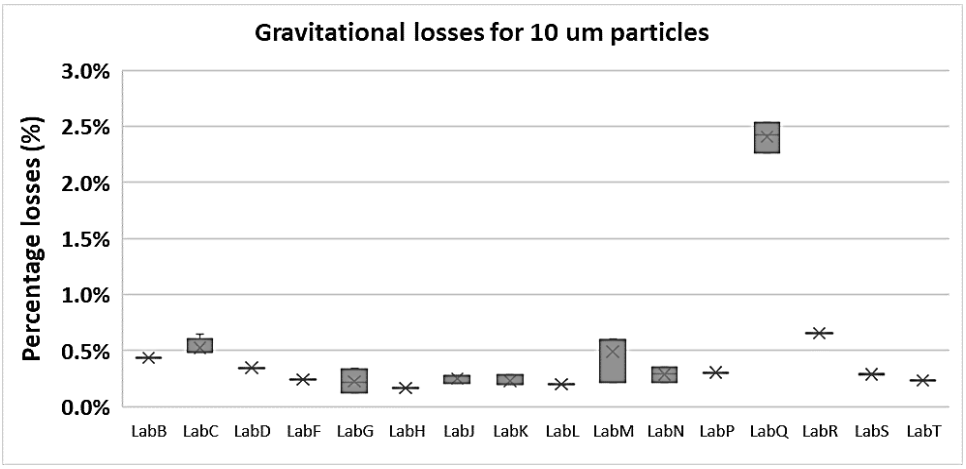

105. The lower Reynolds number was close to 40000 excluding Lab-Q which had generally lower values and cannot ensure a turbulent flow. Gravitational losses for PM2.5 are much lower. Overall, gravitational losses in the tunnel are not of concern.

106. A similar attempt to calculate the gravitational losses for 10 μm particles in the sampling lines is given below (Figure 35). In this case, the calculation applies to the sampling tube and not the sampling probe.

Figure 35

Percent error due to gravitational losses for 10 μm particles in the sampling lines. The following assumptions have been considered: d_a=10 μm, $V_{settling}$=0.00304 m/s, p_{air}=1.2 kg/m^3, μ=1.83E-05, L_{ref}=1 m.

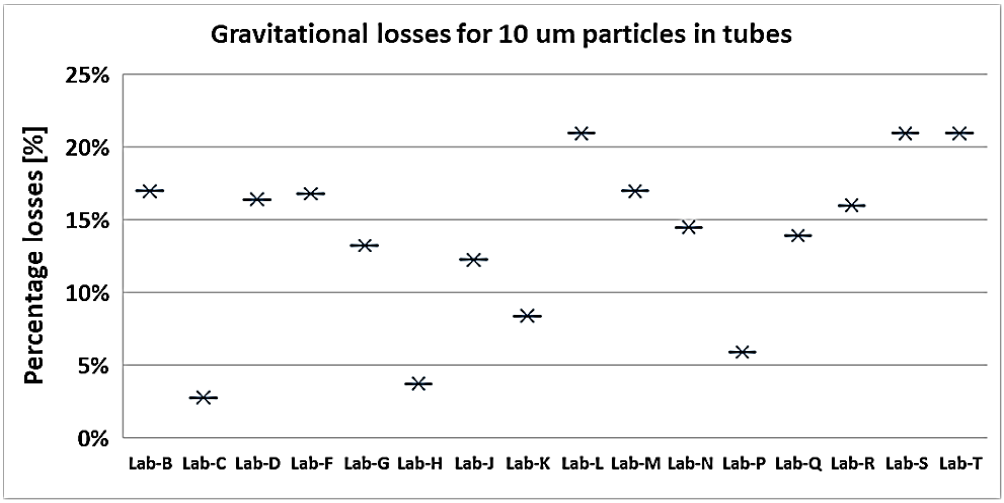

107. As shown in Figure 35, gravitational losses can become more critical in tubes compared to ducts. In the ILS conditions, losses of up to 20% are expected for 10 μm for certain testing facilities; however, the overall influence on the PM10 fraction is expected to be lower. In any case, it was decided to minimize these losses to the extent possible. For this reason, a combination of long lines with large tube diameters and low flows is no longer possible in the UN GTR. However, an optimization taking into account also possible inertial losses is required and discussed below.

108. Figure 36 illustrates the theoretical percent error due to inertial losses in the PM2.5 (left-hand side) and PM10 (right-hand side) measurement as a function of the sample flow/tunnel air speed and the tube/tunnel inner diameter for PM sampling tubes (upper part) and the sampling tunnel (lower part), respectively. From the graphs, it is apparent that inertial impaction on bends can become excessive under certain conditions. In the sampling tunnel, inertial losses increase when the cooling air speed is high. On the other hand, in sampling tubes, inertial losses increase when a high sampling flow is combined with low tube inner diameters.

109. An attempt to calculate the inertial losses for 10 μm particles in the different setups during the ILS is given below. The calculations were performed for all applied flows taking into account the inner diameter of the sampling tunnel. In all cases, a 90° bend has been considered in the layout. As shown in Figure 37, the inertial losses in the tunnel are expected to be moderate (up to 20%) to low (typically lower than 10%) under typical ILS operating conditions. They can become more critical at high air tunnel speeds like in the case of Lab-F (54 km/h), Lab-H (67 km/h), and Lab-G with Br5 (74 km/h). However, the overall influence on the PM10 fraction will be even lower. Overall, inertial losses in the tunnel seem not to be of concern when a maximum of one 90° bend is applied and the tunnel flow remains within the typical ILS values.

Figure 36

Percent error due to inertial losses in the PM2.5 and PM10 measurement as a function of the sample flow/tunnel air speed and the tube/tunnel inner diameter for PM sampling tubes and the sampling tunnel.

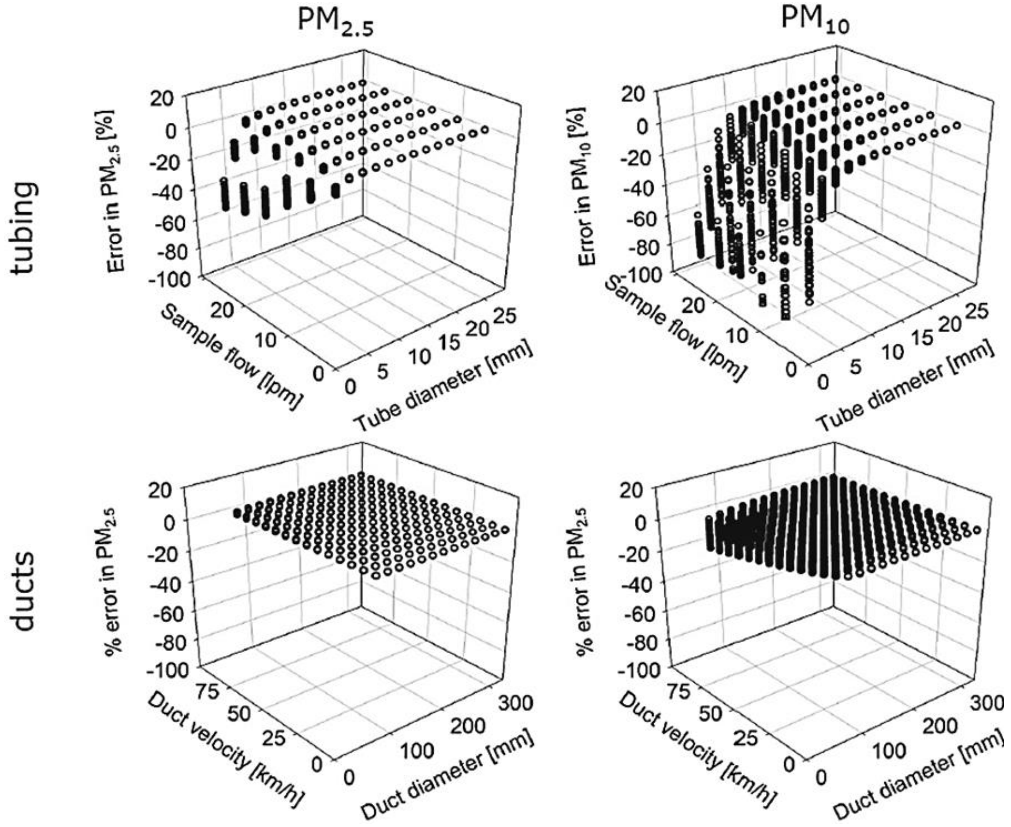

Figure 37

Percent error due to inertial losses for 10 µm particles in the tunnel. The following assumptions have been considered: d_a=10 µm, $V_{settling}$=0.00304 m/s, p_{air}=1.2 kg/m3, µ=1.83E-05, t_{rel}=0.00031 s, one 90° bend.

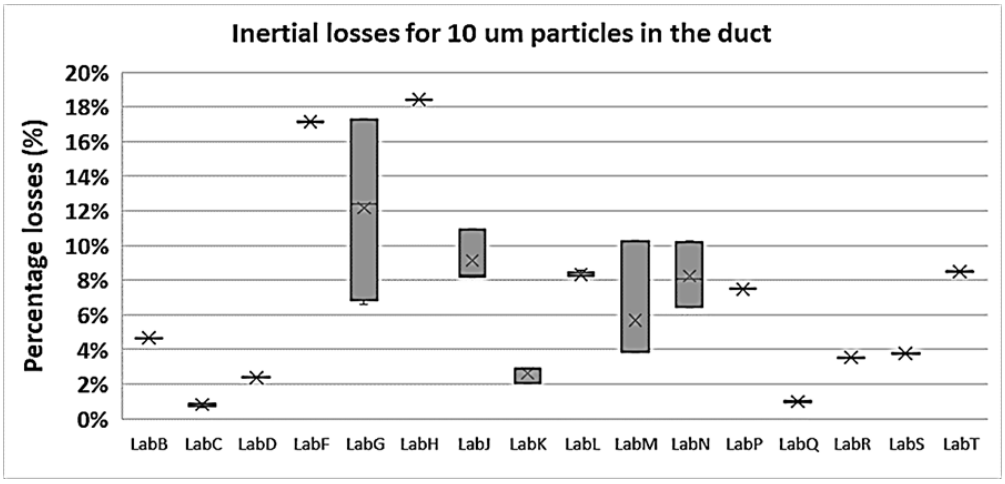

110. Inertial losses of 10 µm particles in the sampling lines were calculated. In this case, the calculation applies to the sampling tube and not the sampling probe. As shown in Figure 38, inertial losses can become very much critical in tubes even with one bend only. Labs H, P, and C experienced very high losses that compromised the overall PM10 fraction – high inertial losses explain the very low PM10 emissions of these labs compared to the average as calculated in the Annex. Again, attention shall be paid to avoid combinations of low diameters with very high flows.

Figure 38

Percent error due to inertial losses for 10 µm particles in the sampling lines. The following assumptions have been considered: d_a=10 µm, $V_{settling}$=0.00304 m/s, p_{air}=1.2 kg/m^3, µ=1.83E-05, t_{rel}=0.00031 s, one 90° bend.

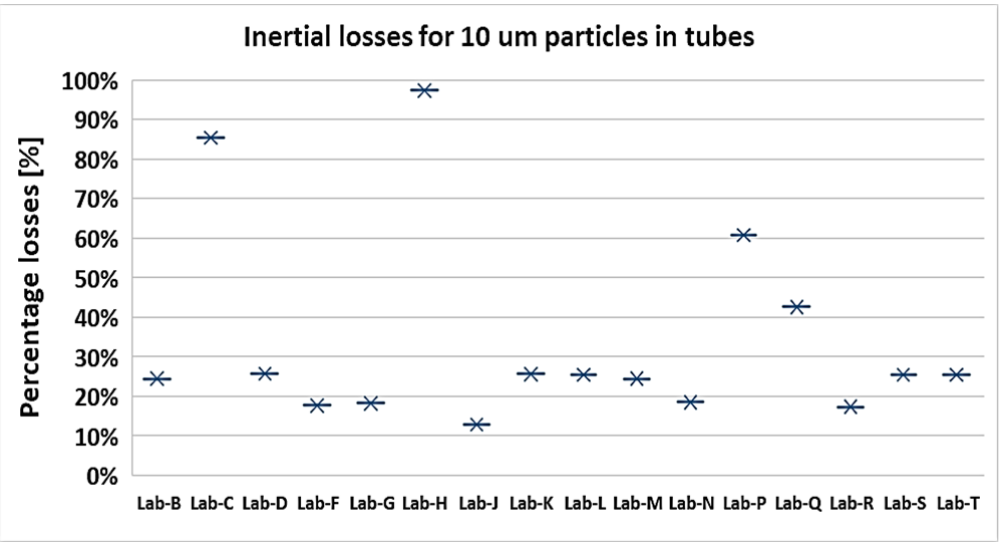

111. The PMP stakeholders acknowledged that bends are one of the most important reasons for losses of PM in the system. The ideal situation would be to completely avoid bends. However, since they provide flexibility in the design of the layout it was decided to allow for this option. Based on the results presented above, it was decided to allow a maximum of a 90° bend for the sampling tunnel – when a bend is applied the bending radius shall be at least two times the inner diameter of the sampling tunnel. Similarly, a maximum of a 90° bend for the sampling tubes is allowed – in this case when a bend is applied the bending radius shall be at least four times the inner diameter of the probe and twenty-five times the inner diameter of the sampling line, respectively.

112. A minimum diameter of 175 mm and a maximum of 225 mm for the sampling tunnel were mandated. Based on the ILS results, the duct diameter does not seem to have an important influence on particle gravitational or inertial losses. However, based on the ILS results, there is a clear need for harmonizing the protocol and further restricting the possible designs. This is the reason for limiting the options between 175-225 mm. This range of diameters allows for the selection of the appropriate layout based on the testing facilities needs without restricting it to one "non-flexible" option. It can accommodate a layout with three or four sampling probes depending on the needs of the testing facility. Finally, it seems that it covers the needs of the different markets.

113. Additionally, a minimum diameter of 10 mm and a maximum of 20 mm for the sampling lines was mandated – a minimum diameter of 10 mm and a maximum of 18 mm for the probes applies. These dimensions are expected to result in minimized PM losses when typical tunnel and sampling flows are applied. The testing facility is allowed to select the optimal diameters depending on the PM sampling flow rate. For example, when high flows are applied (i.e., >> 10 lpm) then tube diameters of close to 20 mm are more appropriate. For low flows (i.e., 8 lpm) tube diameters of close to 10 mm are more appropriate. The Reynolds number alone cannot be used as an indicator since minimizing gravitational losses would require higher Re values, whereas minimizing inertial losses would require lower Re values. The overall length of the probes from the sampling nozzle tip to the inlet of the PM separation device shall not exceed 1 m. Similarly, the overall length of the sampling line from the outlet of the cyclonic separator to the tip of the filter holder shall not exceed 1 m in total.

114. It was discussed in the TF2 that care shall be taken for placing the sampling probes appropriately in the tunnel. When there is not enough distance (i.e., more than 6 duct diameters) one could have improper mixing especially at lower cooling speeds and the PM10 sample probe could show bias. For this reason, it was proposed to place the PM10 probe towards the bottom of the duct and not the top (Figure 10). Additionally, since PM2.5 is a

subset of PM10, the two probes should be at the same plane (both low) not diametrically opposed. In such a case, and especially with a horizontal duct design, the gravitational settling rate would be similar for both PM2.5 and PM10.

115. The nozzles shall be appropriate to ensure isokinetic sampling for both PM10 and PM2.5 – their selection shall depend on the applied tunnel air flow rate. Additional specifications for the nozzles in accordance with ISO 9096 have been mandated. Nozzles – as well as all the surfaces that come into contact with the aerosol – shall be made of stainless steel with an electropolished finish. Electropolishing was introduced to ensure ultra-clean and ultra-fine surfaces. Unlike mechanical finishing, electropolishing does not smear, bend, stress or fracture the crystalline metal surface. Also, electropolishing is an ideal solution for corrosion because electropolishing removes iron contaminants from the stainless-steel duct surface. Finally, nozzles shall be placed with their axis parallel to that of the sampling tunnel making sure that the aspiration angle remains lower or equal to 15° to ensure isoaxial sampling.

116. Based on the specification described in the previous paragraphs, losses of lower than 25% are expected for 10 um particles – the overall losses for the entire PM10 fraction shall be much lower.

117. PM Sampling Devices: Figure 39 plots the PM10 filter load against the PM10 emissions for all tests carried out during the ILS. Among others, it is shown that all levels of PM10 emission factors may be linked with moderate to high PM10 filter load depending on the air flow. Additionally, most of the ILS tests were completed with PM10 filter loads higher than 1 mg with the highest PM fraction being deposited in the PM2.5-PM10 stage. More specifically, testing of full friction brakes results in filter loadings of 2.0-5.0 mg for PM10 and 1.0-2.0 for PM2.5. Six out of eight testing facilities that used impactors had errors in the PM measurement; however, these are not necessarily linked to the impactor as other problems in the layouts exist. On the other hand, six out of eight labs that measured without obvious errors applied cyclones for PM sampling.

Figure 39
PM10 filter load in mg against the PM10 emissions in mg/km for all tests carried out during the ILS.

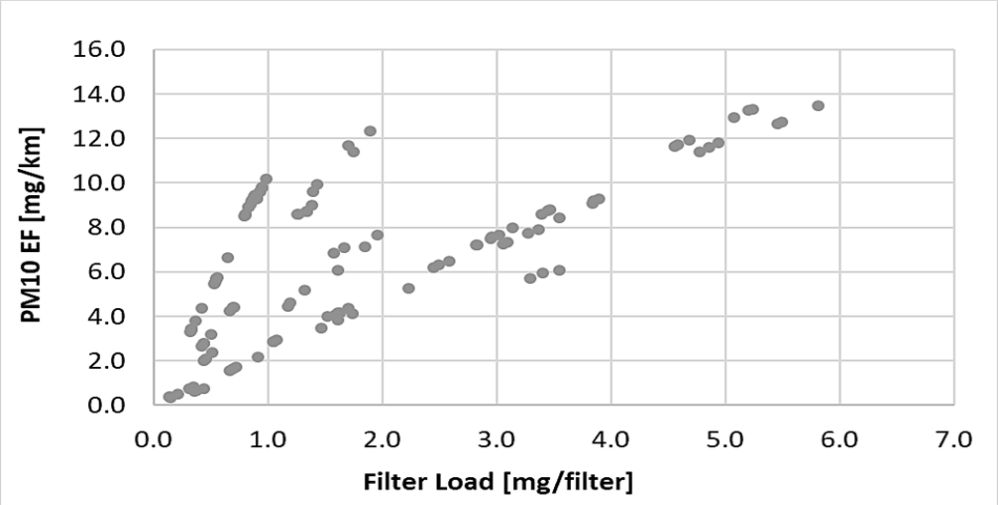

118. As a rule of thumb – but also mentioned in the specifications of some impactor manufacturers –, impactors shall not collect more than 1 mg per impaction stage because they can introduce clogging or bouncing phenomena. During the ILS, 65% of the tests with impactors resulted in a high PM10 filter load (75th percentile is 3.9 mg/filter) due to the long duration of the test. This may compromise both PM10 and PM2.5 measurements especially when considering that also non-friction braking tests will be carried out at full-friction conditions. Additionally, cyclones have less need for cleaning and the contamination impact on the particle separation curve is lower. For these reasons, TF2 unanimously decided to mandate the use of cyclones for PM sampling in the UN GTR. More specifically, single

PM10 and PM2.5 cyclonic separators followed by gravimetrical filter holders shall be used for the collection of the PM10 and PM2.5 samples. Commercially available cyclonic separators with cut-off sizes of 10 μm and 2.5 μm shall be used for the collection of the PM10 and PM2.5 samples, respectively. Specifications for the size-dependent separation efficiency have also been defined following the example in ISO 25597:2013. The efficiency envelopes have been slightly adjusted based on the calibration certificates submitted by the laboratories during the ILS. Finally, the cyclonic separators shall be placed right at the end of the probe exiting the tunnel to minimize losses and possible tubing pollution. No specifications for pre-classifiers are defined.

119. The filters shall be mounted in a dedicated filter holder. The filter holder shall be located as close as possible to the cyclonic separator's outlet to minimize aerosol transfer. Specifications for the filter holder assembly have been defined following ISO 16000:37. It has been agreed that the temperature at the filter holder shall follow the specification for the entire sample path and shall always remain above 15 °C to avoid condensation phenomena. Some stakeholders suggested that multiple PM measurements should be enabled by allowing a switch system for PM measurement in the filter holder. The reason for not agreeing with this option relates to the application of a flow-splitting mechanism in this type of system. Flow splitters have been shown to have a negative impact on PM10 measurement. This is due to the bigger size of brake particles compared to any other particles regulated in the automotive sector. These particles are prone to higher losses when flow splitters are applied. For this reason, it is not allowed to use flow splitters anywhere between the sampling probe and the filter for PM measurement. The PMP could discuss the possibility of allowing such a system in a future amendment of the UN GTR if it is proven that the particle losses are negligible. However, so far no experimental data for large particles in the micron range have been provided.

120. Sampling media: Regarding the sampling media, there were no changes with respect to the initial TF2 recommendations. It was agreed that fluorocarbon-coated glass fibre filters or fluorocarbon membrane filters shall be used for the PM10 and PM2.5 measurements. In addition, specific efficiency requirements were provided – these shall be certified by the filter supplier. PM data shall be validated using reference filters that match the sample filter media.

121. Weighing Procedure: The weighing room environmental conditions were initially specified at 22±1°C and 50±5% RH. The ILS data demonstrated that regulating the weighing room environmental conditions at 22±2°C and 45±8% RH – in line with other regulations – does not have any measurable impact on PM or PN emissions. Four testing facilities applied the updated weighing room environmental conditions and all of them submitted acceptable PM data. Additionally, the weighing balance resolution was agreed to be at least 1 μg in line with the initial TF2 specification – several testing facilities did not follow this specification and all of them submitted questionable results (not necessarily linked to the weighing balance resolution as other problems in the layouts exist). Finally, specific calibration requirements were also defined for the PM weighing balance. More details regarding the weighing room and weighing balance specifications are provided in the UN GTR text.

122. During the ILS, the testing facilities were instructed to precondition the filters for a minimum of 24 h in standard temperature and humidity conditions (22±3°C and 50±10% RH) before performing the initial weighing procedure. One testing facility submitted data of blank filters used during the ILS, which had been stored in a petri dish for 3 weeks without any significant change in mass (<5μg). For the sake of better automation, it was recommended to allow placing the filters in the holders before starting the bedding section (i.e., approximately 24 h before the emissions measurement section). Indeed, it was agreed to precondition the filters at 22±2°C and 45±8% RH for a minimum of 2 hours before performing the initial weighing procedure, store the filters in a closed petri dish (or equivalent) or sealed filter holder until testing without specifying a time limit and place the filter in the filter holder within 1h of its removal from the weighing chamber.

123. Additionally, the testing facilities were instructed to precondition the filters after sampling for a minimum of 1h in standard temperature and humidity conditions (22±3°C and 50±10% RH) before performing the final weighing procedure. During the ILS, there were cases where loaded filters were transferred after 150 h or more to the weighing room. Some testing facilities expressed concerns about such a high duration and for not defining a

maximum allowed time after testing in which the filters shall be transferred in the weighing room. For this reason, it was mandated to take the filters to the conditioning room within 8 hours after testing is completed. Some stakeholders expressed a concern that this restriction would compromise the automation of the procedure and will not allow for testing over weekends. However, the group decided to proceed with the introduction of this specification to avoid the risk of compromising the measurement by losing part of the deposited material and specifically semi-volatile particles. This provision was relaxed in the first amendment of the GTR No. 24 following the submission of a robust dataset at the PMP IWG. Finally, it was agreed to precondition the filters at 22±2°C and 45±8% RH for a minimum of 2 hours before performing the final weighing procedure. Longer preconditioning duration is not required since brake samples are expected to be generally more "stable" compared to e.g. exhaust samples.

124. During the ILS, the testing facilities were instructed to weigh the PM filters twice. When the difference between the first and second measurements was higher than 30 µg the filter shall have been measured for a third time. If the difference between the second and third measurements was higher than 30 µg the measurement was invalid. Some stakeholders advised that provisions for buoyancy correction shall be introduced in the UN GTR. Indeed, a paragraph following the relevant specifications defined in the UN GTR15 was introduced. Additionally, a slightly modified weighing procedure was proposed and adopted unanimously by the TF2 members. The main difference compared to the initial ILS TF2 method is that when the difference between the first and second measurements is greater than 30 µg the testing facility shall perform two additional measurements instead of one. Depending on the results there are different scenarios on how to proceed with the calculations. More details regarding the weighing procedure and buoyancy correction are provided in the UN GTR text.

125. PM emissions calculation: During the ILS, the testing facilities were requested to report the PM emissions of the tested brakes in mass per distance driven. The current version of the UN GTR provides a detailed description for the calculation of the PM2.5 and PM10 emissions for the tested brake following Equations 12.7 and 12.8, respectively. For the calculation, it is necessary to calculate the PM2.5 and PM10 filter mass load in mg, the average normalized air flow in the PM2.5 and PM10 sampling nozzles in normal l/min, the average normalized air flow in the sampling tunnel in normal m³/h (the letter N is used in the UN GTR for normal eg Nm^3/h), and the total distance driven during the WLTP-Brake cycle in km. The calculation is straightforward when a full-friction brake is tested. On the other hand, for the non full-friction brakes it is necessary to apply a correction factor that reflects the expected friction braking share of the vehicle on which the tested brake is mounted. This factor is defined as the friction braking share coefficient (c) and depends on the vehicle type. The calculation of the final PM2.5 and PM10 emissions for the tested brake in the UN GTR follows Equations 12.9 and 12.10, respectively. The testing facility shall apply the friction braking share coefficient that corresponds to the vehicle type of which the parameters were used for testing the brake. The friction braking share coefficients for the different vehicle types are given in Table 19. The ILS data indicate that PM emissions increase almost linearly with the dissipated kinetic energy. More specifically, an increase of 36% in energy results in an increase of 31% and 23% in PM10 and PM2.5 emissions, respectively. Therefore, the application of the friction braking share coefficients is expected to reflect real-world PM emissions in a satisfactory way.

Table 19
Friction braking share coefficients for all vehicle types. The nomenclature for the different types of vehicles is provided in the definitions section of the UN GTR.

Brake type	*Vehicle Type*	*Friction Braking*
Full-friction braking	ICE and other vehicle types not covered in the non-friction braking categories in this Table	1.0
Non-friction braking	NOVC-HEV Cat.1	0.63

Brake type	*Vehicle Type*	*Friction Braking*
	NOVC-HEV Cat.2	0.45
	OVC-HEV	0.30
	PEV	0.15

126. The friction braking share coefficients were calculated using input from the PMP stakeholders. At first, JRC carried out an analysis based on vehicle tests performed on a chassis dynamometer over the WLTC cycle. The JRC methodology is based on an energy balance at the wheels level over the test cycle. The following effects are accounted for: vehicle resistances, internal combustion engine (ICE) motoring, electric machine (EM) energy recuperation, and, lastly, friction braking. The overall concept is summarized in Figure 40. The friction braking energy share is calculated from the other three parameters which are obtained from vehicle data during the chassis dynamometer test. More details about the method and the equations used are available in the TF4 – Minutes of Meeting #20. The c values in Table 19 have been updated in the first amendment of the GTR to reflect the correct calculation when shifting from testing on the chassis dyno to calculating the brake dyno-based c factors. Additionally, the vehicle category NOVC-HEV Cat. 0 has been added to reflect mild-hybrids with battery capacity between 12-20V. The second amendment added fuel cell vehicles.

Table 19
Friction braking share coefficients for all vehicle types. The nomenclature for the different types of vehicles is provided in the definitions section of the GTR.

Brake type	*Vehicle Type*	*Friction Braking Share Coefficient (c)*
Full-friction braking	ICE and other vehicle types not covered in the non-friction braking categories in this Table	1.0
Non-friction braking*	NOVC-HEV Cat. 0	0.90
	NOVC-HEV Cat. 1	0.72
	NOVC-HEV Cat. 2	0.52
	OVC-HEV	0.34
	PEV	0.17

**Note*: Testing facilities may use vehicle-specific friction braking share coefficients measured and calculated according to Annex C of this UN GTR.

Figure 40
Schematic of the energy balance at the wheels at the JRC method for the calculation of the friction energy share.

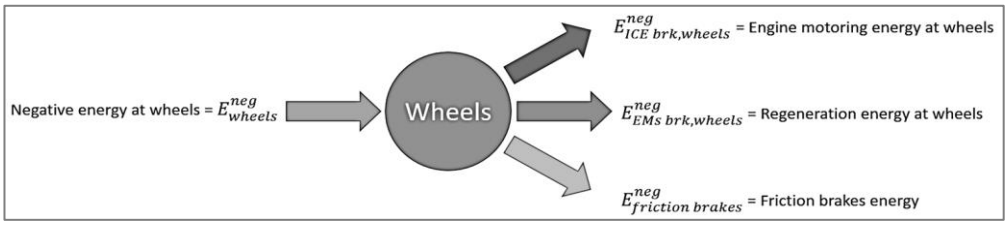

127. In addition to the JRC data, other stakeholders submitted measurement and simulation data following a similar approach. Table 20 summarizes the obtained results for different vehicle types. The friction braking share coefficients were elaborated considering the worst-performing vehicle in each category based on the available data. JRC did not perform chassis dyno data over the WLTP-Brake cycle. Therefore, the problem with the initial data was that the friction share was calculated over a different cycle than the WLTP-Brake cycle. However, OICA presented data showing a low increase in the friction share when shifting from the

WLTC exhaust to the WLTP-Brake cycle at low friction shares and an approximately 20% increase at higher friction shares. Therefore, the final coefficients have been elaborated by applying a 20% correction to take into account the change of cycle (last column in Table 20). Two JRC tests with the Battery electric vehicle EV2 have been treated as outliers due to their high values of friction share compared to other JRC and third-party data. As a result, the friction braking share coefficient for pure electric vehicle (PEV) was defined to 15% (updated to 17% when correcting the denominator). A brake dynamometer test with an off-vehicle charging hybrid electric vehicle (OVC-HEV) shows that when a full regenerative capability is assumed the friction share is calculated to be 24% – this is by 20% reduced compared to the final friction braking coefficient defined for the OVC-HEV (i.e., 30% updated to 34% when correcting the denominator). Only one data point was submitted for not-off vehicle charging NOVC-HEV Cat. 2 (full hybrid) showing a friction energy share of 38% at full regenerative capability (brake dynamometer test over the WLTP-Brake cycle) – the final friction braking share coefficient was defined at 45% (updated to 52% when correcting the denominator) following a 20% increase to account for the phenomenon described above. Finally, a friction braking share coefficient of 63% (updated to 72% when correcting the denominator) is defined for the NOVC-HEV Cat. 1 type. The friction braking share coefficient of NOVC-HEV Cat. 0 has been set to 90% based on the data submitted by a PMP stakeholder.

128. OICA submitted data showing generally lower friction share coefficients during the PMP on 23.11.2022 and 13.12.2022. This data was collected from six OEMs including 55 vehicles. However, this dataset does not cover either the full range of the market available vehicles for all OEMs or the full range of vehicle models within the six OEMs. Additionally, the data was submitted in such a format that it was not possible for JRC to validate its accuracy and make additional calculations or crosschecks against the rest of the data. Figure 41 shows the data from JRC and OICA. A detailed testing methodology to determine vehicle-specific friction braking share coefficients has been elaborated by the PMP and is included in the first amendment to this GTR to solve the problem of non-accurate friction braking share coefficients. Details regarding the method, supporting data, and the development phase have been added in Annex B of the current technical report.

Figure 41

Friction braking share coefficients for WLTP Brake. JRC data (green dots, bigger circle denote >1 data points) and OICA data (boxplot including data from 55 vehicles). The point in red represents a full-hybrid vehicle (NOVC-HEV).

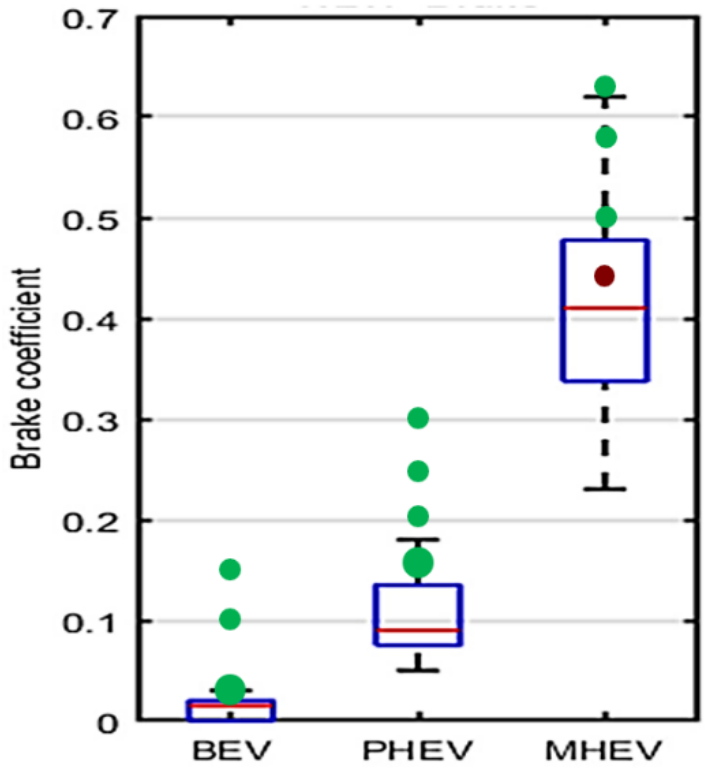

129. The friction braking share coefficients presented in Table 19 shall also be used to select the parent of the brake emissions family when the same brake is mounted on different vehicles and vehicle types. The reason for using the friction braking share coefficient for the definition of the parent of the brake emissions family relates to the need for testing the brake by applying the parameters of the vehicle configuration that is expected to result in higher PM emissions. Some stakeholders proposed to use the heavier vehicle as the parent of the brake emissions family by calculating the product of vehicle mass and brake force distribution; however, this would result in testing most brakes that are mounted in several vehicle types using the PEV configuration. In such a case, another calculation step would be necessary to report the actual emissions for a different vehicle type (e.g., NOVC) – in other words, an extrapolation of the measured emissions with the PEV parameters to lower testing inertia would be required. This step would introduce an additional source of error; therefore, it was rejected by some stakeholders. On the other hand, the current proposal ensures that testing almost always takes place using the parameters of the vehicle configuration which results in higher PM emissions. More details regarding the family concept are provided in the text of the UN GTR. It shall be noted that the first version of the GTR provided guidance on brake emissions testing of OEM brakes. The concept of the families for aftermarket brakes was elaborated and introduced in the first amendment of the GTR. This includes grouping of brake systems and parts based on the friction material surface area (disc brakes) and the brake drum diameter (drum brakes). Each brake pad and shoe material constitute a unique family. Additionally, the type of calliper (floating or fixed), the vehicle axle where the brake is located (front or rear), the brake disc (cast iron, coated cast iron, carbon-ceramic, other) or drum (cast iron, other) material, and the brake disc surface form (plain or not plain) have been considered to define the families. These are summarized in Tables 5.1. and 5.2. of the GTR No. 24. The concept of identical brakes has also been defined and decided to be treated as non-original replacement parts.

Table 20
Friction braking share coefficients for different vehicles tested and verified by the JRC. Cells in grey denote vehicles tested at the JRC on a chassis dynamometer. Cells in white denote either brakes tested on the brake dynamometer, or vehicles tested by other third parties, or simulations.

Vehicle	*Type*	*Test type*	*Cycle*	*Engine Motoring Energy [%]*	*Regeneration Braking Energy [%]*	*Friction Brakes Energy (FBE) [%]*	*Extrapolated FBE at the WLTP-Brake Cycle [%]*
Battery EV1	PEV	Full vehicle	WLTC	0.0	96.2	3.8	4.6
Battery EV2	PEV	Full vehicle	WLTC	0.0	85.3	14.7	17.7
Battery EV2	PEV	Full vehicle	WLTC	0.0	85.5	14.5	17.4
Battery EV2	PEV	Full vehicle	WLTC	0.0	87.2	12.8	15.3
Battery EV3	PEV	Full vehicle	WLTC	0.0	91.5	8.5	10.2
Battery EV4	PEV	Brake dyno	WLTP-Brake	0.0	97.5	2.5	2.5
Battery EV5	PEV	Brake dyno	WLTP-Brake	0.0	96.1	3.9	3.9
Plug-in HEV1	OVC-HEV	Full vehicle	WLTC	2.9	79.5	17.6	21.2
Plug-in HEV1	OVC-HEV	Full vehicle	WLTC	1.7	84.6	13.7	16.4
Plug-in HEV1	OVC-HEV	Brake dyno	WLTP-Brake	0.0	76.0	24.0	24.0
Plug-in HEV2	OVC-HEV	Full vehicle	WLTC	2.5	72.2	25.2	30.3
Plug-in HEV3	OVC-HEV	Simulation	WLTC	0.0	86.1	13.9	16.7
Plug-in HEV3	OVC-HEV	Simulation	WLTP-Brake	0.0	82.9	17.1	17.1
Plug-in HEV4	OVC-HEV	Brake dyno	WLTP-Brake	0.0	83.0	17.0	17.0
Plug-in HEV4	OVC-HEV	Brake dyno	WLTP-Brake	0.0	83.7	16.3	16.3
Full	NOVC-HEV Cat.2	Brake dyno	WLTP-Brake Trip #10	0.0	61.9	38.1	38.1

Vehicle	*Type*	*Test type*	*Cycle*	*Engine Motoring Energy [%]*	*Regeneration Braking Energy [%]*	*Friction Brakes Energy (FBE) [%]*	*Extrapolated FBE at the WLTP-Brake Cycle [%]*
HEV1							
Mild HEV1	NOVC-HEV Cat.1	Full vehicle	WLTC	13.4	38.6	48.0	57.6
Mild HEV1	NOVC-HEV Cat.1	Full vehicle	WLTC	24.7	33.6	41.7	50.1
Mild HEV2	NOVC-HEV Cat.1	Full vehicle	WLTC	3.5	43.8	52.8	63.3

2. Measurement of PN concentration

130. The high-level minimum specifications for the PN measurement can be found in the TF2 guidelines deliverable [9]. The methodology relied on the exhaust emissions relevant requirements. The TF2 defined minimum specifications regarding: (a) the sampling plane, which was placed at least 5 and 2 diameters downstream and upstream of any flow disturbance, respectively; (b) the pre-classifier, which featured a cut-off diameter between 2.5 and 10 μm; (c) the sampling line, which was designed such as the residence time remains below than 1.5 s; (d) a diluter, which was calibrated with particle number concentration reduction factor (PCRF) at 15 nm, 30 nm, 50 nm, and 100 nm; with ratios: $PCRF_{15}/PCRF_{100} \leq 2$, $PCRF_{30}/PCRF_{100} \leq 1.3$, $PCRF_{50}/PCRF_{100} \leq 1.2$; (e) a full flow Particle Number Counter (PNC) which featured a counting efficiency of 65% (±15%) at 10 nm and >90% at 15 nm. Note that all PNCs are Condensation Particle Counter (CPC), so the terms are used interchangeably (usually CPC was used at the ILS, PNC in the regulation). Optionally solid particles could be measured by applying thermal preconditioning of the sample. This included hot dilution 10:1 with temperature ≥150 °C, but not higher than 350 °C. No particular provisions were prescribed as the gravitational and inertial losses of nanoparticles are small. The only requirements regarding the use of short tubing length (e.g., residence time <1.5 s) ensured minimum diffusional and agglomeration losses. The results and lessons learned from the ILS (see Annex) were the basis of the UN GTR proposal. Figure 42 gives an example of the UN GTR proposed PN layout. The positioning and dimensions of the different elements are provided for illustrative purposes; therefore, exact conformance with the figure is not required. Four paragraphs were introduced in the UN GTR.

12.2.1. Describes the sample extraction from the sampling plane;

12.2.2. Discusses the sample treatment and conditioning for the diluter and volatile particle remover (VPR);

12.2.3. Describes the particle number counter (PNC);

12.2.4. Describes the PN emissions calculation.

Figure 42
Indicative setup for PN measurements.

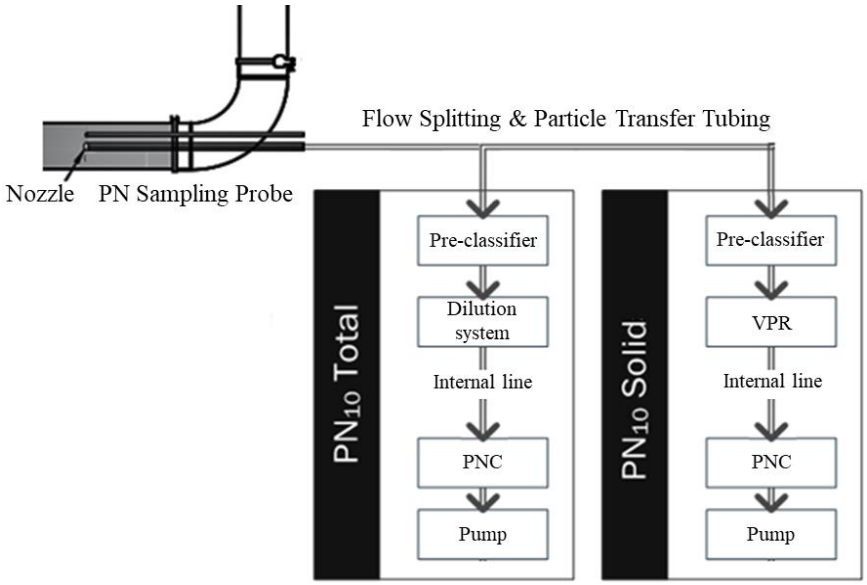

131. The TF2 guidelines were revised based on the ILS experience and theoretical estimations of the contribution of each parameter to the PN results. To assess the importance of various parameters on the PN results, two *scenarios* were examined:

(a) PN emissions of $<10^{10}$ #/km consisting of a mode peaking at 0.8-1.5 μm;

(b) PN emissions with additionally a one order of magnitude higher nucleation mode $>10^{10}$ #/km peaking at 10-30 nm.

132. Panels on the left in the Figures given below plot scenario (i) regarding the impact on PN emissions. On the other hand, panels on the right in the Figures given below plot scenario (ii) regarding the impact on PN emissions.

133. Transport and Extraction: Figure 43 presents the percent error of PN calculated for different values of the aspiration angle for the two PN scenarios. It is demonstrated that non-isoaxial (anisoaxial) sampling has negligible impact for both scenarios (<3%). Nevertheless, it was decided to keep a maximum 15° anisoaxial sampling since it is something that can be easily achieved, even with bare eyes. The same applies to PM sampling.

Figure 43
Impact of anisoaxial sampling on PN emissions for the two PN scenarios. On the left-hand side scenario (i) is plotted. On the right-hand side scenario (ii) is plotted.

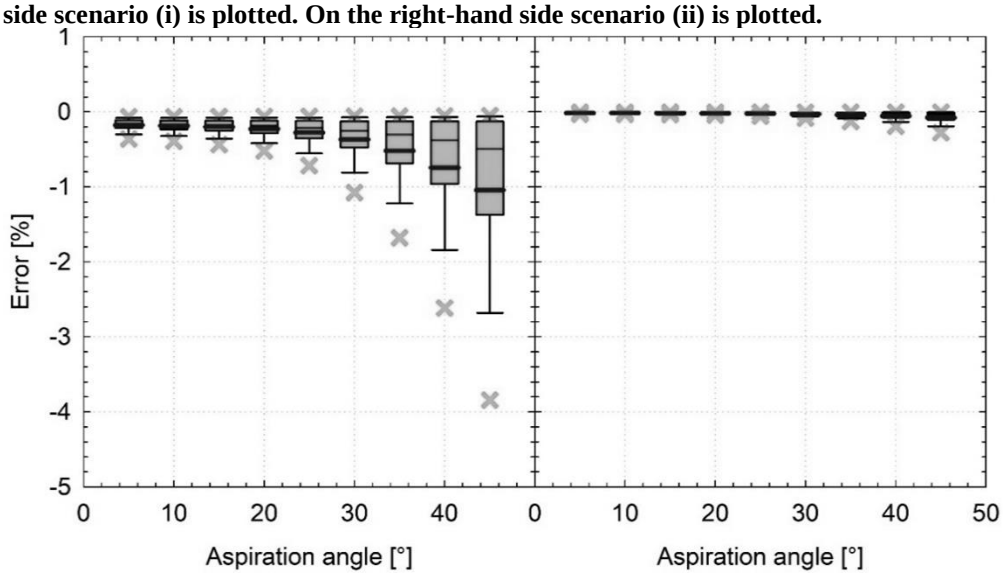

134. Figure 44 presents the percent error of PN calculated for different values of the isokinetic ratio for the two PN scenarios. It is demonstrated that anisokinetic sampling is not important when nucleation mode particles dominate (scenario (ii)). On the other hand, in the absence of nucleation particles (scenario i) for ratios 0.9 to 1.15 (as for PM) the impact is negligible (<5%) and reaches 10-15% at deviations of ±0.4. For this reason, it was decided to relax the isokinetic requirement to 0.6-1.5.

135. The effect of inertial deposition on bends was also estimated to be negligible (<3%) in all cases (Figure 45). Nevertheless, a 10 mm minimum tube diameter was introduced. The minimum diameter (nozzle or tubing between diluter and PNC) was set to 4 mm in order to avoid clogging effects, rather than minimize inertial losses. In all cases up to one bend (with appropriate bend radius) was allowed.

136. The gravitational losses were in general low, except for very low flow rates combined with large tube diameters (Figure 46). To avoid such cases, it was decided to restrict the maximum tube diameter to 20 mm, and introduce maximum residence times, that indirectly restrict the minimum flow rates.

Figure 44
Impact of anisokinetic sampling on PN emissions for the two PN scenarios

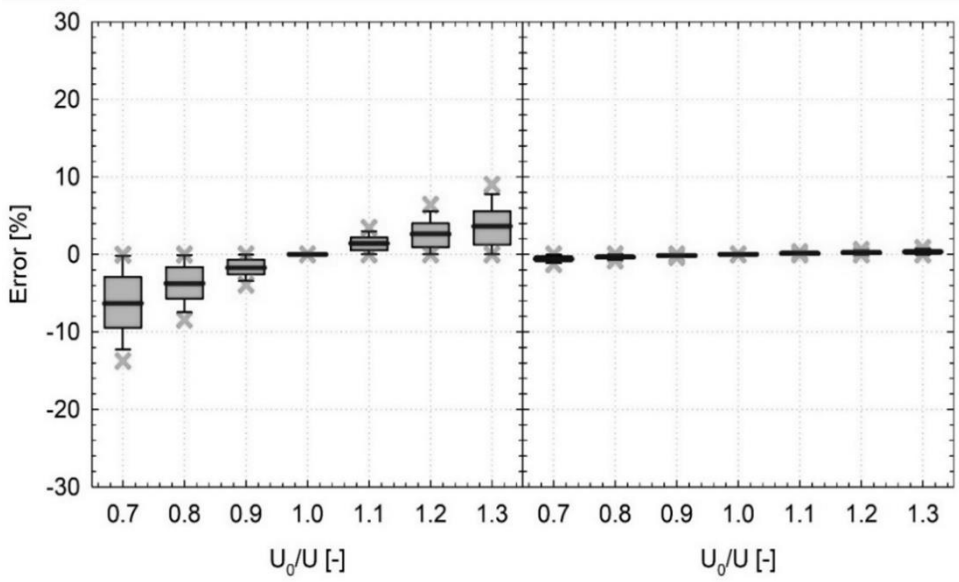

Figure 45
Inertial deposition on bends. On the left-hand side scenario (i) is plotted.

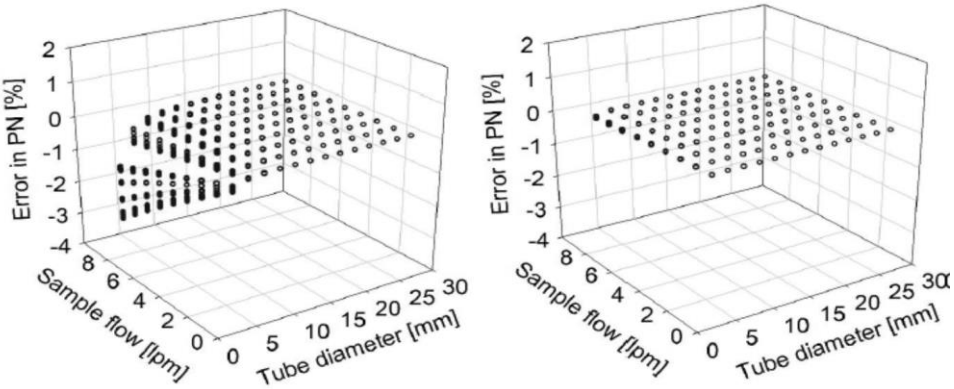

Figure 46
Gravitational losses for length of 1 m. On the left-hand side scenario (i) is plotted.

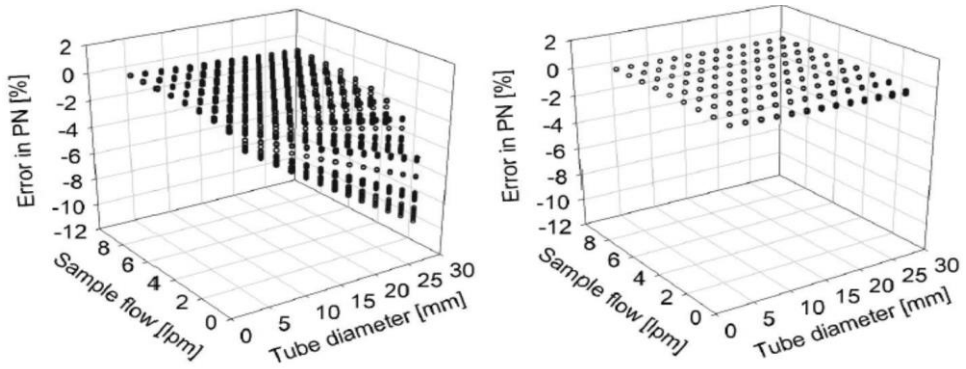

137. Pre-classifier: One issue raised by the instrument manufacturers was that micrometer particles can contaminate the particle systems having a big impact on measurement accuracy. For example, partly blocked orifices have different dilution ratios and the typical pressure measurements cannot identify this change. Figure 47 plots the impact of a 2.5 μm pre-classifier on the detected PN fraction. It is shown that the undetected fraction increases with the particle size. When the peak in the particle size distribution is >1.5 μm, the undetected fraction can exceed 25%. On the other hand, it is shown that the presence of a pre-classifier is not important (<2%) when the nucleation mode dominates.

Figure 47
(a) Impact of a 2.5 μm pre-classifier on PN concentration; (b) ratio of PN to PM10 for various geometric mean diameters (GMDs). Dotted line shows approximately the background level for a 1000 m^3/h tunnel flow rate.

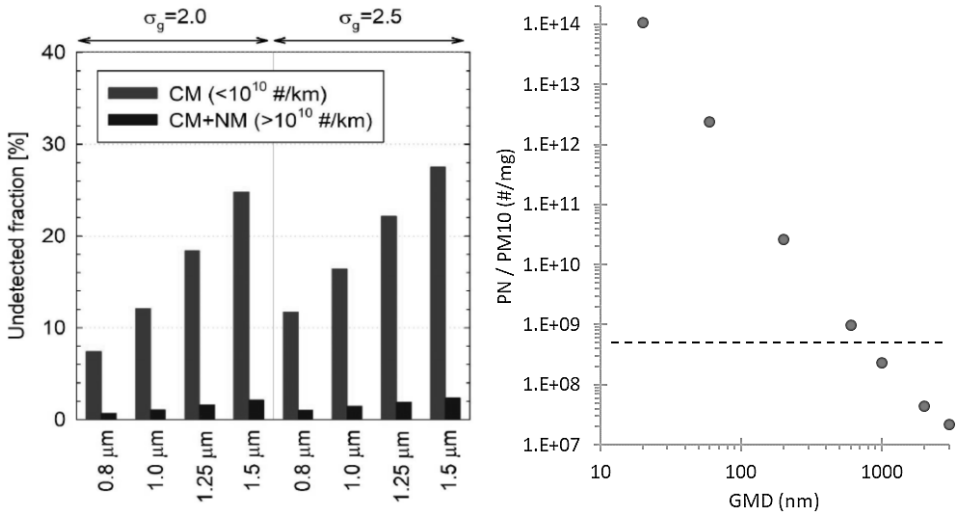

138. To assess the significance of losing large particles, Figure 47 (right panel) shows the ratio of PN to PM10 for various geometric mean diameters (GMD) and assuming unit density. For example, for GMD = 200 nm, PN emissions of 2.6E10 #/km would correspond to PM10 mass of 1 mg/km. The same mass would correspond to less than 4.3E8 #/km for particles 1000 nm or larger, which is at the background level of the PN setup (dotted line in Fig. 47 – more details are discussed below). Thus, the importance of PN measurement for large particle distributions is minor if there is a mass limit. In other words, the number concentration of large particles can be meaningful only if their mass emissions are very high [10].

139. PN background: One of the ILS findings was that the PN background (tunnel and PN system) was in some cases at the same level as the brake emissions (see Figure 18). For this reason, a strict requirement that the PN concentration at the tunnel measured with the PN system must not exceed 20 #/cm^3 was set. More details are discussed in the paragraph related to cooling air cleaning. For a typical tunnel flow rate of 1000 m^3/h the limit of 20 #/cm^3

translates to 4.5E+08 #/km and it is at least one order of magnitude lower than the typical PN concentrations measured at the ILS with the disc brakes. For this reason, the testing facility shall not subtract the background concentration values when reporting the TPN10 and SPN10 concentration values of the brake emissions measurement section.

Sample Treatment and Conditioning:

140. Dilution system – The dilution system ensures that the particle concentration at the inlet of the particle number counter (PNC) is below the single counting mode. For most PNCs, the maximum concentration is around 1-5E+04 #/cm^3 (Figure 48 – a). Figure 48 (b) shows the maximum PN concentration measured by the CPCs as a function of the tunnel flow in the ILS. These concentration levels correspond to a maximum PN concentration in the tunnel of 1E6 #/cm^3 for the tests with solid particles and 1E7 #/cm^3 for the tests with volatile particles. These concentrations translate to a necessary dilution of around 20:1 to 200:1. However, for some brakes the maximum tunnel concentration was <1E+05 #/cm^3. Based on this background and other input from measurements in the literature, a minimum dilution of 10:1 was specified without defining an upper limit. The only requirements for the diluter are (i) the PCRF ratios, which remained the same as in the guidelines (and the exhaust emissions regulation); and (ii) the temperature of the diluted sample will be <38 °C. The second requirement was added to ensure that there is no active heating at any part of the system. A lower temperature was not deemed to be necessary because the temperature in the saturator of the PNC is typically around 38-40°C, thus some evaporation will take place there.

Figure 48
(a) Measured and certified maximum PN concentrations for the ILS CPCs; (b) Maximum tunnel TPN10 concentrations measured by the CPCs in the ILS as a function of the tunnel flow.

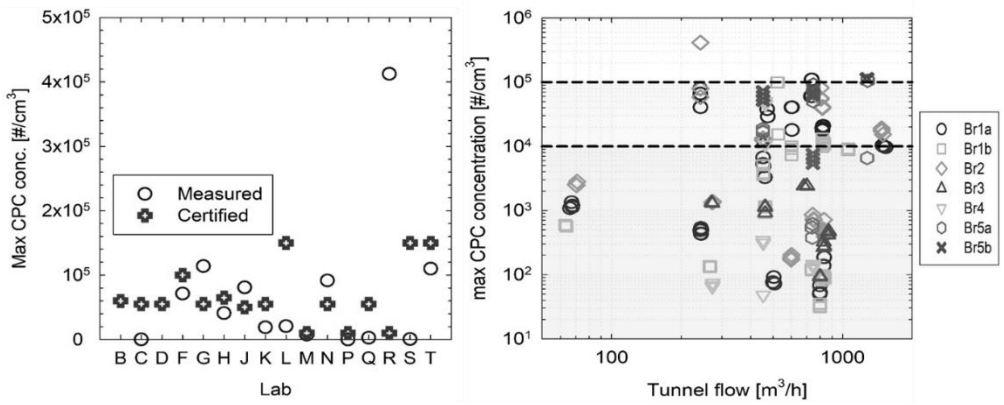

141. Volatile Particle Remover (VPR) – The thermal pre-treatment of the system for solid particles follows the technical requirements of the exhaust PN systems, with two differences: (i) The primary dilution of the VPR for brake emissions measurement does not need heating to 150 °C; however, the VPR needs a catalytic stripper at 350°C. The volatile removal efficiency requirements with tetracontane particles are identical (i.e., 99.9% removal of tetracontane particles with count median diameter >50 nm and mass >1 mg/m^3) to the exhaust system; (ii) The primary dilution factor of the brakes system is undefined as long as the total dilution is at least 10:1. On the other hand, in exhaust PN systems the primary dilution is required to be at least 10:1. The transfer tube between diluter or VPR and PNC has similar requirements as with the exhaust systems: The residence time shall be shorter than 1 s (vs. 0.8 s with the exhaust systems) and the inner diameter shall be 4 mm or larger.

142. The flow of the diluter or VPR should not deviate more than 10% from the mean during a test. The accuracy of the flow measurement should be within 5%. This value is higher than for PM measurements (2.5%) due to the minor importance of isokinetic sampling for PN. Furthermore, the PN system's flow rate is not necessarily used in the calculation of PN emissions. The flow of the PNC should be checked monthly with a calibrated flowmeter and should be within 5% of its nominal flow rate.

143. PN measurement device: Particle Number Counter (PNC) – The technical specifications of the PNC were based on the exhaust PNCs. One important effect reported in

some campaigns was the underestimation of the PNC counts due to flow changes caused by clogging. For this reason, a full-flow PNC is mandated allowing for regular monitoring of the sample flow (using an external flowmeter) which is directly used for the reported number concentrations from measured counts. While clogging may also eventually affect their performance it would be easy to verify on-site. Additionally, the PNC needs to operate in single counting mode where the accuracy is the highest. The counting efficiencies at nominal particle sizes of 10 nm and 15 nm electrical mobility diameter have to be 65±15% and >90%, respectively (including any calibration factor).

144. The following checks have been mandated to verify the correct operation of the PNC: (i) The flow into the PNC shall have a measured value within ±5% of the PNC nominal flow rate when checked with a calibrated flow meter (ii) A zero check on the PNC using a filter of appropriate performance at the PNC inlet shall report a concentration of ≤0.2 #/cm³. Upon removal of the filter, the PNC shall show an increase in measured concentration and a return to 0.2 #/cm³ or less on replacement of the filter; (iii) With a HEPA filter at the inlet of the diluter or VPR, the concentration measured by the PNC should be <0.5 #/cm^3 – this check shall be carried out both before and after the brake emissions test (iv) The PCRF corrected PNC concentration should be <20 #/cm^3 measuring from the tunnel with the flow for the emissions tests – no braking shall take place.

145. Flow splitting: For PN measurements it is allowed to use a flow splitter for the two systems measuring TPN10 and SPN10 under the following conditions: (i) the splitter has a flow angle <20° for each outlet; (ii) the two flow rates at the two branches are equal (within 5%); (iii) the splitter introduces <5% particle losses at 15 nm and 1.5 µm. Experience from calibration of PNCs has shown that the losses at the splitter are <1% for 15 nm particles and thus its impact on the PN results should be negligible. This validation shall be performed by the testing facility once during the installation of the system. Two particle generators probably will be needed: one for bigger particles (1.5 µm) and one for smaller particles (15 nm).

146. PN emissions calculation: During the ILS, the testing facilities were requested to report the TPN10 and SPN10 (where applicable) emissions of the tested brakes in number of particles per distance driven. The current version of the UN GTR provides a detailed description for the calculation of the TPN10 and SPN10 emissions following Equations 12.11 and 12.12, respectively. For the calculation, it is necessary to calculate the average normalised and PCRF-corrected TPN10 and SPN10 emissions in #/cm^3, the average normalized air flow in the sampling tunnel in m³/h, and the average actual velocity of the WLTP-Brake cycle in km/h (the letter N is used for Normal in the UN GTR). Like in the case of PM emissions, the calculation is straightforward when a full-friction brake is tested. On the other hand, for non-friction braking it is necessary to apply a correction factor that reflects the expected friction braking share of the vehicle on which the tested brake is mounted (Table 19). The calculation of the final TPN10 and SPN10 emissions for the tested brake in the UN GTR follows Equations 12.13 and 12.14, respectively. The testing facility shall apply the friction braking share coefficient that corresponds to the vehicle type of which the parameters were used for testing the brake.

147. The ILS data indicate that TPN10 emissions increase with the dissipated kinetic energy. More specifically, an increase of 36% in energy results in an increase of 91% in TPN10 emissions (values are averaged over the results of four testing facilities). However, during these tests there were no volatile nucleation modes. The application of friction coefficients for each vehicle category assumes a linear correlation between PN emissions and braking friction energy. While for SPN10 – which is a metric close to PM – this can be assumed to be true (see PM measurement), for TPN10 this is not necessarily and always true. As OICA pointed out, more data are necessary to support this conclusion. Clearly, the difficulty is for cases where there is a volatile nucleation mode that could be absent in low friction energies. Such cases would not be covered correctly by the friction coefficients. It should be emphasized though that the formation of volatile particles increases more than two order of magnitudes the emissions and the emission limits take into account also the higher variability. Additionally, volatile particle formation is dictated by one or two braking events; therefore, it is important to understand whether the different brakes have the potential of emitting such particles under real-world applications (e.g., a PEV vehicle braking used under

full battery conditions). Thus, even if the friction coefficients are not correct in such cases, they capture the "potential" of volatile particles formation which in principle should be minimum. More data will be collected in the future to allow for possible corrections in the method.

148. Figure 49 presents total and solid PN concentration during a test of Lab T with Br1Fa. It is shown in the graph that the TPN10 emissions increased during high temperature/high speed stops at the end of WLTP Brake Trip 10. During the actual event, TPN10 concentrations are 3-5 orders of magnitude higher than SPN10. The overall effect results in a cycle-average emissions 100-fold higher than for SPN10.

Figure 49
Total and Solid PN concentration during a test of Lab T for Br1Fa.

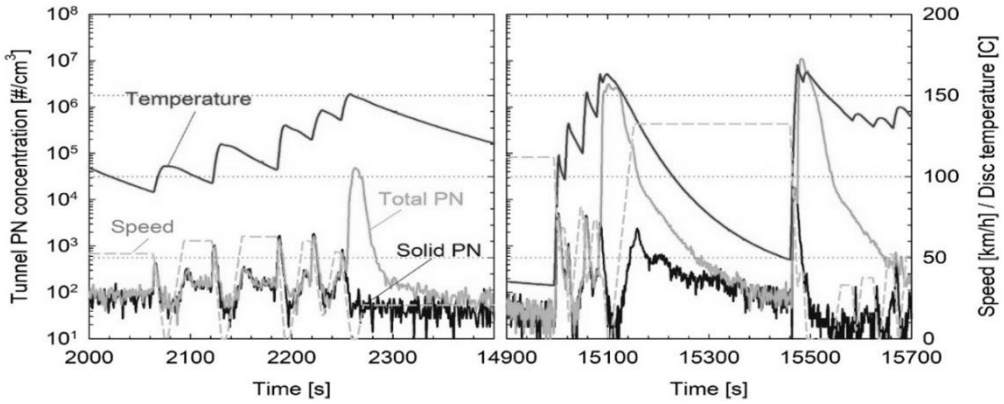

149. While for SPN10 the reproducibility (expressed as Coefficient of Variation – CoV) was 25-61% (more details are discussed in the Annex), for TPN10 this value was as high as 323% when all data are considered. The reason is the presence of a nucleation mode that can impact the result at least one order of magnitude. It is a common understanding that when the brake components (brake disk, brake pad, or both) reach a specific temperature – which depends on the brake system – volatiles originating from the organic binder material in the pad can be emitted. The subsequent cooling forms a volatile nucleation mode. It is not clear why only one lab measured such volatile nucleation mode (Figure 49). One explanation is the bedding procedure that due to the cooling in between the cycles, did not reach high temperatures and did not condition adequately the pads. One other possible explanation is the topical super-saturation ratios in the enclosure, which depend, among other factors, on the air flow profile. The standardization of the enclosure design and dimensions will partly address this issue. However, more tests are necessary for a better understanding. The important message though is that TPN10, should be treated as an indicator of volatile particles formation potential, with high value of reproducibility.

150. Calibration: The calibration requirements follow standard procedures of other regulations (e.g., for exhaust emissions). Typically, annual maintenance and calibration is required. The largest part covers the calibration requirements for the PNC, diluter, and VPR. The text is based on the exhaust emissions regulation. The only difference is that silver particles are additionally allowed for the calibration of the PNC. At the moment the PMP group has no opinion on the calibration material. More studies are necessary to find (if necessary) material representative of brake particles and suitable for calibration. The detailed calibration requirements are provided in the text of the UN GTR.

151. Filtration systems: Active and passive filters are defined for the first time in the first amendment of the GTR. Testing of such systems for emissions is allowed provided that all specifications defined in the GTR (e.g. temperature, dimensions, flow control, etc.) are met. In case of active brake filtering devices, the testing facility shall use dedicated signals to activate the filtering function at the brake event start time. The active filtering function may be deactivated up to maximum 5 seconds after the brake event end time. Additional provisions specifying the use of filtration systems in the context of brake emissions measurement will be introduced in the next amendment to this GTR.

Annex

Annex A – ILS high-level results

1. Introduction: Four disc and one drum brake system were tested during the interlaboratory study (ILS) in various configurations. Table A-1 lists the vehicle and brake parameters for the five brakes tested. Br1a is the reference brake with a typical ECE pad and Br1b is its non-asbestos organic friction pad (NAO) counterpart. Br2 and Br3 are standard disc brakes larger than the reference brake. The drum brake (Br4) mounts on the rear axle of a compact passenger car. Br5a and Br5b represent a typical N1 vehicle category brake tested under different load conditions (0% and 90% of the maximum payload). Table A-2 provides an overview of the final test matrix.

Table A-1
Characteristics of tested brakes.

Brake ID	*Axle*	*Vehicle Test Mass [kg]*	*Test Inertia [kg·m²]*	*Tyre Rolling Radius [mm]*	*Friction Material*	*$WL_{n\text{-}f}$/DM Ratio [-]*
Br1Fa	Front	1600	49.3	315	ECE	88.1
Br1Fb	Front	1600	49.3	315	NAO	88.1
Br2	Front	1668	50.8	321	ECE	44.6
Br3	Front	2623	112.1	383	ECE	50.7
Br4	Rear	1253	16.1	314	-	44.7
Br5La	Front	2500	86.7	345	ECE	90.1
Br5Lb	Front	3390	117.6	345	ECE	122.1

Table A-2
Final test matrix of the ILS. Grey cells denote planned but not completed tests.

	Br1Fa	*Br1Fb*	*Br2*	*Br3*	*Br4*	*Br5La*	*Br5Lb*	*Repeatability*	*Alternative bedding*
Lab B	√	√	√	√				√	√
Lab C	√	√	√	√					
Lab D	√	√	√		√				
Lab F	√	√	√	√	√	√	√		
Lab G	√	√	√			√	√		
Lab H	√	√	√						
Lab J	√	√	√						
Lab K	√	√	√					√	
Lab L	√	√	√	√				√	√
Lab M	√	√	√	√	√	√	√	√	
Lab N	√	√	√	√	√	√	√		√
Lab P	√	√	√						

	Br1Fa	*Br1Fb*	*Br2*	*Br3*	*Br4*	*Br5La*	*Br5Lb*	*Repeatability*	*Alternative bedding*
Lab Q	√	√	√					√	
Lab R	√	√	√						
Lab S	√	√	√	√					
Lab T	√	√	√		√				
Lab X	√	√	√			√	√		

2. 17 testing facilities declared their interest to participate to the ILS. Lab X did not manage to prepare for the testing campaign on time; therefore, it withdrew from the ILS. On the other hand, Labs B and Q reported significant measurement errors related to the dyno control and the overall testing layout. As a consequence, they requested for their results not to be considered in the subsequent analysis. Br1 and Br2 were mandatory for all testing facilities. The rest of the brakes, the alternative bedding and repeatability tests were carried out on a volunteer basis.

3. The main testing specifications were defined for the ILS by the TF2 and were published on the PMP website on 14.07.2021 [9]. The testing facilities were requested to follow all the specifications defined therein. However, this was not the case, as it was found that the testing facilities did not comply with one or more of the defined specifications. Table A-3 summarises the main non-compliances reported during the ILS based on each testing facility's declaration.

Table A-3
Most important non-compliant parameters with the TF2 specifications. Non-compliances in bold indicate parameters more relevant to PM/PN measurement errors.

Testing facility	*Most important non-compliances*
Lab-B	Speed violations, System background, Dyno climatics control, Microbalance resolution, Non-appropriate filters conditioning, **Impactor substrate coating, Pre-classifier cutpoint, Air Flow deviations**
Lab-C	1Hz Dyno climatics control (RH), **Calliper orientation, Application of the cycle at low friction work**, Air flow measurement location, **One filter for three PM10 – PM2.5 measurements**
Lab-D	Speed violations, System background, **Dyno climatics control, Microbalance resolution, Calliper Orientation**, Non-appropriate filters conditioning, No use of dilution system, **Cycle duration, No PM2.5 measurement**
Lab-F	System background, 1Hz Dyno climatics (RH), **Disc rotation direction, Calliper Orientation**, non-compliance with the weighing room specs, **PM flowsplit angle**
Lab-G	Initial trips temperature, No use of dilution system, Air flow measurement location, **Air Flow deviations**
Lab-H	System background, non-compliance with the weighing room specs, **Charge neutralizer, Microbalance resolution**, Non-appropriate filters conditioning, No use of dilution system
Lab-J	Non-compliance with the weighing room specs, **Impactor substrate coating**, Non-appropriate filters conditioning, No use of dilution system

Testing facility	*Most important non-compliances*
Lab-K	**Calliper orientation, Sampling plane location (0D)**, No use of dilution system, **No use of recommended impactor substrates**
Lab-L	**Calliper orientation, Sampling plane location (5.5D)**, Non-compliance with the weighing room specs, Air flow measurement location, **Air Flow deviations**
Lab-M	**Calliper orientation**, No use of reference filters, Non-appropriate filters conditioning, Non-compliance with the weighing room specs
Lab-N	
Lab-P	Initial trips temperature, System background, **Calliper orientation**, Air flow measurement location, **Application of the cycle at low friction work**
Lab-Q	Initial trips temperature, **Sampler/filter combination, Flow rate deviation, Application of the cycle at low friction work**
Lab-R	Initial trips temperature, System background, No use of reference filters, **Charge neutralizer**, No use of dilution system, **Pre-classifier cutoff, One filter for three PM10 measurements**
Lab-S	Non-compliance with the weighing room specs
Lab-T	Initial trips temperature, No use of reference filters, **Microbalance resolution**

4. The main objectives of the interlaboratory study are summarised to the following working items:

- Verify the feasibility and applicability of the defined specifications for sampling and measuring brake emission particles (TF2 Output);
- Provide recommendations to the TF2 on further improving and/or extending the set of the defined specifications;
- Examine the repeatability and reproducibility of PM and PN emission measurements with the application of the defined specifications;
- Examine the repeatability and reproducibility of specific test conditions with the application of the defined specifications;
- Propose alternatives that can improve the efficiency of some of the methods and specifications proposed (i.e., bedding procedure).

5. PM measurements: Figure A-1 summarizes the measured PM2.5 and PM10 emissions from all testing facilities for all tested brakes. It is observed that the reference brake emits an average of 5.0 mg/km per brake, while its NAO counterpart emits approximately 2.2 mg/km. Br2 and Br3 emit PM10 at similar levels of about 9.0 mg/km per brake corner. The drum brake exhibits substantially lower PM10 emissions at the level of 0.5 mg/km. Finally, increasing the payload of the N1 brake results in an increase of PM10 emissions in an almost linear way.

6. Similar trends are observed for PM2.5 emissions. The reference brake emits almost twice as high compared to its NAO counterpart. The drum brake exhibits substantially low PM2.5 compared to the disc brakes. The increase of the payload of the N1 brake by 36% results in an increase of PM2.5 emissions by almost 25%. PM2.5 is typically between 35-42% of PM10 for all tested disc brakes, whereas for the drum brake, the PM2.5 to PM10 ratio is substantially higher (almost 60%).

Figure A-1

PM10 (above) and PM2.5 (below) measurements from all testing facilities for all tested brakes. Data from Labs B and Q have not been introduced following a request by the testing facilities. Error bars represent the standard deviation of the measurement.

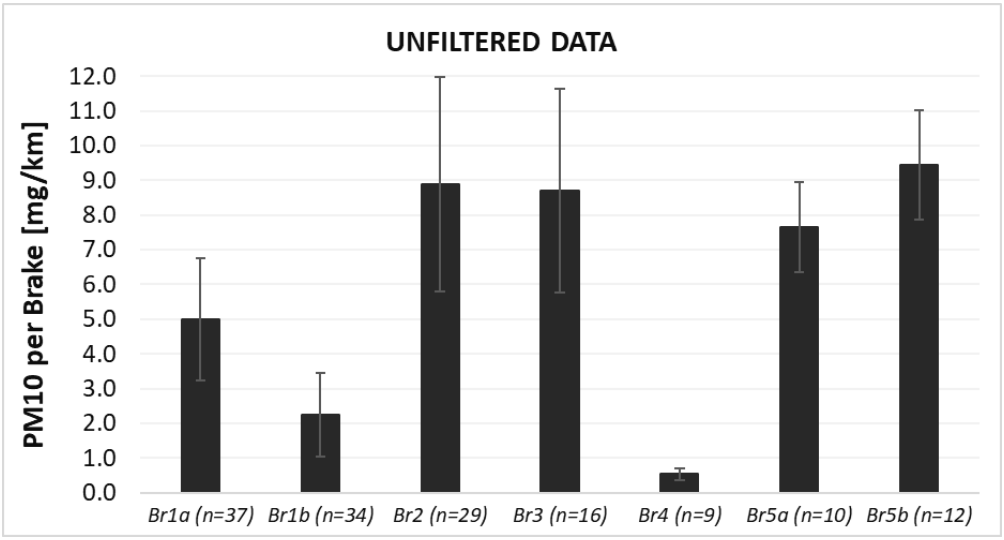

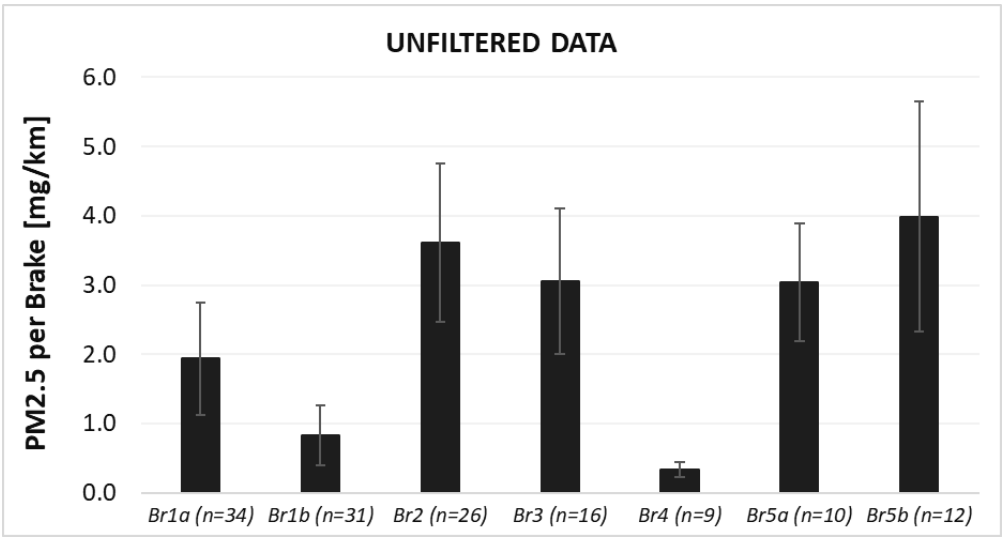

7. Table A-4 summarizes the PM emissions results as well as the PM measurement variability. The PM10 measurement variability – defined as the ratio of the standard deviation to the average PM10 value – ranges between 17% and 35%. These values are considered acceptable taking into account the general non-compliance of the testing facilities with the protocol discussed in Table A-3. It is expected that the introduction of stricter specifications for the PM mass measurement – along with the mandatory compliance of the testing facilities with the protocol with the introduction of the UN GTR – will result in a much lower PM10 measurement variability.

Table A-4

PM2.5 and PM10 measurements from all testing facilities for all tested brakes. The PM2.5 to PM10 ratio and the wear rate are also shown.

	Br1a	*Br1b*	*Br2*	*Br3*	*Br4*	*Br5a*	*Br5b*
PM10 [mg/km]	**5.0**	**2.2**	**8.9**	**8.7**	**0.5**	**7.7**	**9.4**
StDev	1.8	1.2	3.1	2.9	0.2	1.3	1.6

	Br1a	*Br1b*	*Br2*	*Br3*	*Br4*	*Br5a*	*Br5b*
[mg/km]							
Measurement Variability	35%	54%	35%	34%	31%	17%	17%
Number of measurements	37	34	29	16	9	10	12
PM2.5	**1.9**	**0.8**	**3.6**	**3.1**	**0.3**	**3.0**	**4.0**
[mg/km]							
StDev	0.8	0.4	1.1	1.1	0.1	0.9	1.7
[mg/km]							
Measurement Variability	42%	52%	32%	34%	33%	28%	42%
Number of measurements	34	31	26	16	9	10	12
Mass Loss	**14.9**	**4.9**	**20.9**	**23.7**	**2.3**	**16.1**	**19.3**
[mg/km]							
StDev	1.9	2.4	2.1	1.3	1.8	1.7	1.0
[mg/km]							
Measurement Variability	12.9%	48.2%	10.0%	5.5%	76.3%	10.3%	5.1%
Number of measurements	10	9	8	4	3	4	3
PM2.5/PM10 Ratio	**39%**	**37%**	**41%**	**35%**	**61%**	**40%**	**42%**

8. Br1b shows a higher variability compared to the other brakes (54%); however, this is attributed to the brake material which exhibited a strange emissions behaviour. More specifically, three testing facilities reported an average PM10 of 0.6±0.2 mg/km (mass loss of 1.8±0.2 mg/km), whereas seven testing facilities reported an average PM10 of 3.0±0.7 mg/km (mass loss of 6.5±0.9 mg/km). Practically, Br1b "behaves" as if there were two different brakes and this is demonstrated by studying its mass loss. JRC was not able to confirm that Br1b was identical for all testing facilities; therefore, it is not possible to draw any conclusion regarding the PM measurement variability using this particular brake. However, it has been decided to mandate the mass loss measurement because it provides useful information regarding the tested brake and may prove useful when evaluating the results of a measurement campaign. The results demonstrate that a repeatable and reproducible mass loss measurement is already achievable.

9. Table A-4 shows that the PM2.5 measurement variability is at a similar level with PM10. Slightly higher measurement variability was observed with Br1a and Br5b; however, this is attributed to three outlying measurements (2 measurements with Br1a carried out by Lab M and 1 measurement with Br5b carried out by Lab G). Again, Br1b comes with higher measurement variability due to the phenomenon described above. More specifically, three testing facilities reported an average PM2.5 of 0.3±0.1 mg/km (mass loss of 1.8±0.2 mg/km), whereas seven testing facilities reported an average PM10 of 0.9±0.2 mg/km (mass loss of 6.5±0.9 mg/km). Overall, it is expected that the introduction of stricter specifications will result in a much lower PM2.5 measurement variability.

10. PN Measurements: Figure A-2 summarizes the measured TPN10 and SPN10 emissions from all testing facilities for all tested brakes. It is observed that the reference brake emits an average of 1.9E+10 #/km per brake; however, with this brake, Lab-T reported the formulation of volatile particles thus resulting in an increased overall average value as well as an increased variability of the measurement. No other testing facility observed volatile particles, neither with Br1a nor with any other brake, during the ILS. The NAO disc brake exhibits the lowest TPN10 emissions along with the drum brake at the level of 2.0E+09 #/km per brake. Br2 emits relatively high TPN10 at a level of about 1.1E+10 #/km per brake corner. Finally, increasing the payload of the N1 brake by 36% results in an increase of TPN10 emissions of approximately 90%. However, with only a few data points it is not possible to extract a solid conclusion regarding the relationship between testing inertia and TPN10 emissions. More data are required to investigate and establish – or not – such a relationship.

11. Slightly different trends are observed for SPN10 emissions. The reference brake emits much lower emissions due to the absence of volatile particles. The NAO brake exhibits substantially low SPN10 compared to the other disc brakes – actually Br1b exhibited the lowest SPN10 emissions among all tested brakes. Again, Br2 emits the highest SPN10 at a level of about 9.3E+09 #/km per brake corner – more than one order of magnitude lower than the regulatory limit for exhaust emissions. The drum brake exhibits generally low SPN10 emissions in line with all other measured parameters. The influence of increasing payload of the N1 brake to SPN10 emissions was not possible to be investigated since Labs F, G, M, and N did not measure SPN10 with these brakes. Relevant data will be required in the future to investigate and establish – or not – a relationship between testing inertia and SPN10 emissions.

Figure A-2

TPN10 (above) and SPN10 (below) measurements from all testing facilities for all tested brakes. Data from Labs B and Q have not been introduced following a request by the testing facilities. Error bars represent the standard deviation of the measurement.

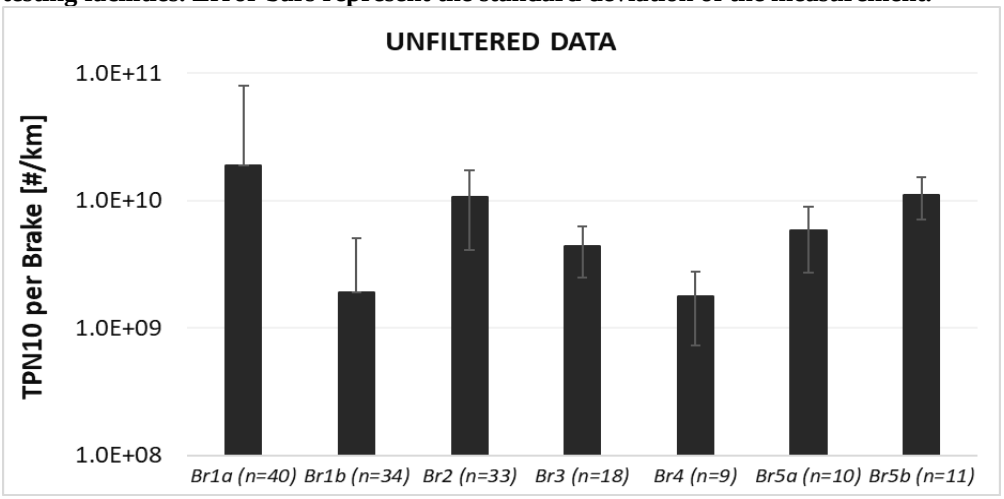

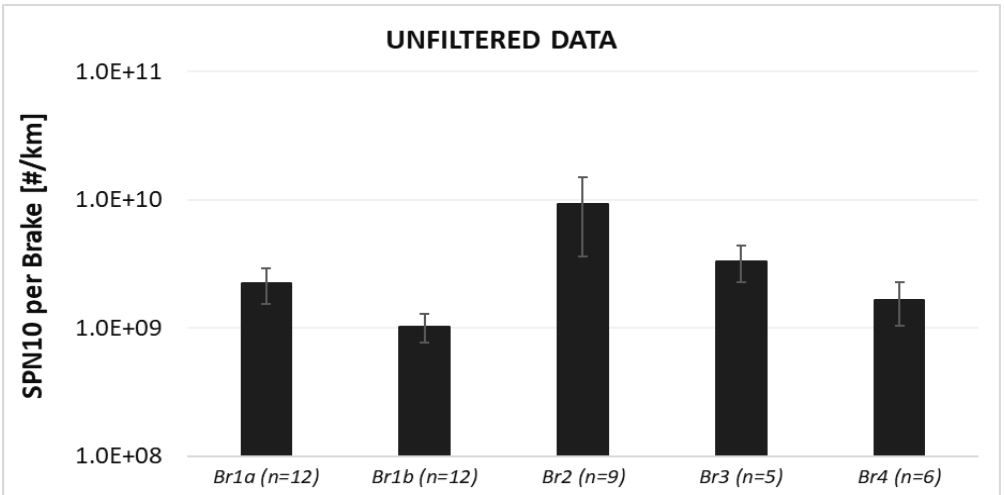

12. Table A-5 summarizes the PN emission results. The TPN10 measurement variability ranges between 36% and 323%. Br1a exhibits the highest variability (323%) due to volatile particle emissions reported by Lab T. Br1b also exhibits a high measurement variability due to the "strange" emissions behaviour described in the previous paragraphs. When the two different emission blocks are considered for Br1b the TPN10 variability is 31.6% and 35.8%, respectively. These values are considered acceptable taking into account the general non-compliance of the testing facilities with the protocol discussed in Table A-3. It is expected that the introduction of stricter specifications for the PN measurement – along with the mandatory compliance of the testing facilities with the protocol with the introduction of the UN GTR – will result in a much lower TPN10 measurement variability.

13. Regarding volatile particles, it became apparent from the ILS that more data are required to investigate and understand their formulation. At a first glance, the presence of volatile particles results in a very high – non acceptable – measurement variability; however, this remains an important aspect since volatiles – when present – dictate the overall TPN10 emissions and are emitted as a result of a few single brake events. Therefore, it is of high importance to enable the measurement of such particles in the UN GTR with the aim of understanding the mechanism behind its formation as well as investigating how frequently this phenomenon happens with the currently available brakes in the market.

14. Table A-5 shows that the SPN10 measurement variability is much better compared to TPN10. Much lower measurement variability was observed with the reference brake. This is normal since volatile particles are not measured with SPN10. Br1b comes with low measurement variability despite the difference in its behaviour – the variability is comparable to that of TPN10 when the two blocks are considered. The measurement variability of the SPN10 measurement for Br2, Br3, and Br4 is comparable to that of TPN10 for the same brakes. Unfortunately, it was not possible to assess the SPN10 measurement variability of Br5 due to lack of related measurements. Once more, it is expected that the introduction of stricter specifications will result in an improved SPN10 measurement variability.

Table A-5
TPN10 and SPN10 measurements from all testing facilities for all tested brakes. Measurement variability is also shown.

	Br1a	*Br1b*	*Br2*	*Br3*	*Br4*	*Br5a*	*Br5b*
TPN10 [#/km]	**1.9E+10**	**1.9E+09**	**1.1E+10**	**4.4E+09**	**1.8E+09**	**5.8E+09**	**1.1E+10**
StDev [#/km]	6.1E+10	3.2E+09	6.7E+09	1.9E+09	1.0E+09	3.1E+09	4.1E+09
Measurement Variability	322.9%	169.8%	62.0%	43.0%	58.3%	53.0%	36.0%
Number of measurements	40	34	33	18	9	10	11
SPN10 [#/km]	**2.2E+09**	**1.0E+09**	**9.3E+09**	**3.3E+09**	**1.7E+09**	**N/A**	**N/A**
StDev [#/km]	6.8E+08	2.6E+08	5.7E+09	1.1E+09	6.3E+08	N/A	N/A
Measurement Variability	30.9%	25.3%	61.0%	32.3%	37.8%	N/A	N/A
Number of measurements	12	12	9	5	6	0	0

Annex B – Development of the vehicle-specific friction braking share coefficients

15. Introduction: Annex C (introduced with the first amendment) describes the procedure to determine vehicle-specific friction braking share coefficients for use with the Global Technical Regulation on the measurement of brake wear particulate matter and particle number emissions from brakes used on Light-Duty vehicles up to 3.5 t. It is intended for vehicles that are capable of some level of regenerative braking and may be used as an alternative to the templated friction braking share coefficients given in Table 5.3. of UN GTR No. 24 for improved accuracy.

16. Scope and Principle of Method: The vehicle specific friction braking share coefficient is defined in UN GTR No. 24 as the fraction of deceleration energy absorbed by the friction brakes (after accounting for road load) with regenerative braking active. It applies to all vehicles belonging to the specific 'vehicle family' (the term was changed to 'vehicle electrification family' in the second amendment). It is a calculated parameter based on measurements of the subject vehicle on a fully UN GTR No. 15 compliant chassis dynamometer. Based on studies conducted in the development of Annex C, the WLTP-Brake cycle, or WLTP-Brake Trip #10 cycle were selected as test cycles over which the friction braking share coefficient may be determined.

The methodology is based on measuring friction brake energy (directly or by proven surrogate) over the prescribed drive cycle. To measure friction brake power, all brake positions on the vehicle are equipped with external sensors to determine the brake torque at each of the wheels. These data are combined with the velocity of the vehicle data and integrated over time to determine the dissipated friction braking energy.

The friction braking share coefficient, c, is calculated dividing the "deceleration energy dissipated by the friction brakes" W_{brake} by the "total deceleration energy reduced by 13 per cent to account for the road loads", W_{ref}, as shown in Equation B1:

$$c = \frac{W_{brake}}{W_{ref}} \qquad \text{(Eq. B1)}$$

The total deceleration energy is calculated from the cycle (velocity profile) and vehicle test mass. It is multiplied by 0.87 (13% reduction) to match the methodology for accounting for road load in the single brake inertia dynamometer procedure for the emission measurement.

The declared value can be increased by the manufacturer by up to 0.05 absolute or 50% relative, whichever is greater. The second amendment added that Contracting Parties adopting additional requirements to this GTR (e.g. durability, in-service conformity) may allow manufacturers to additionally declare values up to the values of Table 5.3 of the GTR.

17. Methods to determine friction brake energy: Friction brake torque may be measured either indirectly, by means of installing hydraulic pressure sensors and scaling by the appropriate pressure to torque gain factors (Cp.b, measured by running the front and rear brakes for the subject vehicle over the WLTP-Brake cycle on a dynamometer fully compliant to UN GTR No. 24), or directly, by use of installed piezoelectric torque sensors.

18. Pressure Method: To determine the friction brake energy by the "pressure method", hydraulic pressure transducers are installed close to each brake position. An example is shown in Figure B-1. The pressure data for each brake recorded over the duration of the WLTP-Brake or the WLTP-Brake Trip #10 drive cycle and that exceed the threshold pressure required to develop torque, are multiplied by the corresponding torque to pressure ratio, $C_{p,b}$, to create a torque trace for each brake. These traces are then multiplied by the corresponding wheel rotational speed for each brake to get braking power, and the braking power signal is integrated over time to result in work energy absorbed by each brake. The work energy of each brake position is added to result in the total friction brake work for the vehicle over the drive cycle.

How this pressure is determined was not included in the GTR. Proposals to determine it in the brake dyno laboratory showed for the same brake different values during ILS3. This was attributed to several potential factors such as unusual pressure oscillations or slow rise times that can arise due to improper brake bleed or servo controller settings. Analysis of the data also showed that for disc brakes a value of 1 bar could cover all applications. For this reason, in the second amendment it was decided to set a fixed value of 1 bar for disc brakes and 3.5 bar for drum brakes.

Figure B-1

Brake pressure sensor (left-hand side) and examples of mounting of brake pressure sensors (P) at brake pipes of the tested vehicles (right-hand side).

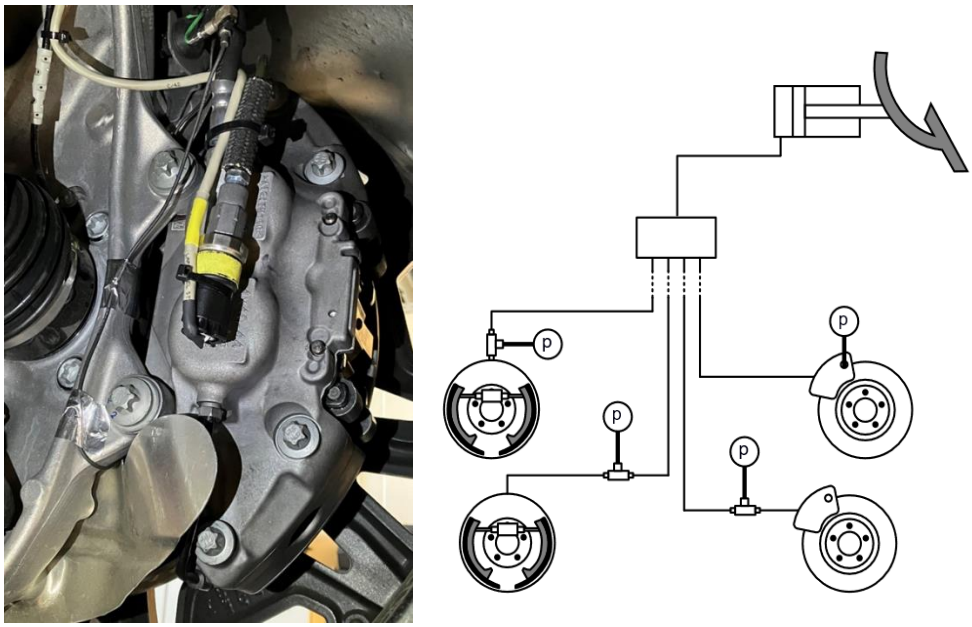

19. Use of alternative signals (such as CAN-Bus or On-Board Diagnostics) are permitted so long as equivalency to the prescribed methods is established (the equivalency criterion is defined in Annex C of the UN GTR No. 24). An example of this is shown in Figure B-2:

Figure B-2

Example comparison External Torque Sensor, External Pressure Sensor, and CAN based Pressure derived braking torque.

20. Torque method (piezoelectric torque sensors): Friction brake torque may be measured directly using installed piezoelectric sensors, an example of which is depicted in

Figure B-3. Friction brake power and total friction brake torque over the drive cycle are computed in an identical manner as for the Pressure Method, with the exception that it is no longer necessary to multiply recorded pressure by the brake torque to pressure ratio to calculate brake torque; this is instead measured directly:

Figure B-3
Brake torque sensor (left), and fully installed (right).

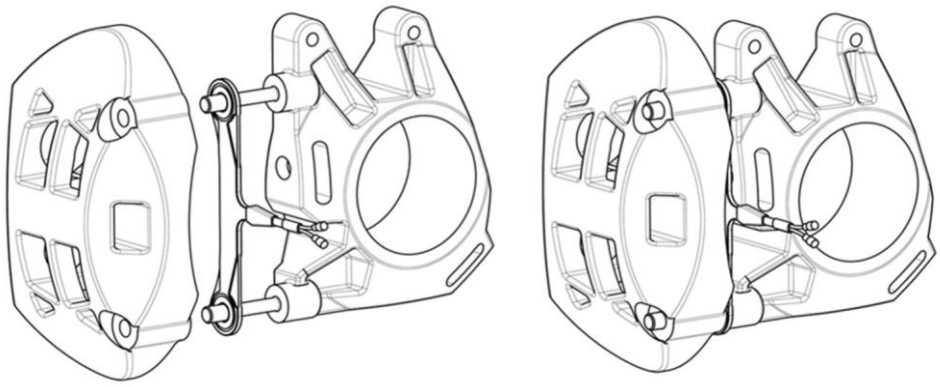

21. Test setup and test cycles: To minimize the effort and keep comparability to other vehicle tests on the chassis dyno (e.g. range determination or exhaust emission measurement) the vehicle shall be conditioned according to the provisions of WTLP (exhaust) following the local regulation or GTR 15.

After conditioning and soaking of the vehicle, the measurement shall be performed using the complete WLTP Brake Cycle. Alternatively, Trip #10 of the cycle may be used. However, the complete cycle will be considered the master if differences occur. Annex C provides information on criteria, requirements, and the determination of equivalency.

22. Application of the method and results: Vehicles representing the electrification concepts NOVC-HEV Cat.1/Cat2, OVC-HEV, and PEV were tested by OICA laboratories applying the methods as described above. The vehicles and some base information is given in Table B-1. NOVC-HEV vehicles were conditioned as prescribed by GTR-15 and defining an intermediate state of charge. OVC-HEVs and PEVs were charged to 100% and tested without recharging. The reference deceleration energy was calculated from the known vehicle test mass.

Table B-1
Summary of vehicles and base information tested with friction share method on the chassis dynanometer

Vehicle	Type	Engine power [kW]	Battery capacity [kWh] netto	Vehicle Mass [kg] approx.
Vehicle 1	OVC-HEV	145+100	31	3000
Vehicle 2	NOV-HEV Cat.2	109+135	1.1	1900
Vehicle 3	OVC-HEV	324	10	2300
Vehicle 4	PEV	385	105.2	2700
Vehicle 5	NOVC-HEV Cat.1	114	0.45	1400
Vehicle 6	PEV	560	83.7	2500
Vehicle 7	PEV	100	81	3400
Vehicle 8	NOVC-HEV Cat.1	225	0.92	2400
Vehicle 9L	OVC-HEV	160	10.4	1750

Vehicle	Type	Engine power [kW]	Battery capacity [kWh] netto	Vehicle Mass [kg] approx.
Vehicle 9H	OVC-HEV	160	10.4	2100
Vehicle 10	PEV	198	76	2200
Vehicle 11	PEV	100	81	3500

23. The test results of friction share determined at WLTP-Brake Trip #10 and full WLTP-Brake cycle are shown in Figure B4. In the general the friction share determined at WLTP-Brake-Trip 10 is on a relative basis some percent higher. Instead of introducing uncertainty, the PMP group decided to use a factor of 1, however fixing that in case of doubt the result determined at the full WLTP-Brake cycle is decisive.

Figure B-4
Deviation of friction share determined at WLTP-Trip 10 from full WLTP-Brake cycle measured by direct torque method (O) pressure method without pressure threshold (squares).

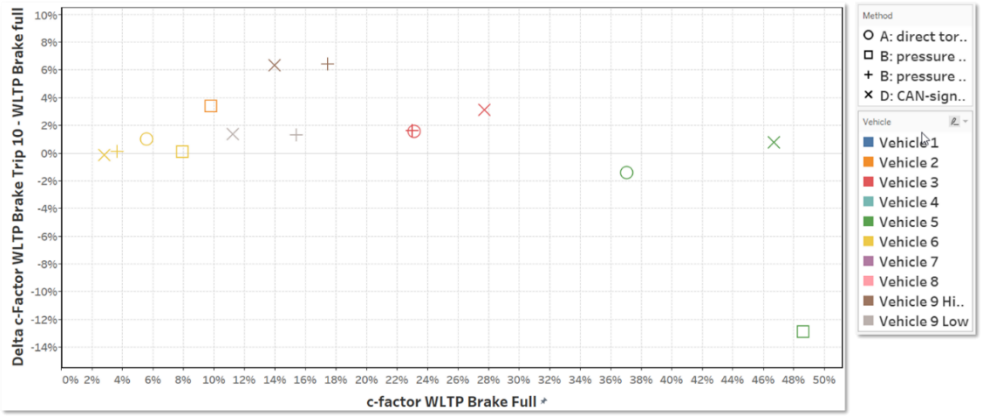

24. Besides the master methods (pressure and torque measurement), the torque signals available at the vehicle CAN were investigated. In Figure C-5 the friction share coefficient determined by Method D (CAN) is plotted against the c-factor determined by the pressure method. The data shows that the two methods correlate with a slope close to unity. For use in Annex-C of the GTR, an equivalency criterion needed to be defined. In order to deal with increasing relative deviations at small friction shares it was agreed to have two criteria: either the absolute deviation of ±2%, or a relative deviation of ±10% (JRC-proposal) needs to be fulfilled in order to demonstrate equivalency. OICA suggested ±20% as relative criterion. Figures B-5a and B-5b show the data and the criterion ±10% or ±20%, respectively. From the available data so far, it is evident that several correlation data points would not meet the relative criterion of ±10%.

Figure B-5

Correlation of friction share coefficients determined by alternative (CAN) method (D) and pressure method (B). a.) The lines show absolute deviation of ±2% (green dotted) and relative deviation ±10% (blue solid) b.) the identical data is shown with absolute deviation of ±2% (green dotted) and relative deviation ±20% (blue solid).

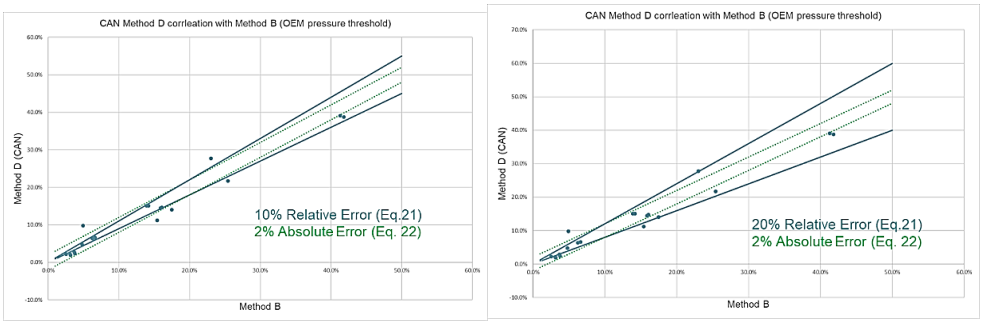

25. Aggressive / Smooth braking criteria: In addition to the criterion of speed trace tolerances defined in the GTR, criteria of smoothness of the braking style were added in the second amendment, as they could have an influence on the c factor. As in other regulations, SAE J2951 drive quality criteria were assessed. Square Speed Error (RMSEE), Inertial Work Rating (IWR), and inertial power difference rating (IPDR) were finally introduced with the second amendment. The limit values were determined based on inputs of different braking styles from OICA, technical services and JRC.

Figure B-6

Results of the study on braking criteria.

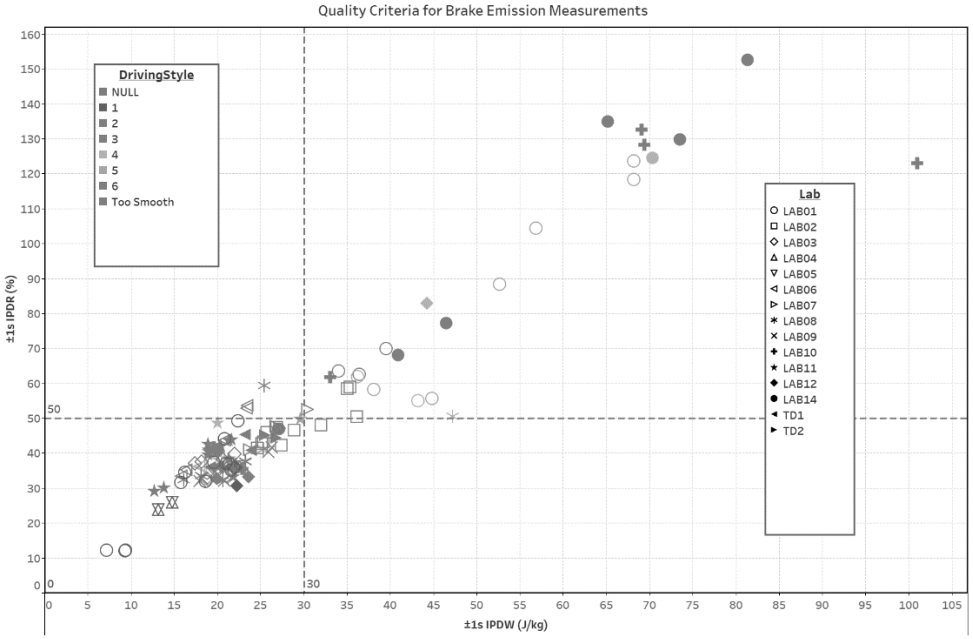

Annex C – ILS3 high-level results

1. Introduction: Three disc brake systems were tested during the third interlaboratory study (ILS3). The main objectives of ILS3 were to.

- Examine the repeatability and reproducibility of PM and PN emission measurements with the application of the GTR-24 protocol;
- Understand the capability of participating labs to carry out brake PM and PN emission measurements in accordance with the GTR-24;
- Help the laboratories to finetune their setup and improve their processes;
- Provide recommendations to the PMP on further improving and finetuning the defined specifications in the GTR-24 (for the second amendment);

2. The ILS3 was organised in two phases.

Phase 1 with the BMW X5 brake was used a reference to compare results obtained in ILS3 with those previously obtained using the same brake during the second ILS.

Phase 2 was completed with two additional brakes: Ford Puma and JLR brake. Both phase 1 and phase 2 included 5 WLTP-Brake cycles for bedding followed by 3 WLTP-Brake cycles for emission measurements. During phase 2, a fourth WLTP-Brake emission cycle was added with a constant cooling airflow for all laboratories and selected dynamometer signals were recorded at a higher resolution of 250 Hz. The key points of investigation using the fourth cycle were to understand the flow effects on brake temperatures, friction work evaluations, and threshold pressure.

All three brakes were tested using two samples M1 and M2 (different batches) for each brake.

Figure C-1
ILS3 methodology.

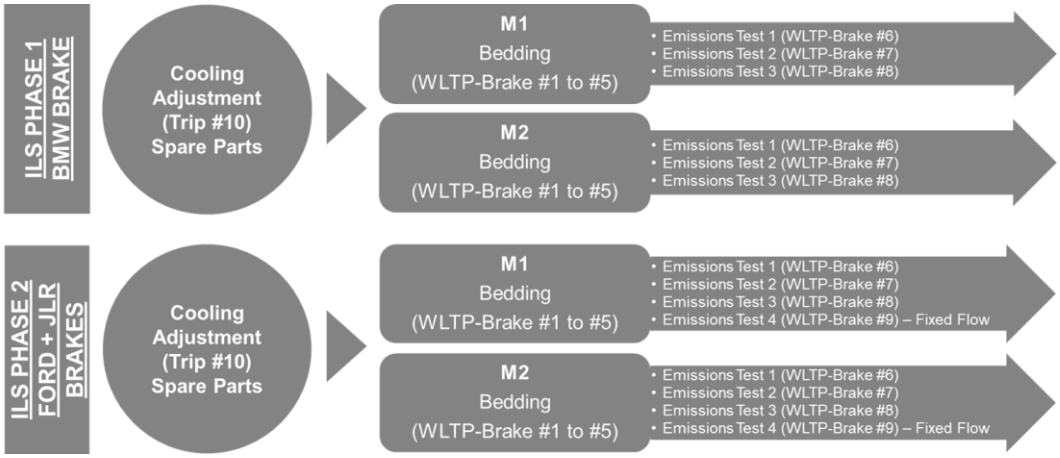

3. A total of 16 test facilities originally enrolled in the study. From initial evaluations of the test setup and other factors, two labs (B, H) withdrew from the entire ILS3 study and one lab (L) withdrew from the ILS3 phase 1. Lab L finetuned their setup and continued their participation in the ILS3 phase 2. Data analytics were carried out for all the brakes by the ILS3 ‘small group’.

Table C-1
Final test matrix of the ILS3. w=withdrawn; nc=not compliant.

	BMW M1	BMW M2	FORD M1	FORD M2	JLR M1	JLR M2
Lab A	√	√	√	√	√	√
Lab B	w	w	w	w	w	w
Lab C	√	√	√	√	√	√
Lab D	√	√	√	√	√	√
Lab E	√	√	√	√	√	√
Lab F	√	√	√	√	√	√
Lab G	√	√	√	√	√	√
Lab H	w	w	w	w	w	w
Lab I	√	√	√	√	√	√
Lab J	√	√	√	√	√	√
Lab K	√	√	√	√	√	√
Lab L	nc	nc	√	√	√	√
Lab M	√	√	√	√	√	√
Lab N	√	√	√	√	√	√
Lab O	√	√	√	√	√	√
Lab P	√	√	√	√	√	nc

4. The small group analysed the data submitted by labs in various files such as equipment and testing checklists, EBF files, TBF files, PM filter measurements, brake parts wear measurements, and the GTR test reports. As a part of this exercise, datapoints which were either self-declared by labs as non-compliant or those assessed by the small group were excluded from further data analysis. Such exclusions were presented in the PMP forum accordingly.

5. The cycle-to-cycle repeatability of PM10 EF within each lab for both BMW X5 and the Ford Puma brakes had an average of about 3%. The cycle-to-cycle CoV of PM10 EF for the JLR brake was about five times higher compared to X5 and Puma brakes (similar in absolute value). One of the key differentiators between JLR and the other two brakes was that the former was made up of NAO friction material while the latter two constituted of low metallics. Similar to PM10, the cycle-to-cycle CoV of PM2.5 EF for the JLR brake was about three times higher compared to X5 and Puma brakes. The JLR brake with low EFs (PM10: 1.4 mg/km) was attributed to the higher CoV compared to the other brakes. Nevertheless, the CoV of PM2.5 EFs was nearly the same (25%-28%) for all the three brakes.

6. The cooling airflow for each brake was determined by each lab using the method described in GTR24 Paragraph 10. In addition, all labs used a common normalised airflow of 975 N.m3/h ±10% in the fourth emission cycle of phase 2. The subsequent results revealed no significant difference in brake temperatures (delta < 10 °C) when the labs either used individual airflow setpoints or when they all used the same airflow (with ±10% tolerance). The effect of airflow on emission factors was inconclusive due to different trends observed between M1 and M2 samples tested only once.

7 The coefficient of variation (CoV) of PM10 emission factor (EF) reduced from 27% in ILS2 to 16% in ILS3. The difference in PM10 EF (mg/km) measured between ILS2 and ILS3 was within 5%.

Figure C-2
Test results.

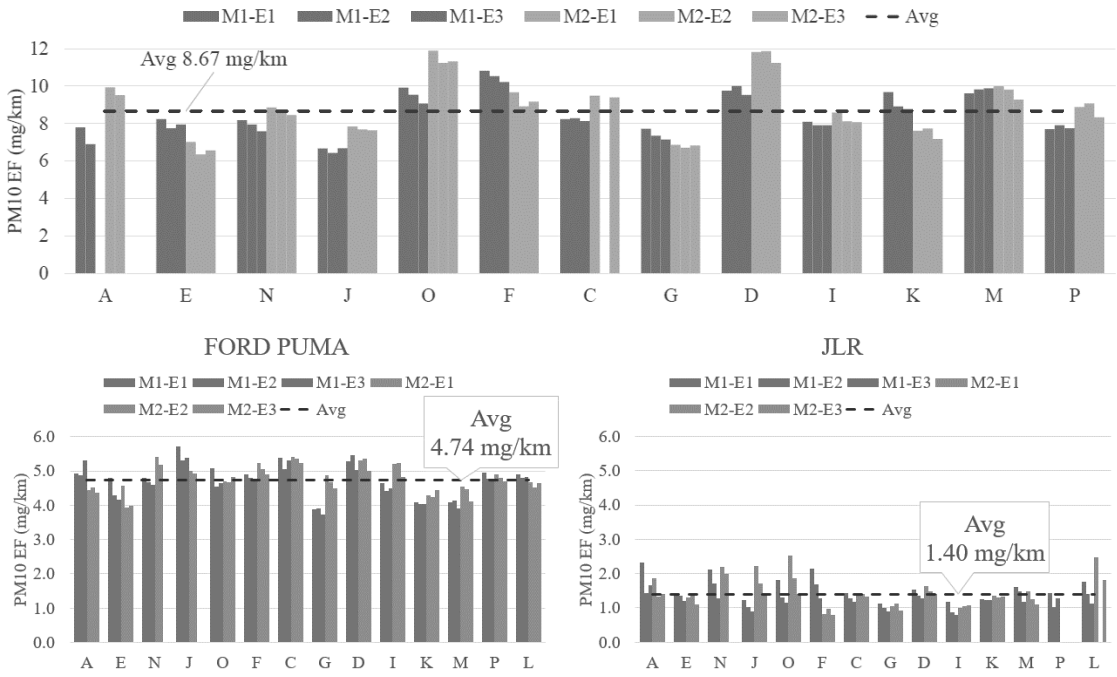

References

[1] Grigoratos, T.; Giechaskiel, B. Preliminary analysis on PM data from the ILS. PMP Web Conference 29.03.2022. https://wiki.unece.org/display/trans/PMP+Web+Conference+29.03.2022

[2] Agudelo et al. 2020. High-fidelity modelling and characterization of dynamometer enclosure interactions using a DOE approach for brake emissions measurements. 50th PMP Meeting – April 3-4 2020. https://wiki.unece.org/display/trans/PMP+50th+Session

[3] https://wiki.unece.org/display/trans/PMP+39th+session - PMP-39-02 NEPE - Driving Conditions Summary Report.pdf

[4] Mathissen M., Grochowicz J., Schmidt C., Vogt R., Zum Hagen F., Grabiec T., Steven H., Grigoratos T.; A novel real-world braking cycle for studying brake wear particle emissions; Wear, Volumes 414–415, 2018, 219-226, https://doi.org/10.1016/j.wear.2018.07.020

[5] Mathissen M., Grochowicz J., Schmidt C., Vogt R., Zum Hagen F., Grabiec T., Steven H., Grigoratos T.; WLTP-based Real-World Brake Wear Cycle, Mendeley Data 1 (2018), https://doi.org/10.17632/dkp376g3m8.1

[6] UNECE (2020) – Informal Document GRPE-81-12 (2020). (PMP) Brake Emissions Protocol – Part 1. Available online: https://www.unece.org/trans/main/wp29/wp29wgs/wp29grpe/grpeinf81.html.

[7] Grigoratos, T.; Agudelo, C.; Grochowicz, J.; Gramstat, S.; Robere, M.; Perricone, G.; Sin, A.; Paulus, A.; Zessinger, M.; Hortet, A.; et al. Statistical Assessment and Temperature Study from the Interlaboratory Application of the WLTP–Brake Cycle. Atmosphere 2020, 11, 1309

[8] Hesse, D.; Hamatschek, C.; Augsburg, K.; Weigelt, T.; Prahst, A.; Gramstat, S. Testing of Alternative Disc Brakes and Friction Materials Regarding Brake Wear Particle Emissions and Temperature Behaviour. Atmosphere 2021, 12, 436. https://doi.org/10.3390/atmos12040436

[9] PMP brake protocol - testing specifications.pdf – Minimum specifications for measuring and characterizing brake emissions – Available at https://wiki.unece.org/display/trans/PMP+Web+Conference+15.07.2021

[10] Grigoratos, T.; Mamakos, A.; Arndt, M.; Lugovyy, D.; Anderson, R.; Hafenmayer, C.; Moisio, M.; Vanhanen, J.; Frazee, R.; Agudelo, C.; Giechaskiel, B. Characterization of Particle Number Setups for Measuring Brake Particle Emissions and Comparison with Exhaust Setups. Atmosphere 2023, 14, 103. https://doi.org/10.3390/atmos14010103